

**IDENTIFICATION OF POTENTIAL INHIBITORS AGAINST
E.coli MUR ENZYMES THROUGH VIRTUAL SCREENING AND
in vitro ASSAY**

Thesis Submitted for the Award of the Degree of

DOCTOR OF PHILOSOPHY
in

Microbiology

By

Vinita Gaur

Registration Number: 42000147

Supervised By

Dr Ashish Vyas (12386)

Department of Microbiology (Professor)

**School of Bioengineering & Biosciences, Lovely Professional University,
Punjab, India**



**LOVELY PROFESSIONAL UNIVERSITY, PUNJAB
2025**

DECLARATION

I hereby declared that the presented work in the thesis entitled “Identification of potential inhibitors against *E. coli* Mur enzymes through virtual screening and *in vitro* assay” in fulfilment of degree of **Doctor of Philosophy (Ph. D.)** is outcome of research work carried out by me under the supervision of Dr. Ashish Vyas, working as Professor & Head, in the Department of Microbiology/School of Bioengineering & Biosciences of Lovely Professional University, Punjab, India. In keeping with general practice of reporting scientific observations, due acknowledgements have been made whenever work described here has been based on findings of other investigator. This work has not been submitted in part or full to any other University or Institute for the award of any degree.

A handwritten signature in blue ink, appearing to read 'Vinita', is written over a light blue horizontal line.

(Signature of Scholar)

Name of the scholar: Vinita Gaur

Registration No.:42000147

Department/school: Department of Microbiology/ School of Bioengineering and Biosciences
Lovely Professional University,

Punjab, India

CERTIFICATE

This is to certify that the work reported in the Ph. D. thesis entitled “Identification of potential inhibitors against *E. coli* Mur enzymes through virtual screening and *in vitro* assay” submitted in fulfillment of the requirement for the award of degree of **Doctor of Philosophy (Ph.D.)** in the Department of Microbiology/School of Bioengineering & Biosciences, is a research work carried out by Vinita Gaur , 42000147, is bonafide record of his/her original work carried out under my supervision and that no part of thesis has been submitted for any other degree, diploma or equivalent course.

(Signature of Supervisor)

Name of supervisor: Dr. Ashish Vyas

Designation: Professor and Head

Department/school: Department of Microbiology/ School of Bioengineering and Biosciences

University: Lovely Professional University, Jalandhar-Delhi, G.T. Road (NH-1), Phagwara, Punjab (INDIA) -144411

Affectionately
Dedicated
To
My Beloved Parents

Abstract

Antibiotic-resistant bacteria are increasingly causing serious infections day by day, and their frequency is rising steadily. Overuse of antimicrobial agents has resulted in the emergence, recurrence, and spread of antibiotic resistance in commensal flora and targeted bacterial pathogens, making it one of the main drivers of the rapid spread of antimicrobial resistance. The active export systems present in bacterial membranes, the prevention of antibiotics penetrating pathogenic bacterial cells, the enzymatic degradation of antimicrobial agents, the development of thick biofilms, the alteration of antimicrobial targets, and the protection of some bacterial sites of action from antibiotics are a few examples of antimicrobial resistance mechanisms. In addition, multidrug-resistant bacteria have evolved systems that allow genetic determinants of resistance to be transferred from DNA to pathogenic species. The relatively limited number of antibacterial medications that are already available in the market necessitates the creation of novel medications that are targeted at carefully selected biological drug targets. Among the novel targets, the biosynthetic pathway involved in bacterial cell wall formation is a particularly appealing and remarkable source of antibacterial targets. In this regard, Mur enzymes are crucial for the synthesis of bacterial cell wall and present a prime candidate for the synthesis of inhibitors directed against microorganisms resistant to antibiotics.

Main purpose of the present study is the identification of possible inhibitors which may be developed as an appropriate, effective, and specific *Escherichia coli* MurD enzyme pathway inhibitor to boost therapeutic effectiveness and circumvent drug resistance by employing *in silico* and *in vitro* studies. Main objectives of the present study are identification of prospective compounds having ability to bind efficiently with the selected MurD enzyme (PDB ID 2UUP) of *Escherichia coli* by utilizing High Throughput virtual screening (HTVS), Standard precision (SP) screening and Extra-precision (docking-XP) docking of a large number of small compound libraries containing about 0.3 million compounds. Smaller libraries like FDA-approved Drug Library, Bioactive compound library, along with natural product libraries from this larger set of libraries that contain various diverse compounds in terms of structure, medically active compounds, as well as cell-permeable compounds that have been confirmed for their bioactivity, water-soluble and chemically stable compounds, and containing structural motifs that have been

substantiated by nature for better biological response were taken into consideration in an effort to increase the likelihood of finding a better biological agent to act as an inhibitor against the targeted enzyme. The lead molecules obtained after HTVS, and SP screening were further subjected to extra-precision docking calculations to find the best lead molecules using Glide module of Schrodinger software. After XP screening, top 20 virtual hits (marked from S1 to S20) were selected. The majority of virtual hits were interacting with the residues found within the catalytic area of the chosen target enzyme through hydrogen bonding, pi-cation and pi- pi stacking interactions, as determined by extra-precision docking studies. The stability of highest virtual hit (S1- WZB117) was further studied based on molecular dynamics studies for 100ns. The analysis of interactions over the course of the 100 ns trajectory revealed that the protein and residue Gly73 interacted through hydrogen bond interactions. The residues Glu164 as well as Tyr187 also interacted through a water bridge interaction with the protein (enzyme) molecule. Based on the S1-2UUP (protein molecule) complex's calculation of binding free energy by utilizing the MM-GBSA technique, van der Waals, hydrogen bonding, lipophilic, along with Coulomb energy components have been identified as favorable contributors to the ligand binding.

The final twenty lead molecules were also subjected to ADMET (Absorption, Distribution, Metabolism, Excretion and Toxicity) prediction studies using Qikprop module of Schrodinger software. One of the most crucial factors in determining how new medications affect or pose a risk to human health is their qualities relating to absorption, distribution, metabolism, excretion, and toxicity (ADMET). The early stages of drug development have relied heavily on the estimation of pharmacokinetic parameters to guide hit-to-lead optimization efforts. Most of the virtual hits displayed favourable ADMET properties like the n-octanol/water-octanol/water efficient (QPlogPo/w), QPlogKhsa (Prediction of binding to Human Serum Albumin), the anticipated blood brain barrier (QPlog BB), Caco-2 permeability, the percentage of oral absorption by humans, SASA (Solvent Accessible Surface Area), FOSA, FISA, PISA, and Phi (carbon and connected hydrogen) components of SASA fall within the permissible range as predicted in Qikprop manual of Schrodinger expect few properties which required structural modification of that particular compound.

The antibacterial efficacy of the two most effective virtual hits against Gram-positive and Gram-negative pathogens was examined. Further testing was done to assess the *in vitro* efficacy of the top two virtual hits versus *Escherichia coli* (ATCC 8739), *Pseudomonas aeruginosa* (ATCC 9027), and *Staphylococcus aureus* (ATCC 6538), and *Bacillus subtilis* (ATCC 6633) for assessment of their Minimum inhibitory concentration (MIC) against these organisms. The compound S1 (WZB117) demonstrated a MIC value of 40 µg /ml against *Escherichia coli* (ATCC 8739) and 50 µg/ml value when tested against *Pseudomonas aeruginosa* (ATCC 9027) respectively, showing a moderate inhibitory effect against the tested Gram-negative organisms. Against *Staphylococcus aureus* (ATCC 6538) the compound S1 demonstrated a MIC value of 30 µg /ml and against the Gram-positive *Bacillus subtilis* (ATCC 6633) of 20 µg /ml respectively, displaying remarkable activity against the tested organisms. The compound S2 (EPZ015666) was not found to be effective against the tested Gram-negative organisms of *Escherichia coli* (ATCC 8739) and *Pseudomonas aeruginosa* (ATCC 9027) at the highest tested level pertaining to 100 µg/ml. In contrast, compound S2 (EPZ015666) demonstrated moderate value of MIC of 50 µg/ml against *Staphylococcus aureus* (ATCC 6538) and a MIC value of 40 µg /ml against *Bacillus subtilis* (ATCC 6633).

The top two virtual hits were also tested for determination of The Minimum bactericidal concentration (MBC) against the *Escherichia coli* (ATCC 8739), *Pseudomonas aeruginosa* (ATCC 9027), *Staphylococcus aureus* (ATCC 6538), *Bacillus subtilis* (ATCC 6633) strains. In terms of MBC, compound S1 was found to be effective against *Escherichia coli* (ATCC 8739), *Pseudomonas aeruginosa* (ATCC 9027), *Staphylococcus aureus* (ATCC 6538) and *Bacillus subtilis* (ATCC 6633) at 50 µg/ml, 100 µg/ml, 30 µg/ml, and 20 µg/ml respectively. Compound S2 showed MBC of 50µg/ml against *Staphylococcus aureus* (ATCC 6538) and 40µg/ml against *Bacillus subtilis* (ATCC 6633), however it was ineffective against *Escherichia coli* (ATCC 8739) and *Pseudomonas aeruginosa* (ATCC 9027). Finally, the effect of the top two lead molecules on the morphology of various tested bacterial strains displayed cellular damage at their MIC concentration when studied using scanning electron microscopy (SEM).

So, compounds screened against the MurD enzyme can be further studied as starting points for *in vivo* studies to develop potential drugs.

Acknowledgment

First, I express thanks to the almighty God for enabling me to finish my research work effectively and calmly. My tenure at LPU was a magnificent and spectacular experience that will be very helpful to me in the future as I work to establish my own identity in the community. The driving force and source of motivation that helped me to finish my thesis in its current shape was everyone's unwavering support and inspiration. It seemed almost unbelievable to acknowledge the ongoing guidance, cooperation, love, care, and wisdom I received from my mentors. My sincere gratitude goes out to everyone that helped me, and I am extremely pleased with how content I feel right now.

It gives me great pleasure to convey my deep appreciation and sense of gratitude to my guide, **Prof. Dr. Ashish Vyas**, for his invaluable advice, unwavering support, and most importantly, for trusting in me. I am grateful to him for allowing me to work with him on this challenging issue and for his unwavering patience and kind support throughout. Throughout my thesis, he has served as a consistent source of inspiration. His diligence, genuineness, and excitement for research have really inspired me.

My deep gratitude to **Dr. Surojit Bera**, Assistant Professor, Department of Microbiology, Lovely Professional University, for his kind support, guidance, and invaluable advice in my difficult time. He exemplifies among best researcher for his passion in research. I also extend my sincere thanks to **Dr. Minhaj**, Associate Professor (HOL), Department of Biochemistry, Lovely Professional University, for providing the necessary laboratory consumables during my research work.

I am especially thankful to the faculty members, Central Instrumentation Facility (CIF) of Lovely Professional University (LPU) whose expertise and guidance have greatly influenced my approach to this research. Additionally, I appreciate the resources and facilities provided by the department, which enabled me to conduct my work effectively.

My overwhelming thanks go to **Mr. Ashok Mittal** (Chancellor), **Mrs. Rashmi Mittal** (Pro-Chancellor), and **Dr. Loviraj Gupta** (Pro Vice-Chancellor & Executive Dean) LPU for their

inspiration and assistance. I would also like to thank **Dr. Monika Gulati** (Registrar) for her co-operation and support.

I heartily acknowledge **Dr. Neeta Raj Sharma**, Senior Dean of the School of Bioengineering and Biosciences, for her excellent cooperation, support, and guidance during my research project. She also significantly expanded my knowledge and never ceased to inspire me. Her genuine assistance and unwavering support have my sincere gratitude.

I would like to convey my appreciation to Mr. John, Mr. Virender Singh, Mr. Sunny Gupta, and Mr. Kuldeep, for providing all the necessary laboratory amenities to me to conduct the experiments for my project.

My sincere gratitude to everyone I encountered while pursuing my doctorate for their kind companionship, discussions, assistance, and friendship. A special thanks goes out to my parents, who have always been there for me, believing in me and my abilities since I was a young child.

I wish to sincerely thank everyone for contributing to the wonderful experience that I've experienced during my research work.



(Vinita Gaur)

PREFACE

One of the primary challenges of the global healthcare system is the swift development of antibiotic resistance variants among bacteria because of the progressive and excessive consumption use of antibiotics. It has placed at risk the established methods for effectively preventing and treating a variety of diseases brought on by numerous infectious agents. So, there is a need for the development of newer drugs directed against novel targets (Mur enzymes) of bacterial pathogens. There is the presence of a larger variation in the requirement and furnishing of novel antimicrobial drugs with the innovative mode of action to circumvent the intricacy related to resistance against antimicrobials due to multiphase means of exploration and development of antibacterial medications. As drug resistance is a Global problem, the resistance to antibiotics has been identified by the World Health Organization (WHO) as among the most urgent issues facing humanity today. So, WHO has also emphasized the development of novel inhibitors at a faster rate to counter the problem of increasing drug resistance.

In the present study, a number of small chemical libraries containing about 3,00,000 compounds were selected and docked against *E. coli* MurD (PDB ID 2UUP) enzyme using high throughput virtual screening (HTVS), standard- precision (SP) screening, along with the Extra- precision (XP) screening using Glide module of Schrodinger software. Various interactions between the highest virtual hits and the amino acid residues placed within the catalytic pocket of the enzyme were analyzed. The ADMET (Absorption, Distribution, Metabolism, Excretion, and Toxicity) properties of the lead molecules were studied further. The top two lead molecules were further evaluated for their antibacterial efficacy against variety of bacterial species and their effect on bacterial morphology was also studied using SEM (Scanning Electron Microscopy). Thus, the current study will be helpful in the identification of novel prospective *E. coli* bacterial Mur D enzyme inhibitors that might be further explored by the pharmaceutical industry for use as possible medications.

Index:

- 1. Introduction**
- 2. Review of Literature**
- 3. Hypothesis**
- 4. Objectives**
- 5. Materials & methods**
- 6. Results & Discussion**
- 7. Conclusion & future remarks**

Bibliography

List of Publications

Appendix

Table of Contents

	Page No.
1. Introduction	23
1.1 New Challenges in targeting Mur Enzymes	30
2. Review Of Literature	35
2.1. Genetic properties and characteristics of MurD enzyme regulation	36
2.2. Functional characteristics & properties of Mur D enzyme	38
2.3 Structural Features of MurD Enzyme	41
2.4. Inhibitors of MurD Enzyme	43
3. Hypothesis	57
4. Objectives	59
5. Materials & methods	61
5.1. Retrieval of MurD enzyme structure and preparation for molecular docking	63
5.2 Preparation of Ligand Molecules & Grid Generation	64
5.3 Maestro (molecular modelling environment) molecular docking; GLIDE (Grid based ligand docking with energetics)	65
5.4. GLIDE-HTVS (High-throughput virtual screening)	65
5.5. GLIDE- Standard Precision (SP) Docking	67
5.6. GLIDE Extra precision (XP)	67
5.7. Molecular Dynamics simulation studies	68
5.8. Binding Free Energy Calculation studies	70
5.9. Absorption, Distribution, Metabolism, Excretion and Toxicity (ADMET) studies	71
5.10. <i>in vitro</i> validation of lead compounds	72
5.10 (a). Antibacterial Activity Assay	72
5.10 (b). Determination of Minimum Inhibitory Concentration (MIC)	73
5.10 (c). Calculation of Minimum Bactericidal Concentration (MBC)	74
5.10 (d). To Study the Effect of Lead Compounds on Bacterial Cell Morphology	74

6. Results & Discussion	76
6.1 Identification of potential lead molecules by molecular docking : HTVS, SP & XP Screening of compound libraries	77
6.2. Molecular dynamics simulation studies	124
6.3. Binding Free Energy Calculation studies	128
6.4. Prediction of ADMET properties of potential lead molecules	132
6.5 Determination of Antibacterial Activity	143
6.6 Determination of Minimum Inhibitory Concentration (MIC)	148
6.7: Determination of Minimum Bactericidal Concentration (MBC)	157
6.8 To Study the Effect of Lead Compounds on Bacterial Cell Morphology	158
7. Conclusion & Future Remarks	161
Bibliography	165
Publications	176
Appendix	181

List of Tables

Table 2.1: Comparative effectiveness of Mur D enzymes from different bacterial strains

Table 2.2: Various substituent groups that are linked to Phenoxyacetohydrazide ring to constitute structures from 4a-4k

Table 5.1: Selected enzyme target with respective PDB identification for X-ray crystal structure

Table 6.1: Lead molecules obtained after HTVS screening of various libraries

Table 6.2: Lead molecules obtained after SP (Standard-Precision) screening

Table 6.3 :Lead molecules obtained after XP screening studies

Table 6.4: Extra- precision docking scores of top 20 virtual hits against MurD (2UUP) enzyme target

Table 6.5: Binding free energy (ΔG Bind in kcal/mol) values in the WZB117-2UUP complex based on post-simulation MM-GBSA

Table 6.6: Binding energy calculation of the virtual hit S1-2UUP complex and non-bonded interaction energies from MM-GBSA trajectories.

Table 6.7: Predicted ADMET parameters of top 20 virtual hits

Table 6.8: Evaluated ADMET parameters of the lead molecules by Qikprop

Table 6.9: Predicted Lipinski parameters of top 20 lead molecules

Table 6.10: Chemical structures of various lead molecules against MurD

Table 6.11: Antibacterial studies of compounds S1 & S2 against *Escherichia coli* (ATCC 8739)

Table 6.12: Antibacterial studies of compounds S1 & S2 against *Pseudomonas aeruginosa* (ATCC 9027)

Table 6.13: Antibacterial studies of compounds S1 & S2 against *Staphylococcus aureus* (ATCC 6538)

Table.6.14 : Antibacterial studies of compounds S1 & S2 against *Bacillus subtilis* (ATCC 6633)

Table 6.15: MIC determination of compound S1 against *Escherichia coli* (ATCC 8739)

Table 6.16: MIC determination of compound S1 against *Pseudomonas aeruginosa* (ATCC 9027)

Table 6.17: MIC determination of compound S1 against *Staphylococcus aureus* (ATCC 6538)

Table 6.18: MIC determination of compound S1 against *Bacillus subtilis* (ATCC 6633)

Table 6.19: MIC determination of compound S2 against *Escherichia coli* (ATCC 8739)

Table 6.20: MIC determination of compound S2 against *Pseudomonas aeruginosa* (ATCC 9027)

Table 6.21: MIC determination of compound S2 against *Staphylococcus aureus* (ATCC 6538)

Table 6.22: MIC determination value of compound S2 against *Bacillus subtilis* (ATCC 6633)

Table 6.23: MIC values against tested bacterial strains

Table 6.24: MBC values against tested bacterial strains

List of Figures

Figure 1.1: Cytoplasmic steps of Peptidoglycan synthesis

Figure 1.2: Mechanism of Action of Mur D enzyme

Figure 2.1: Basic chemical structure of a sulphonamide inhibitor

Figure 2.2 A: Chemical structure of 2-oxoindolinylidene based inhibitor

Figure 2.2 B: Chemical structure of 2- Thioxothiazolidin-4-one ring

Figure 2.3: Chemical structures of D1, D2, D3, and D4 compounds, which were developed by altering the 2-thioxothiazolidin-4-one ring

Figure 2.4: Chemical structure of inhibitor H5

Figure 2.5 A: Chemical formula of ATP-dependent kinase (aza-stilbene derivative) inhibitor

Figure 2.5 B: Chemical formulae of compounds ZINC19221101 & ZINC12454357

Figure 2.6: Chemical formula of Parent phenoxyacetohydrazide structure

Figure 2.7: Chemical formulae of Aza-stilbene derivatives marked as compound 30 and 31

Figure 2.8: Chemical structure of compound ChEMBL426262

Figure 5.1: Flow chart of Methodology

Figure 5.2: Parameters used for GLIDE-HTVS/XP molecular docking

Figure 6.1a: Ligand interaction diagram of virtual hit S1 (WZB117) with MurD (2UUP)

Figure 6.1b: Ribbon presentation diagram of MurD (2UUP)-S1 (WZB117) complex

Figure 6.2a: Ligand interaction diagram of virtual hit S2 (EPZ015666) with MurD (2UUP)

Figure 6.2b: Ribbon presentation of the MurD (2UUP)-S2 (EPZ015666) complex

Figure 6.3a: Ligand interaction diagram of compound S3 (SCH727965) with MurD (2UUP)

Figure 6.3b: Ribbon presentation of MurD (2UUP) –S3 (SCH727965) complex

Figure 6.4a: Ligand interaction diagram of compound S4 (Phloretin) with MurD (2UUP);

Figure 6.4b: Ribbon presentation of MurD (2UUP) –S4 (Phloretin) complex

Figure 6.5a: Ligand interaction diagram of compound S5 (S9428 Brazilin) with MurD (2UUP)

Figure 6.5b: Ribbon presentation of MurD (2UUP) –S5 (S9428 Brazilin) complex

Figure 6.6a: Ligand interaction diagram of compound S6 (CRT0066101) with MurD (2UUP)

Figure 6.6b: Ribbon presentation of MurD (2UUP) –S6 (CRT0066101) complex

Figure 6.7a: Ligand interaction diagram of compound S7 (EPI-001) with MurD (2UUP)

Figure 6.7b: Ribbon presentation of MurD (2UUP) –S7 (EPI-001) complex

Figure 6.8a: Ligand interaction diagram of compound S8 (TWS119) with MurD (2UUP)

Figure 6.8b: Ribbon presentation of MurD (2UUP) –S8 (TWS119) complex

Figure 6.9a: Ligand interaction diagram of compound S9 (UM171) with MurD (2UUP)

Figure 6.9b: Ribbon presentation of MurD (2UUP) –S9 (UM171) complex

Figure 6.10a: Ligand interaction diagram of compound S10 (CP868569) with MurD (2UUP);

Figure 6.10b: Ribbon presentation of MurD (2UUP) –S10 (CP868569) complex

Figure 6.11a: Ligand interaction diagram of compound S11 (TAK-659) with MurD (2UUP);

Figure 6.11b: Ribbon presentation of MurD (2UUP) –S11 (TAK-659) complex

Figure 6.12a: Ligand interaction diagram of compound S12 (AZD7762) with MurD (2UUP) ;

Figure 6.12b: Ribbon presentation of MurD (2UUP) –S12 (AZD7762) complex

Figure 6.13a: Ligand interaction diagram of compound S13 (S9395 N-Benzoyl-(2R,3S)-3-phenylisoserine) with MurD (2UUP);

Figure 6.13b: Ribbon presentation of MurD (2UUP) –S13 (S9395 N-Benzoyl-(2R,3S)-3-phenylisoserine) complex

Figure 6.14a: Ligand interaction diagram of compound S14 (S9395 N-Benzoyl-(2R,3S)-3-phenylisoserine) with MurD (2UUP);

Figure 6.14b: Ribbon presentation of MurD (2UUP) –S14 (S9395 N-Benzoyl-(2R,3S)-3-phenylisoserine) complex

Figure 6.15a: Ligand interaction diagram of compound S15 (631305) with MurD (2UUP)

Figure 6.15b: Ribbon presentation of MurD (2UUP) –S15 (631305) complex

Figure 6.16a: Ligand interaction diagram of compound S16 (333718) with MurD (2UUP)

Figure 6.16b: Ribbon presentation of MurD (2UUP) –S16 (333718) complex

Figure 6.17a: Ligand interaction diagram of compound S17 (S4722) with MurD (2UUP)

Figure 6.17b: Ribbon presentation of MurD (2UUP) –S17 (S4722) complex

Figure 6.18a: Ligand interaction diagram of compound S18 (CNX-774) with MurD (2UUP)

Figure 6.18b: Ribbon presentation of MurD (2UUP) –S18 (CNX-774) complex

Figure 6.19a: Ligand interaction diagram of compound S19 (KENACORT (triamcinolone) with MurD (2UUP)

Figure 6.19b: Ribbon presentation of MurD (2UUP) –S19 (KENACORT (triamcinolone) complex

Figure 6.20a: Ligand interaction diagram of compound S20 (Floxuridine) with MurD (2UUP)

Figure 6.20b: Ribbon presentation of MurD (2UUP) –S20 (Floxuridine) complex

Figure 6.21: Time-dependent root mean square deviation (RMSD) of the WZB117 (S1)-Mur D complex during 100 ns of MD simulation

Figure 6.22: Individual amino acids' Root mean square fluctuation (RMSF) plot of WZB117 (S1)-MurD complex

Figure 6.23a: Binding interactions of ligand (WZB117) (S1) with Mur D (2UUP) during MD Simulation of 100 ns

Figure 6.23b: Interaction fraction of various residues (WZB117 (S1)-MurD (2UUP) Complex)

Fig 6.24: Top two virtual lead molecules

Figure 6.25a: Antibacterial studies of compound S1 against *Escherichia coli* (ATCC 8739)

Figure 6.25b: Antibacterial studies of compound S2 against *Escherichia coli* (ATCC 8739)

Figure 6.26a: Antibacterial studies of compound S1 against *Pseudomonas aeruginosa* (ATCC 9027)

Figure 6.26b: Antibacterial studies of compound S2 against *Pseudomonas aeruginosa* (ATCC 9027)

Figure 6.27a : Antibacterial studies of compound S1 against *Staphylococcus aureus* (ATCC 6538)

Figure 6.27b: Antibacterial studies of compound S2 against *Staphylococcus aureus* (ATCC 6538)

Figure 6.28a : Antibacterial studies of compound S1 against *Bacillus subtilis* (ATCC 6633)

Figure 6.28b: Antibacterial studies of compound S2 against *Bacillus subtilis* (ATCC 6633)

Figure 6.29: Concentration (compound S1) vs inhibition % chart against *Escherichia coli* (ATCC 8739)

Figure 6.30: Concentration (compound S1) vs inhibition % chart against *Pseudomonas aeruginosa* (ATCC 9027)

Figure 6.31: Concentration (compound S1) vs inhibition % chart against *Staphylococcus aureus* (ATCC 6538)

Figure 6.32: Concentration (compound S1) vs inhibition % chart against *Bacillus subtilis* (ATCC 6633)

Figure 6.33: Concentration (compound S2) vs inhibition % chart against *Staphylococcus aureus* (ATCC 6538)

Figure 6.34: Concentration (compound S2) vs inhibition % chart against *Bacillus subtilis* (ATCC 6633)

Figure 6.35a: SEM image of untreated *Escherichia coli* (ATCC 8739)

Figure 6.35b: SEM image of Compound S1 treated *Escherichia coli* (ATCC 8739)

Figure 6.35c: SEM image of untreated *Pseudomonas aeruginosa* (ATCC 9027)

Figure 6.35d: SEM image of Compound S1 treated *Pseudomonas aeruginosa* (ATCC 9027)

Figure 6.35e: SEM image of untreated *Staphylococcus aureus* (ATCC 6538)

Figure 6.35f: SEM image of Compound S1 treated *Staphylococcus aureus* (ATCC 6538)

Figure 6.35 g: SEM image of untreated *Bacillus subtilis* (ATCC 6633)

Figure 6.35 h: SEM image of Compound S1 treated *Bacillus subtilis* (ATCC 6633)

Figure 6.35 i: SEM image of untreated *Staphylococcus aureus* (ATCC 6538)

Figure 6.35j: SEM image of Compound S2 treated *Staphylococcus aureus* (ATCC 6538)

Figure 6.35 k: SEM image of untreated *Bacillus subtilis* (ATCC 6633)

Figure 6.35 l: SEM image of Compound S2 treated *Bacillus subtilis* (ATCC 6633)

List of Appendix

Muller Hinton Agar

Muller Hinton Broth

Nutrient Broth Medium

Tryptic Soya Broth

Phosphate Buffered saline

Abbreviations:

PG: Peptidoglycan

UDP-GlcNAc: UDP-N-acetylglucosamine

UDP-MurNAc : UDP- N-acetylmuramic acid

UDP-Mpp: UDP-N-acetylmuramyl-pentapeptide

PEP: Phosphoenolpyruvate

UNAG: UDP- N-acetylglucosamine

UMA: UDP N-acetylmuramoyl-l-alanine

HTS: High Throughput Screening

GLIDE : Grid based ligand docking with energetics

GLIDE HTVS: GLIDE High Throughput Virtual Screening

GLIDE XP : GLIDE Extra precision

ADMET : Absorption, Distribution, Metabolism, Excretion and Toxicity

MIC: Minimum Inhibitory Concentration

CADD: Computer Aided Drug Design

Chapter 1

Introduction

Introduction:

One of the most significant efforts of the 20th century that has significantly improved the quality of human existence has been the discovery and advancement of newer antibiotics against diverse bacterial illnesses. In order to combat different Gram-positive and Gram-negative infections, new antibiotics have been developed. However, this enormous achievement has come at a cost, so the pharmaceutical industry is producing fewer new medications at the same time that more and more bacterial pathogens are reported to be becoming resistant to the most clinically effective antibiotics. This is partially because creating medications has less opportunities for profitability because it costs a lot of money and resources to conduct clinical studies before an antibiotic is developed (Naclerio & Sintim, 2020). Incidences of resistance are being reported against most of the currently useful antibiotics like tetracyclines, aminoglycosides, macrolides, quinolones, β -lactams as well as polymyxin which is considered as the final category of drugs (Kahler et al., 2018). One of the most crucial public health problems across the world is the dreadful increase and dissemination of resistance mechanisms among bacterial pathogens against the most clinically useful antibiotics which are further complexing the treatment of various infectious diseases leading to great human distress, mortality, and an increase in health care costs at alarming levels. Because of the very limited number of effective antibacterial drugs available, there is a requirement for the design and development of newer drugs directed against judiciously selected targets. One of the best and most notable sources of antibacterial targets is the metabolic pathway of cell wall formation in bacteria (Kouidmi et al., 2014; Gaur et al., 2023).

Among the main components of the bacterial cell wall, that is commonly referred to as peptidoglycan (PG) or murein and it maintains the cell stable and in its correct structural state. The cytoplasm, periplasm, along with membrane are the three cellular compartments where synthesis of peptidoglycan is accomplished by sequential action of various enzymes (Miyachiro et al., 2019). The Mur enzymes associated with the biosynthesis of cell walls are distinct targets for antibacterial agents. Peptidoglycan (murein) is a polymer of polysaccharides composed of alternating units of n-acetylglucosamine (GlcNAc) and N-acetylmuramic acid (MurNAc) to which a pentapeptide is joined. Nucleotide precursors are generated in the cell's cytoplasm, wherein PG synthesis commences.

These nucleotide precursors include UDP-GlcNAc which is produced from fructose-6-phosphate, the process brought about by the Glm (N-acetylglucosamine-1-phosphate transferase) enzymes (Belete, 2019) .

The bacterial cell wall (PG) biosynthesis is an intricate mechanism that occurs in two stages. The first stage is carried out within the cytoplasm that leads to the generation of single units of N-acetylglucosamine-N-acetylmuramyl pentapeptide. The Mur A enzyme catalyzes this step, which entails moving an enol pyruvate residue from phosphoenolpyruvate (PEP) to UDP-N-acetylglucosamine's third position. The enolpyruvate moiety is reduced to D-lactate in the second step, generating UDP-N-acetylmuramate. This reaction is catalyzed by Mur B enzyme. A series of ATP-dependent amino acid ligases adds new pentapeptide side chains to a substantially reduced D-lactyl group leading to creation of UDP-N- acetylmuramyl pentapeptide (El Zoeiby et al., 2003) (Fig.1.1). Role played by the Mur C enzyme is the catalysis of transferal of 1 alanine to UDP-MurNAc nucleotide precursor. MurD enzyme functions by catalyzing the addition of α glutamic acid to UDP-MurNAc- α -Ala. This reaction is ATP dependent process and involves the formation of acyl- phosphate and tetrahedral intermediate (Šink et al., 2013) . The structure of Mur enzymes in bacteria is highly conserved like most of the other enzymes associated with peptidoglycan synthesis and there are no homologs in humans (Nikolaidis et al., 2014). Mur ligases (Mur C to Mur F) are ATP dependent enzymes whose structure and function have been well characterized. Further they share common active sites, so are the potential targets for inhibitors with multitargets (Smith, 2006). The widespread presence of the Mur pathway in bacteria and associated Mur enzymes have been recognized as prospective targets for antibiotics. Nevertheless, the screening and creation of pharmacological inhibitors for the Mur enzymes proved ineffective, and very few commercial chemotherapy drugs were created by specifically targeting the Mur enzyme (Sheng et al., 2014).

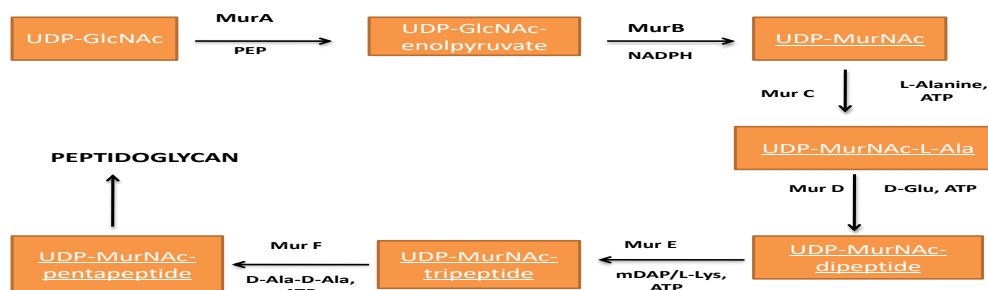


Figure 1.1 Cytoplasmic steps during Peptidoglycan synthesis

Mur ligases (Mur C, D, E, and F) are among the most intriguing groups of targets that can be used in the search for novel medications. Numerous investigations on Mur ligases have been conducted over the past ten years, leading to the identification of a distinct and varied class of inhibitors. Every Mur ligase shares a shared kinetic mechanism and a consistent means of activity (Hrast et al., 2019). Each Mur ligase also contain a significantly preserved region for ATP binding which contain amino acids that vary by 22-26%. Mur ligases also share a P-loop with a high plentitude of glycine amino acid residues and a variety of other residues, including glutamic acid as well as histidine, which take part in maintaining proper functioning of Mg^{2+} ions (El Zoeiby et al., 2003). Notwithstanding likenesses, the configurational framework and residue arrangement in the MurD catalytic site vary amongst various bacterial species, including *Mycobacterium tuberculosis*, *Borrelia burgdorferi*, *Escherichia coli* along with *Staphylococcus aureus* (M. A. Azam & Jupudi, 2020). There is a comparable domain topology in the crystal structures of ATP dependent Mur ligases from various bacteria, whereas the condensing amino acid or dipeptide residue is bound by the C-terminal domain, the N-terminal and central domains bind the UDP precursor and ATP, respectively (Chakkyarath & Natarajan, 2019). The N-terminal domains, on the other hand, show variations, with Mur C and Mur D showing a higher degree of similarity when compared with Mur E and Mur F. There is a correlation between these variations and the UDP precursor substrate lengths. The Mur ligases' ATP binding site is a highly conserved area, with sequence identities varying from 22% to 26% (Hrast et al., 2019). Many researchers have studied compounds, including phosphinates, phosphates, and N-

acetylmuramic acid analogs, as inhibitors of the *Escherichia coli* MurD enzyme. But these substances didn't provide encouraging findings (Gegnás et al., 1998; Gobec et al., 2001; Štrancar et al., 2006).

The stem of five amino acids of N-acetylmuramic acid which is synthesized in the course of biosynthesis of cell wall of bacteria, is added by the crucial activity of the MurD enzyme and other Mur ligases. The MurD enzyme's structure and mode of action has been well-studied (Zdouc et al., 2018). The attachment of the D-glutamic acid with UDP-MurNAc-l-Ala (UMA), generates tetrahedral intermediate and acyl-phosphate, is catalyzed by the activity of MurD enzyme. MurD enzyme presents as a prime candidate for the development of new inhibitors since it is very selective for its substrate amino acid residue D-glutamic acid and lacks a homologue within the mammalian cells (Perdih et al., 2014). As an ATP-dependent cytoplasmic Mur ligases, MurD holds about 46,973 Daltons of molecular weight (M. A. Azam & Jupudi, 2020). Enzyme Mur D adds a (d-Glu) amino acid residue to UMA, its substrate. As a result, creation of a single peptide bond takes place, uniting the -COOH group of UDP-N-acetylmuramyl-L-alanine together with the amino residue of D-glutamic acid. An ATP molecule is used in the reaction, which also produces an Adenosine diphosphate (ADP) and releases the orthophosphate group (Fig. 1.2) (Walsh et al., 1999). It is crucial to note that the residues of amino acid located at location of two or three of the mature peptidoglycan's pentapeptide stem may occasionally vary about the various substrate amino acid of the Mur D or Mur E enzyme. For example, in some species' peptidoglycan, d-isoglutamine (d-iGln) or threo-hydroxy-3-glutamic acid are located at location two in place of d-Glutamic acid (Schleifer & Kandler, 1972; Vollmer et al., 2008). The modifications (like amidation, hydroxylation, etc.) that follow the mechanism of ATP-dependent Mur ligases, usually occur at the stage of lipid II synthesis, are the source of these residues. Regarding position 2, in every bacterial species that have been studied thus far, D-Glu serves as MurD's amino acid substrate (Patin et al., 2010). Topologically, Mur ligases are all identical to one another. They consist of two hinges joining three domains together. Among the three substrates-ATP, incoming nucleotides, as well as the amino acid is bound by each domain. The enzymes have a great deal of flexibility. It has been hypothesized

that the central domain only forms the active conformation following combining ATP (Bratkovič et al., 2008).

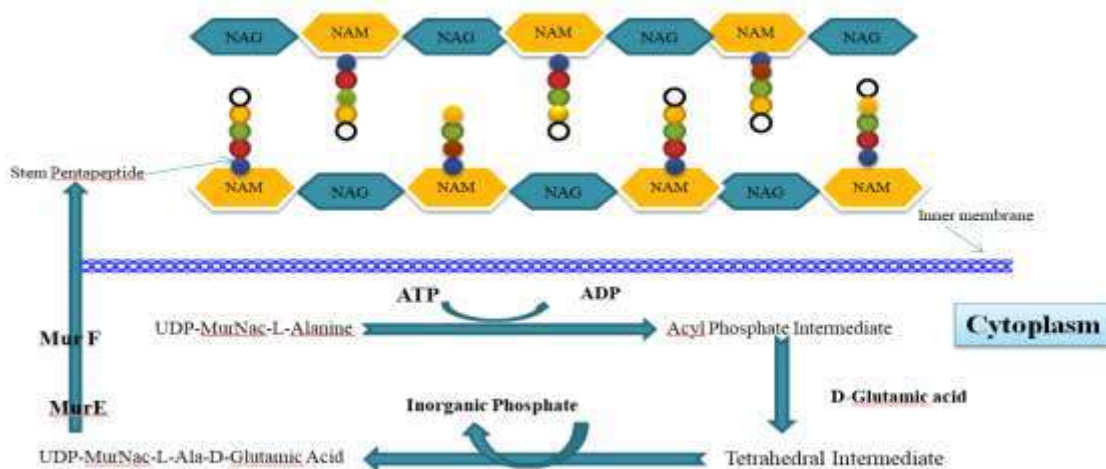


Figure 1.2: Mechanism of Action of Mur D enzyme

There is the presence of a larger variation in the requirement and furnishing of new antimicrobial medications with the innovative mode of action to circumvent the intricacy of resistance mechanism developed among various bacterial species due to multiphase means of exploration and scientific advancement of antibacterial novel compounds. Numerous factors affect the advancement of newer therapeutic agents like unpredictable results against infection with currently available drugs, diversified models of antibiotic usage, confirmation of consequent infections, rigorous approval by various regulatory companies, reduced yield of the concerned industry, several steps involved in clinical trials and limitation of various agencies that regulate the over pricing of drugs (N Sangshetti et al., 2017).

In order to find novel medications, high-throughput screening (HTS) enables the filtering of a large number of biological and chemical substances using automated procedures. Pharmaceutical industries particularly use computerized and robotic processes for the accelerated trial of a large number of potential therapeutic agents for the investigation of targets. HTS primarily aims at identifying new compounds known as "Leads" or "Hits" through screening of compound

libraries that may interact with the selected target in a sought-after design. HTS screening serves as the starting point for the number of steps associated with the development of new drugs and to conjecture the mechanism of various biochemical processes. There are several limitations associated with HTS like its inability to predict the bioavailability of the potential drugs. Despite that, it presents a highly useful technique for the speedy screening of various biological processes to exclude compounds with weak or no result, from the early stages of the investigation. The importance becomes even more pronounced in the era of rising incidences of antibiotic resistance among microbes which necessitates the rapid discovery of novel drugs with newer mechanisms of action ([https:// www.bmglabtech.com](https://www.bmglabtech.com)).

The application of computer-based methods coupled with various laboratory methods plays a very critical role in the investigation of newer drugs and both present as parallel pathways to be conducted side by side. In the current scenario of the rapid development of drug resistance among microbes which is further compounded by high resource devouring and complicated process of recognition and advancement of newer drugs, the use of computer-based methods has emerged as a widely accepted tool with more comprehensive execution and significance among the scientific community. Regularly practiced computer based methods incorporate ligand-based methods of drug designing (pharmacophore), quantitative structure-activity, structure-based drug designing method, and structure-property correlations. Several steps are being aided by the use of computer-based or *in silico* processes like accelerated identification of hits, hit to lead assortment, optimization of processes like absorption, distribution, metabolism, excretion and toxicity (ADMET), and circumventing concerns related to safety. Molecular docking encompasses three primary and crucial objectives; display estimation, virtual screening, and assessment of affinity for binding. Nowadays there exists an accelerated extension of CADD with the elevation of new computation based softwares (like AutoDock, DOCK, FlexX/E, Surflex, GOLD, and Maestro), recognition of new biological targets, and a broadened database of the openly available crystal structures of various target proteins in the biological system. In this context, *in silico* modeling presents a critical tool to reduce the extensive use of resources and to speed up the drug discovery process in a limited period (Kapetanovic, 2008).

1.1 New challenges in targeting Mur Enzymes

The crucial step involving the movement of enolpyruvate moiety coming from phosphoenolpyruvate (PEP) to uridine diphosphate N- acetylglucosamine (UDP-GlcNAc) is catalyzed by the important bacterial enzyme known as UDP-N-acetylglucosamine enolpyruvyl transferase (MurA). The production of the peptidoglycan layer begins with this committed step. Since MurA's catalytic mechanism is well understood, it is conserved in bacteria and lacks a human counterpart, making it a useful target for the development of antibacterial drugs (Jukič et al., 2019). Furthermore, it is a verified target that has a clinically used inhibitor, fosfomycin. The sole antibiotic that targets MurA at the moment is the antibiotic fosfomycin, which binds by a covalent bond to the Cys115 residue present within the MurA active site. This prevents UDP-GlcNAc-enolpyruvate from being released, which ultimately results in disruption of biosynthesis of peptidoglycan layer leading to cell death (Silver, 2017). An analogue of PEP, fosfomycin interacts with MurA in a specific way despite having an electrophilic epoxide moiety (Eschenburg et al., 2005). Fosfomycin is the antibiotic produced by species of *Pseudomonas* & *Streptomyces* that is currently used against MurA as the target (Hendlin et al., 1969). It is a phosphoenolpyruvate (PEP) analogue. Its mode of action involves alkylation of highly conserved cysteine residues on the Mur A enzyme, which is further promoted by attachment of the UDP-GlcNAc with open stage of enzyme molecule. This results in accumulation of large number of peptidoglycan precursors by hindering the catalysis process (Bensen et al., 2012). Despite this, microbes have a well-documented resistance to fosfomycin, which involves a number of mechanisms, including decreased antibiotic uptake, target modification, expression of enzymes involved in antibiotic degradation, and rescue of the UDP-MurNAc biosynthesis pathway. Various resistance species like *Mycobacterium tuberculosis*, *Borrelia burgdorferi* have a Cys-Asp mutation in their Mur A homologs thereby blocks the alkylation step induced by the antibiotic (De Smet et al., 1999). The superfamily comprising enzymes that bind flavin adenine dinucleotide (FAD) includes UDP-N-acetylenolpyruvylglucosamine reductase (MurB), has a FAD molecule as a cofactor. The enzyme takes part in the catalysis leading to reduction of the UDP-N-acetylglucosamine enolpyruvate's enolpyruvyl moiety, which was generated by the MurA enzyme in the preceding

step. In a comparable way, it is a universal enzyme that is conserved throughout bacterial genera and is lacking a homologue in eukaryotes (Benson et al., 1993; Chen et al., 2013) .

The understanding of reaction mechanism has displayed that the preserved residues of enzymes' active sites, alongwith various configurational similarities present a significant opportunity for the simultaneous targeting of all four Mur ligases by numerous inhibitors. One benefit of multiple inhibition by a single agent would be that it would be less vulnerable to high-degree of target-based resistance caused by alterations in a single bacterial gene (Chopra, 2013).

Selleckchem library contains a combination of smaller libraries like the Bioactive compound library, Preclinical/Clinical compound library, FDA-approved drugs library, Natural product library, etc. Selleckchem library contains about 1,20,000 inhibitors to be used for various cell signaling pathways. It also contains about 8000 small molecules with authenticated biological and pharmacological activities. A distinct collection of 3067 approved medications and Active Pharmaceutical Ingredients (API) in pharmacopeia for HTS as well as high content screening (HCS) may be found in Selleckchem's FDA-licensed drug library. Sallelckchem's library containing bioactive compounds has a distinct set of 9127 bioactive substances suitable for high content as well as high throughput screening (HTS and HCS). The majority of these compounds, APIs, natural products, and chemotherapeutic agents are among the compounds that have received FDA approval. These substances are cell permeable, medicinally active, and structurally varied. There is thorough documentation that is organized and includes client testimonials.

These are further validated through NMR and HPLC to ensures enhanced purity. A unique set of 3371 clinical and preclinical substances for high content and high throughput screening (HTS and HCS) is also available in Sallelckchem's chemical library. These compounds are beneficial for drug repurposing, to be use of existing medications to treat new disease indications. Sallelckchem's compound library also contains distinct assortment of 1570 anti-infection substances possessing biological characteristics including antibacterial, antifungal, antiviral etc. It also contains an exclusive set of 836 endogenous human metabolites for use in high content and high throughput screening (HCS) (<https://www.selleckchem.com>). Life Chemical's compound Library containing Bioactive constituents contains about 9,900 drug-like small molecules used for HTS (High throughput screening) against several biological targets like

enzymes, receptor ligands, and ion channel regulators, etc. Its building block library contains small molecules having reactive functional groups that allow the introduction of specific structural motifs into the target molecules (<https://lifechemicals.com>). The Enamine library contains a collection of more than four million compounds for the identification of new hit compounds. Newer compounds have been added to this library through the advancement of newer synthetic approaches providing a large collection of small molecules for drug discovery against several biological targets. The Discovery diversity set of the enamine library contains 10,240 high-quality latest compounds for random screening against new and already established targets because of the high diversity of scaffolds. The essential Fragment library of Enamine contains 320 fragment compounds that have been tested for their water solubility and chemical stability to make them suitable for authentication of newer targets. The natural product-like fragment library contains 4160 structural motifs substantiated by nature for better biological response (<https://enamine.net/compound-libraries>).

ASINEX has developed a unique chemical library for use in antibacterial studies based on its own natural product-like scaffolds, which provide a high degree of structural diversity along with the presence of various polar functional groups and stereogenic centers. A library of small molecule compounds built on an "iminosugar" scaffold has been produced by ASINEX. The chosen compounds fit into a highly particular physicochemical niche among recognized Gram-negative antibiotics (<https://www.asinex.com/antibacterial>). Chem Div library contains a collection of low molecular weight organic compounds which is revised every quarter to reflect new developments in the fields of molecular and cell biology, the availability of novel ligands, general trends in disease areas, and contemporary definitions of lead-like qualities. Chem Div's antibacterial library is a unique set of fifteen thousand chemicals. RNA polymerase enzyme, DNA polymerase III enzyme, peptide deformylase enzyme, cell division protein FtsZ, tRNA ligase, penicillin binding protein, and other proteins are included in the reference target space. The Antiparasite Library at ChemDiv has 25,376 extremely unique and varied chemicals. Chemicals with antibacterial, antifungal, and insecticidal properties make up the collection. These are novel compounds that make claims about their ability to be insecticidal, antifungal,

and antibacterial. Additionally, 2-D topological counterparts for CADD are included in this package (<https://www.chemdiv.com>).

Among the largest collections of synthetic as well as natural compounds in the world is found in the Interbioscreen (IBS) library. Over 4,60,000 synthetic substances (mainly functionalized complex heterocycles) and over 68,000 natural compounds, as well as their derivatives and analogs, are contained in the complete library. The compounds present in the IBS library constitute 30-35% of which are natural compounds that are isolated from various plants, microbes, marine species, etc. About, 40% of these compounds are derivatives that are modified forms derived from various natural compounds like modified forms of alkaloids, terpenoids along with flavonoids. Besides these, the rest 25–30% belong to the category of natural compound mimics, or analogs, such as oxaterpenoids, conjugated isoindole systems, azosteroids, and azocoumarins (<https://www.ibscreen.com>).

Mur enzymes are highly sought after and studied for the development of newer inhibitors. Because bacterial pathogens are developing resistance at a swift rate, there is an urgent need for efficacious therapeutic targets against a very trivial number of antibacterial agents that are currently available. As enzymes catalyzing the various steps of peptidoglycan synthesis are among most suitable targets for newer drug development. Among these, the enzymes taking part in the catalysis of cytoplasmic stages of peptidoglycan synthesis, the MurD enzyme carrying out the second step of peptide stem addition is widely studied because of its indispensable role among bacterial pathogens. Till now a lot of new agents have been studied as potential inhibitors of MurD enzyme with promising initial results but little success is achieved towards the overall development of newer antimicrobial agent. This could be explained by the inhibitors' inability to cross the semi-permeable barrier. Therefore, to get beyond the cell membrane permeability barriers, efforts must be made to develop new inhibitors as well as there is a requirement for structural and chemical alterations to the inhibitors that are already in use. Nowadays, *in silico* or structure-based methods for drug designing is particularly helpful for the rapid development of alternative inhibitors that may impede the reaction of the MurD enzyme catalyzed function.

Using High-throughput screening technique to find novel drugs is not a novel concept; nevertheless, it remains a highly useful technique with regard to the discovery of newer drugs in the era of rising incidences of antibiotic resistance among microbes (<https://www.bmglabtech.com>). The present work aims at a high-throughput screening of numerous natural and synthetic compounds from various commercial libraries to find *Escherichia coli* MurD enzyme inhibitor(s), which may ultimately be used to substitute or expand the scope and use of various therapeutic agents currently available in the clinical domain as inhibitors of the MurD enzyme. The overall goal of this work is to identify the promising compound (s) that could efficiently bind with *E. coli* MurD enzyme and to validate the inhibitor(s) through *in vitro* assay. Within this framework, this study's main objective is to determine putative inhibitors that might be utilized in conjunction with *in silico* investigations as appropriate, strong, and targeted inhibitors of the *Escherichia coli* Mur D enzyme pathway in order to overcome drug resistance and enhance therapeutic efficacy.

Chapter 2

Review of Literature

Review Of Literature :

The stages involved in the biosynthesis of peptidoglycan precursors that take place in bacterial cytoplasm are imperfectly accomplished as targets for antimicrobial agents. Most of the clinical drugs used in the present scenario like β -lactams, vancomycin, and glycopeptides largely aim at target cell wall synthesis steps occurring at succeeding stages of PG synthesis (Tomašić et al., 2010). Excluding MurA enzyme, which is a target for the drug fosfomycin, neither of these enzymes taking part during the cytoplasmic stages of cell wall synthesis is hindered by known antibiotics or chemicals (El Zoeiby et al., 2003). In addition to this, among most bacterial species Mur proteins are profoundly conserved and have common structural motifs (Kouidmi et al., 2014). Furthermore, the need for the generation of newer multitargeted inhibitors assumed to have a bactericidal result with a broad spectrum has arisen because of the fast spread of microorganisms resistant to antibiotics. In this context, Mur enzymes present potential targets of choice for the advancement of new inhibitors which may ultimately be used to replace or extend the use of currently available drugs in clinical settings.

2.1 Genetic properties and characteristics of MurD enzyme regulation

The *murD* gene codes for the enzyme MurD that adds D-glutamic acid residue catalytically during the biosynthesis of bacterial cells. This gene is positioned in the *E. coli* 's 2-min area present in its genome, which is also residence to a group of genes pertaining to envelope A (*envA*) and penicillin-binding protein B (*pbpB*). These genes are present in this region in the order - *pbpB-murEmurF-X-murD-Y-murG*. In this region the chromosomal segments of X and Y code towards certain unspecified proteins while gene E along with the F gene are reported to be located together. The MurD ligase was earlier thought to be the catalytic product of the *murG* gene, but subsequent research verified that the *murD* is located 2.5 kilobases upstream from the *murG* (Mengin-Lecreulx et al., 1989). The *mra* (from murein A) cluster is a term given to the 2-min area found in *Escherichia coli*. This *mra* cluster is reported to harbor seven murein) genes that take part in peptidoglycan synthesis and include *mur* (ATP dependent) ligases, *mraY*, and *ddl* and genes that take part in division of cell (*fts* genes) and genes carrying out biosynthesis pertaining to LPS (lipopolysaccharide) (*envA*) (Hara et al., 1997) . It has also been reported that the *murD* gene in *Mycobacterium tuberculosis* is located within the group of genes close to

genes for *ftsW* that take part in the process of cell division. The MurD genes of *Mycobacterium tuberculosis* and *Escherichia coli* are also reported to have a 64 percent homology (Thakur & Chakraborti, 2008). A preserved sequence is also present in the *mra* (murein) cluster of *Escherichia coli* as well as *Haemophilus influenzae*. But there exist slight differences in the positioning of these genes in Gram-positive bacterial species. Within *Staphylococcus aureus*, *Enterococcus faecalis*, including *Streptococcus pyogenes*, this *pbp1* is located ahead of *mraY*. In contrast, these gene sequences in *Enterococcus faecalis*, *Enterococcus hirae*, and *Streptococcus pyogenes* follows the order *murD*, *murG*, *divIB*, *ftsA*, *ftsZ* (Watanabe et al., 1997). Sequence analysis was used to determine the location of the *murD* in *Staphylococcus aureus*. The genes that code for isoleucyl tRNA synthetase have been identified in the array of genes as *mraY*, *murD*, *divIB*, *ftsA*, *ftsZ*, *orf*, *divIVA* and *ileS*. These genes were expected to be part of the same operon as *Escherichia coli* since they both carried brief intergenic regions and were transcribed by the same DNA fragment (El-Sherbeini et al., 1998). There is presence of 3 genes which possess homology in their sequences when compared with *murE*, *mraY* along with *murD* positioned in the genome of *Escherichia coli* which have been identified to be localized within the *Bacillus subtilis*' 4.4 kb area and is positioned in-between the distal part of the sequences of *spoVD* promoter and the initial site of the *spoVE* (Daniel & Errington, 1993). It has been established that a number of the genes found in the 133" segments of *Bacillus subtilis* and the gene cluster found in the 2min region of *Escherichia coli* share functional similarities. In addition to sharing a gene sequence with *Escherichia coli*, the *Bacillus subtilis* chromosome compared to that of *Escherichia coli* with regard to, it lacks three genes and has a greater proportion of intergenic regions throughout its genome (Daniel & Errington, 1993).

The process of transcription of every single gene reported in the operon designated as *mra* of *Escherichia coli*, in addition to presence of *murD*, is regulated by a single *mra* promoter. Studies on mutant strains of *Escherichia coli* has demonstrated that decreased expression of the *murD* located within the *mra* promoter induces the bacterial cell to lyse, demonstrating the necessity of the *murD* in the survival of bacterial cell (Hara et al., 1997). Given that protein serine-threonine kinases phosphorylate the MurD enzyme, it is possible that they are involved in the regulation of *Mycobacteria's* peptidoglycan production machinery. It was discovered that the phosphorylation

process that is brought about by the labeled kinases (PKnA) of serine/threonine was remarkably influenced by the concentration of Mur D enzyme and the duration of incubation (Thakur & Chakraborti., 2008; Gaur & Bera., 2022).

An open reading frame of 449 amino acids is located in the *Staphylococcus aureus murD* (El-Sherbeini et al., 1998). Enzyme MurD from *Staphylococcus aureus* shares a high degree of similarity with another bacteria, including 54% with *E. coli*, 55% with *Haemophilus influenzae*, 65% with *Bacillus subtilis* & 66% similarity with *Streptococcus pyogens*. Many of the amino acid residues found within the complementary regions belonging to the enzyme MurD ligase including the part regarding to the C-domain that harbors the binding site for ATP molecule are conserved across different bacterial species (El-Sherbeini et al., 1998) .

Nucleotide order of the 12 kb chromosomal segment's *mra* region, which contain the genes coding the Mur ligases are present in the order of *E*, *F*, followed by *D*, *mra Y*, and finally *murG*, have all been established (Ikeda et al., 1990). The 2.6 kb MurD enzyme-encoding gene in *E. coli* is located in the 2 min region present on the chromosome map, localized in the middle of *murF* as well as that of *ftsW* genes. 2 ORFs were identified within this region by sequence decoding: open reading frame D, and ORF Y which is localised downstream to that of *murD*, which codes for the Mur D enzyme. The 438 amino acid protein with molecular weight of about 46,938 Daltons is encoded by the 1314 base pair open reading frame of *murD* (Ikeda et al., 1990).

2.2 Functional characteristics & properties of Mur D ligase:

The MurD enzyme crystal structures from a number of bacteria have been reported by employing a number of ligands for example, of *Escherichia coli* by (Bertrand et al., 1999), of *Thermotoga maritime* by (Favini-Stabile et al., 2013) and of *Streptococcus agalactiae* (serogroup V) by Stein et al., in the year 2010. Additionally, a number of structures are also been generated through comparative modeling of different pathogenic bacteria e.g. of *Staphylococcus aureus* by (M. A. Azam & Jupudi, 2019), of *Leptospira interrogans* by (Amineni et al., 2010) for developing prospective inhibitors through utilizing *in silico* methods. However, in the last few decades, the most thorough and early studies on *Escherichia coli* MurD has been conducted (Bertrand et al., 1997; Kotnik et al., 2007; Humljan et al., 2008). 46,973 Dalton is the molecular weight of MurD ligase (M. A. Azam & Jupudi, 2020). The Mur D transfers a D-glutamic acid amino acid into

UDP-N-acetylmuramyl-L-alanine (UMA), that results in peptide bond formation between the D-glu's (D-glutamic acid) amino residue and -COOH group of UDP-N-acetylmuramyl-L-alanine. An ATP molecule is being utilized during the reaction, it additionally also generates one ADP molecule along with release of an orthophosphate (Walsh et al., 1999).

To comprehend the mode of action, the crystal structures formed by the combination Mur D belonging to *Escherichia coli* together along with multiple ligands and along with gene products, such as the quaternary complex related to the enzyme together with UMA, ADP molecule, Mg^{2+} ion, and Mn^{2+} ion, the product ADP as well as UMA, & the enzyme's binary complex together with UDP-N-acetylmuramoyl-L-alanine-D-glutamate (UMAG), were resolved (Bertrand et al., 1999). The catalytic process comprises gamma phosphate group pertaining to ATP first phosphorylating carboxylic acid group located at the C-terminal portion of the substrate molecule UMA, leading to the creation of an intermediary acyl phosphate. The acyl phosphate gets attacked nucleophilically via the approaching D-glutamic acid's amino group and yielding a tetrahedral intermediate with high-energy. The intermediate is ultimately transformed into the amide product, which liberate an inorganic phosphate group (Bertrand et al., 1999; Humljan et al., 2008). A cleft that exists in-between the central domain joining the C-terminal domains related to the substrate UMA serves as the location where the initial phosphorylation of the substrate occurs. The reactive element in UMA enters the cleft at the domain present at N-terminal, whereas from opposite side ATP molecule enters (Hrast et al., 2019).

MurD ligase necessitates 2 cations with bivalency (Mn^{2+} & Mg^{2+}) in order to transfer a phosphoryl group between two substrates that are anionic as demonstrated by (Bertrand et al., 1999). The cations having a bivalency serve as essential components for ligase activity of the MurD enzyme but are not crucial to the binding of the substrates UMA nor ADP (Kotnik et al., 2007).

The amino acids Leucine15, Threonine16, Aspartic acid 35, Threonine 36, Arginine 37, Glycine 73, and Asparagine138 are the most significant residues of the *Escherichia coli* MurD enzyme that are involved in interactions with the substrate UMA, whereas His183 interacts with Mg^{2+} (Bertrand et al., 1997; Bertrand et al., 1999; Bertrand et al., 2000). Interaction of ADP with

amino acid residues Glycine114, Lysine115, Serine116, Threonine117, Asparagine 271, Arginine 302, and Aspartic acid 317 takes place concurrently. The D-glutamic amino acid interactions involve residues Threonine 321, Lysine 348, Serine 415, Leucine 416, and Phenylalanine 422 (Bertrand et al., 1999). The interaction between enantiomeric glutamic acid derivatives and the MurD enzyme in its closed configuration has demonstrated an 1800 turnover of Leucine13-Glycine14 and Proline 41-Glycine 42 bonds, which caused the domain of N-terminal position to marginally shift the residue leucine13 towards Valine150.

Furthermore, inhibitors' attachment to the active site of the enzyme induces slight contortion in the domain present at central portion, primarily with respect to the amino acids Isoleucine139 alongwith Gly140 (Kotnik et al., 2007). Upon ATP hydrolysis, the resultant ADP molecule attaches to the enzyme's P-loop, where residues 108–116 combine to form a portion of the mononucleotide-binding fold. The ADP molecule connects itself between the domain located at the central region and the domain at the C-terminal position. Studies on the interaction between the MurD enzyme and UMAG (PDB 4UAG) demonstrates enzyme's specificity with respect to its substrate, D-glutamic acid. The γ -carboxylate forms hydrogen bonds with residues Serine at position 415 and Phenylalanine at position 422, while the -COOH group positioned at the alpha position of D-glutamic acid is involved in hydrogen bonding interactions with Threonine residue at position 321 and interacts with nitrogen of Lys348 residue based on charge (Humljan et al., 2008). *Escherichia coli* along with *Haemophilus influenzae* (belonging to group of Gram- negative bacteria) display feedback mechanism of inhibition when concentration of UMA surpasses the level of 15 and 30 μ M, however *Enterococcus faecalis* and *Staphylococcus aureus* being Gram-positive display a minimal impact on the activity of MurD enzymes, irrespective of amount of UMA present in the cell (Table 2.1) (Walsh et al., 1999).

Organism name	KmATP (μ M)	Km UMA(μ M)	Km D-Glu (μ M)	References
<i>Streptococcus pneumoniae</i> (MurD)	2000 (Approx)	96 \pm 39	190 \pm 26	H.Barreteue et al.,2012
<i>Borellia burgdoferi</i> (MurD)	53 \pm 12	63 \pm 30	110 \pm 29	H.Barreteue et al.,2012
<i>M. tuberculosis</i> (MurD)	710 \pm 290	340 \pm 10	700 \pm 180	H.Barreteue et al.,2012
<i>E. coli</i> (MurD)	97 \pm 9	7 \pm 0.6	42 \pm 5	M.Simcic et al.,2014
<i>Staphylococcus aureus</i> (MurD)	5400	41	100	H.Barreteue et al.,2012
<i>E. faecalis</i> (MurD)	47 \pm 4	36 \pm 7	118 \pm 14	Walsh et al.,1999
<i>Haemophilus influenzae</i> (MurD)	102 \pm 6	8 \pm 4	169 \pm 20	Walsh et al.,1999

Table 2.1 Comparative effectiveness of Mur D ligases from different bacteria

2.3 Structural Features of MurD Enzyme

Many of the MurD enzyme's crystal structures have been determined since far and submitted to the PDB. Numerous bacterial species' crystal structures, including the ones from *Escherichia coli* as determined by (Zidar et al., 2011) (Šink et al., 2016) *Thermotoga maritima* by (Favini-Stabile et al., 2013), and *Streptococcus agalactiae* serogroup V by Stein et al. “(2010)” across the open as well as closed stages of enzyme are elucidated. There were significant similarities identified in the domain configuration of MurD crystal structures. The substrate binding pocket of the MurD ligase is comprised of 3 globular domains: one located at N-terminal position, 2nd at central region, and the third at C-terminal position (Bertrand et al., 1997). Domain at N-terminal location primarily attaches to UDP component during UMA's binding. Entire family of Mur enzymes shares a conserved core domain that functions as an ATP-binding area. The interaction of D-glutamic acid within the catalytic site is facilitated by the C-terminal domain. The MurD enzyme's active site is created by the cleft that joins the central along with C-terminal domains (M. A. Azam & Jupudi, 2017). Residual amino acid sequences in the N-terminal domain range from 01 to 93. It consists of four α -helices around five lateral β -sheet strands. C-terminal domain is made up of β -sheet present in antiparallel manner with three strands along with β -sheet with six strands arranged parallel and surrounded by seven α -helices. It can accommodate amino acids ranging from 94 to 298 (Bertrand et al ., 1999).

The shape of these domains undergoes sequential modifications in which open state gives way to closed states via a semi-closed intermediate position during the process of catalytic reaction of the enzyme MurD. After each step of ligand binding, each ligand's domain motion is obliterated. The apo stage of the MurD enzyme has a domain opening and shutting mechanism in addition to

twisting during the catalytic process. When ATP binds, twisting is suppressed, and when an inhibitor binds, the open-closed technique is suppressed (Nakagawa et al., 2021). The MurD ligase from *Escherichia coli* has two open stages: one when it is present in free state along with the other one while it is attached to the UMA (Šink et al., 2016). A novel configuration of Mur D (2XPC) was determined using the ligand 4-aminocyclohexane-1,3-dicarboxyl, by application of NMR spectroscopy methods along with X-ray crystallography. Studies have demonstrated that the interaction of the -COOH group at 3' position within the cyclohexyl ring with nitrogen atom present in Lysine residue at position 348 was charge-based (Sosič et al., 2011).

MurD ligase adopts a semi-closed configuration during catalytic mechanism. Interaction between ligand and MurD causes enzyme to alter shape in multiple ways, which in turn modifies the ligand binding sequence and the enzyme's affinity for the next ligand (Saio et al., 2015). In contrast to other domains, C-domain pertaining to the MurD ligase adopts the maximum distinctive conformations. The MurD enzyme's C-terminus is the most versatile as it does not collaborate with the central domain and shows two non-identical configurations in the same asymmetric segment (Favini-Stabile et al., 2013).

Studies on crystallographic structures of MurD enzyme has thus far indicated that the C-terminal domain may have configured itself to drift toward the center of the structure. This alteration is brought about by the ligand molecule binding, and it leads the enzyme to close (Bertrand et al., 1999; Bertrand et al., 2000). When C-terminal domain present in MurD enzyme (pdb:1EEH) is positioned in different plane when compared to domains present in central & N-terminal locations, there is requirement of greater energy for its closure when opposed to the open form of crystal structure (PDB:1EOD) (Perdih et al., 2014) .

During catalytic process, domain 3 belonging to MurD enzyme traverses through significant conformational substitutions, as demonstrated by the NMR spectra. MurD ligase demonstrates change from open towards closed shape during its Apo state (Saio et al., 2015). On the contrary, the ligand molecule's coupling maintains the enzyme's closed configuration (PDB IDs 2X5O along with 2JFF). The sequence of ligand binding to the Mur D enzyme is as follows: first, ATP

binds to the ubiquity of Mg^{2+} , then UMA binds, and last, the ATP molecule is hydrolyzed. The final step involves the joining of residue D-glutamic amino acid (Saio et al., 2015).

2.4 Inhibitors of Mur D Enzyme

During the synthesis of peptidoglycan, Mur D ligase enzyme catalyzes incorporation of D-glutamic amino acid with alanine amino acid attached to precursor UDP N-acetylmuramoyl-l-alanine (UMA) (M. A. Azam & Jupudi, 2020). MurD ligase forms an amide by catalyzing the starting step of carboxylic acid phosphorylation with the use of an ATP molecule (Humljan et al., 2006). The binding pocket present in the MurD enzyme is comprised of 3 domains of globular structure : domains localized at N-terminal , central , along with C-terminal positions (Bertrand et al., 1997). Domain at N-terminal position remains accountable for attachment of UDP portion of UMA. The whole family of Mur enzymes shares a conserved core domain that functions as an ATP-binding area. The absolute binding of D-glutamic amino acid residue is mediated by domain at C-terminal position. The MurD's binding site is formed by the cleft that separates the central from the C-terminal domains (M. A. Azam & Jupudi, 2017).

The ATP-dependent ligase MurD is one of the enzymes that can potentially be targeted for generation of novel antibacterial medications. Significant role is played by this enzyme in the biosynthesis of peptidoglycan, a constituent of bacterial cell wall. Several configurations of MurD enzymes with ligands crystallized inside their catalytic pocket have been described (Bertrand et al., 1997; Bertrand et al., 1999; Bertrand et al., 2000; Kotnik et al., 2007) providing new inhibitors' design and development a foundation. Considerable advancements have been made in comprehending the structure and catalytic mechanism of the MurD enzyme, which is linked to numerous bacterial strains, including *Escherichia coli*, *Staphylococcus aureus*, *Streptococcus pneumoniae*, *Leptospira interrogans*, and *Borellia burgdoferi*. Additionally, research has been done on orthologs of MurD derived from several detrimental bacteria (Walsh et al., 1999; Barreteau et al., 2012). The synthesis of peptidosulfonamides was done by a novel approach, and it was then applied to a number of newer inhibitors that were tested against microbes that produce peptidoglycan by targeting the ligases MurD and MurE. In this process, new building blocks consisting of N-phthalimido β -aminoethanesulfonyl chlorides were used in production of peptidosulfonamides.

The key step was combining sulfonic acids or their sodium salts with C-protected amino acid after excess SOCl_2 or SOCl_2/DMF (dimethylformamide) converted them into corresponding sulfonyl chlorides. While some of the compounds inhibited MurE, none of them significantly inhibited MurD; one compound's IC_{50} was less than 200 μM , indicating that it could be a viable beginning point for additional research. Using two analogues, molecular modeling simulations were run to look at the lack of inhibitory activity of the compounds (Humljan et al., 2006). To identify potent inhibitors of the MurD enzyme, a series of four N-acylhydrazones were generated and their potential to inhibit MurD was evaluated.

The antibacterial properties of these substances were also investigated *in vitro*. N-acylhydrazone 1 displayed the strongest inhibitory effect among all the compounds tested, demonstrating an IC_{50} value ranging from 230 μM to 123 μM , in relation to *Escherichia coli*. Additionally, this compound demonstrated a low level of antibacterial activity against *Staphylococcus aureus* 8325-4, *Escherichia coli* 1411, and *Escherichia coli* SM1411, which exhibited a MIC level of 128 $\mu\text{g/ml}$ at every instance. The inhibitor lost its entire inhibitory effect against MurD and reduced its inhibitory activity against MurC when one of its hydroxy groups was removed or replaced with a methoxy group (Šink et al., 2008).

Additionally, phosphorylated hydroxyethylamine has been established as a MurC–MurF ligase inhibitor. These inhibitors are promising prospects for the creation of multiple Mur ligase inhibitors due to their IC_{50} levels in the micromolar range. The most effective inhibitor of *Escherichia coli* MurD among the series was found to be 1-(4-ethylphenylsulfonamido)-3-morpholinopropan-2-yl dihydrogen phosphate, which showed 28 percent inhibition at 500 μM level (Sova et al., 2009). Among the compounds that have been described so far, transition state analogue was demonstrated to be strongest inhibitors targeting MurD enzyme belonging to *Escherichia coli* (IC_{50} , 0.68 μM) because it contains phosphinic acid group, having a tetrahedral shape at core containing a dipeptide. Another research team used this discovery as basis to create a new class of inhibitors with similar characteristic (Gegnas et al., 1998). The IC_{50} values of these transition state inhibitors fell between 20 and 78,200 nM. Combining the carbohydrate component and adjusting the stereochemical structure of the α -amino phosphinate produced the strongest inhibitor. The N-(5-phthalimidopentanoyl)-N-[2-(2-ethoxy) acetyl] along with

derivatives of N-(7-oxooctanoyl)-phosphono and phosphinoalanine were examined to determine potential as inhibitors of the MurD ligase (Gobec et al., 2001). Derivatives of N-acetylmuramic acid have also been identified as MurD inhibitors; however, these investigations failed to produce any encouraging findings (Auger et al., 1995). Numerous inhibitors based on N-acyl-d-Glu have been generated. It is noted that those with indole moieties are among the most noteworthy (Victor et al., 1999). Additionally, the Wyeth group's internal screening effort revealed pulvinamide 5 to be a Mur C inhibitor (IC_{50} , 8 μ g/ml). 180 pulvinones were investigated as MurA-D inhibitors considering this finding. Newer compound was shown to have inhibitory effect against MurA-D enzymes in a subsequent effort (IC_{50} , 1 to 6 microgram/ml) (Antane et al., 2006). Additional phosphinate-based inhibitor development led to a novel substance containing the phosphinodipeptide Ala- ψ -(PO_2-CH_2-)-Glu structural motif was produced. The inhibitory action of this chemical against MurE fell into the micromolar range (Štrancar et al., 2006).

Through utilizing high-throughput screening (HTS) plus structural activity relationship (SAR) methods, numerous agents from the natural and synthetic component categories that may function as MurD inhibitors have been found. However, none of the substances have shown effective results in suppressing the MurD enzyme in a clinical setting to date. As a result of the development of computer-aided drug design (CADD) processes in conjunction with HTS, numerous inhibitors of the MurD were additionally recognized and developed by applying *in silico* procedures (Simčič et al., 2014; M. A. Azam & Jupudi., 2017).

The *Escherichia coli* Mur D enzyme was tested against a series of derivatives of sulphonamide derived from naphthalene-N-sulfonyl-D-glutamic acid to examine binding processes of these compounds.

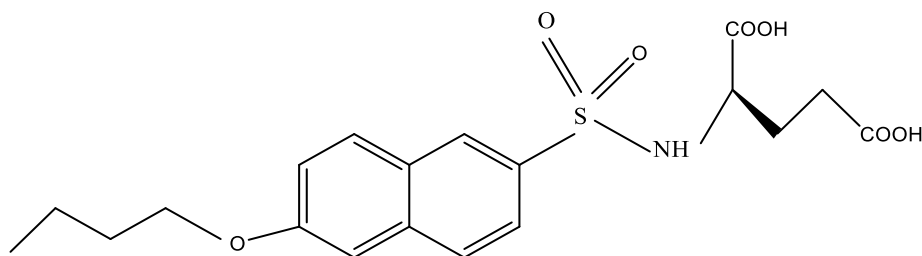
Rigid substitutes were used in place of the D-glutamic acid fraction in these compounds. Stretching forces are a significant factor in the association between sulphonamide inhibitors and their C- and N-terminal domains when creating novel inhibitors, as shown by studies using molecular dynamics (MD) simulation. Additionally, the inhibitor molecule's adaptability to the structural changes of the MurD enzyme was proposed. Centered on the N-sulfonyl-D-glutamic acid fraction, a class of sulphonamide analogues was studied in conjunction with the *Escherichia*

coli Mur D enzyme. Studies were conducted to explore the manner in which these derivatives interacted with the N- & C-terminal domains. (Simčič et al., 2012).

Compounds based on thiazolidine-4-one were structurally modified to produce inhibitors acting simultaneously on two enzymes against MurD as well as MurE from *Staphylococcus aureus* and *Escherichia coli*. The most potent molecule showed a MIC of 8 microgram/ml when tested against *Staphylococcus aureus* along with MRSA, and displayed an IC₅₀ amounts that range from 8.2 to 6.4 μ M when examined about the MurD enzyme from *Staphylococcus aureus* and *Escherichia coli*, respectively (Tomašić et al., 2012). It was found that the inhibitor interfered with the product UDP-MurNAc-L-Ala-D-Glu's binding location (UMAG). Leu 416 residue and Phe161 residue exhibit π - π interactions and hydrophobic interactions, respectively, with the inhibitor. Residues Threonine at position 321, Lysine 348, Serine 415, and Phenylalanine 422 make contribution towards hydrogen bonding with the inhibitor's D-glutamic acid portion (Tomašić et al., 2012).

By using structure activity relationship (SAR), a number of derivatives of Naphthalene-N-sulfonyl-D-glutamic acid were examined to be prospective inhibitors for MurD enzyme from *Escherichia coli*. The IC₅₀ values calculated for the compounds were found to lie between 80 and 600 μ M. Synthesis of compounds that contain sulphonamide (Fig. 2.1) in order to imitate the tetrahedral transition stage that the MurD enzyme goes through when catalyzing a reaction (Humljan et al., 2008). It was determined that the presence of the α -carboxylate group in D-glutamic acid derivatives was necessary for their association with the enzyme. It was found that the carboxamide as well as sulphonamide group of substituent compounds were inert when compared to those with bulky biphenyl and naphthalene substituents, which showed IC₅₀ amounts in the range from 1720 to 810 μ M, respectively. Compared to compounds without this direct interaction, the series whereby the naphthalene moiety was directly associated with the D-Glutamic acid residue through sulphonamide component showed inhibition effect. It was studied that when the side chain's length was enhanced through switching the methyl group for a pentyl group (590 to 170 μ M), an increase in inhibitory activity of three times was observed. It was discovered that arylalkyloxy substituents work better as substituted inhibitors (Humljan et al., 2008).

Figure 2.1. Basic chemical structure of a sulphonamide inhibitor



A new 2-oxoindolinyldene based inhibitor (Fig. 2.2A) has been evaluated targeting the MurD enzyme of *Escherichia coli* through a steady-state kinetic mechanism. For the substrate UMA, the analog displayed a competition-based mechanism of inhibitory effect. This chemical exhibited a MIC level of 128 microgram/ml when tested against isolates of *Enterococcus faecalis* (ATCC 29212) along with *Haemophilus influenzae* (ATCC 49247) (Simčič et al., 2014). Nuclear magnetic resonance (NMR) examination demonstrated the fact that inhibitor displayed interaction with the enzyme's N-terminal as well as central domains however not with its C-terminal domain, in contrast to transition stage analogues. As a result, domain shifts had no effect on its binding. It became apparent that the uracil-binding site included the 2-oxoindolinyldene ring. The MD simulation indicated that the continued stability of the enzyme-inhibitor combination was primarily due to hydrophobic interactions (Simčič et al., 2014).

Using simulation studies and molecular docking, a library of marine natural products was examined to for putative inhibitors of the MurD enzyme from *Staphylococcus aureus*. Two compounds demonstrated an effective contact with the enzyme's binding pocket, potential medicinal benefits, as well as a stable arrangement involving the protein of interest (Zheng et al., 2021). Compound with id (46604) exhibited hydrogen bonding contacts with residues of Glu166, Ser168, Lys328, and Thr330, and also displayed hydrophobic bonding interactions with amino acid residues Lysine19 and Asparagine145. Asn145, Ser168, as well as Lys328 residues have been associated in the formation of H-bonds, while Compound marked as (46608) demonstrated hydrophobic bonding interactions with the residues Threonine 330 and Phenylalanine at position 431 (Zheng et al., 2021).

Using molecular docking and molecular dynamics experiments, 2-Thioxothiazolidin-4-one, (Fig. 2.2B), has been investigated to be possible suppressor of the MurD enzyme from *Staphylococcus*

aureus that was homology-modeled. Three main interactions that were seen in-between the inhibitor & MurD enzyme were mainly H- bonding, pi- pi stacking interactions, along with salt bridge bonding interactions. Main residues that contributed to stabilize the inhibitor-enzyme complex were Lysine19, Glycine147, Tyrosine 148, Lysine 328, Threonine 330, and Phenylalanine 431 residues. The principal forces involved in inhibitor binding were van der Waals interactions and electrostatic solvation energies. The modeled MurD enzyme and the inhibitor were shown to exist a steady arrangement by MD simulation. In the course of compound's *in vitro* verification, its IC₅₀ value of 6.40 μ M demonstrated its ability to inhibit the enzyme. When tested against commercial strains of *Staphylococcus aureus* and MRSA, the putative inhibitory compound showed antibacterial efficacy along with minimum inhibitory concentrations (MIC) of 8 μ g/ml (M. Azam et al., 2019).

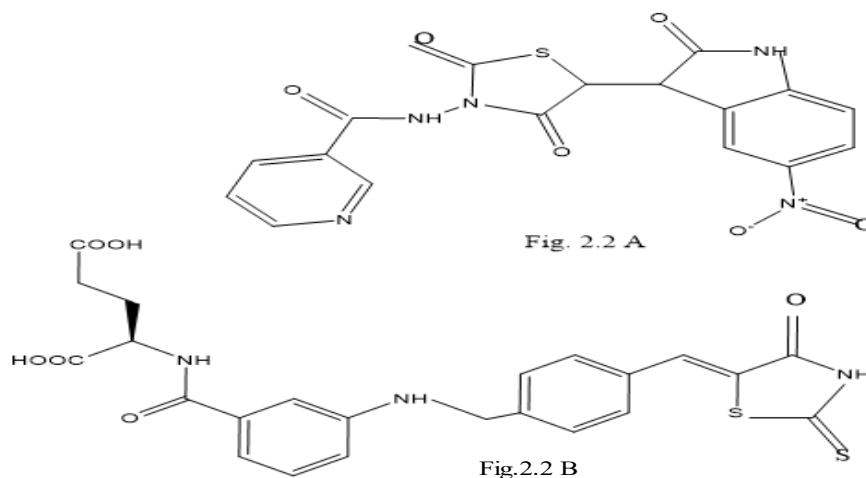


Figure 2.2: 2.2 A: Chemical formula of 2-oxoindolinyldene derived inhibitor; 2.2 B. Chemical formula of 2- Thioxothiazolidin-4-one ring

MD simulation investigations upon the enzyme and 2-thioxothiazolidin-4-one based inhibitor indicated the fact, in addition to the structural characteristics of D-glutamic amino acid residue, configurational flexibilities related to the compound were primarily reliant on rotations of a unit bond about C₆H₄-CO-NH-, C₆H₄-CH₂-NH-C₆H₄- group. Given that the 4-one ring of 2-thioxothiazolidin contributes insignificantly to binding mechanism, numerous novel inhibitors

(designated as compound D1, D2, D3 & D4) (Fig. 2.3) were generated. To enhance the binding affinity, the new inhibitors were created by substituting heterocyclic rings containing N atoms for the D-Glu part, C₆H₄-CO-NH- and a ring of aromatic compounds with -COOH, -OH, and other polar groups. These changes resulted in a rise in the free energy for binding ranging from -61.36 to 83.71 kcal/mol and an improvement in the glide score ranging from -6.75 to -8.88 kcal/mol (Azam et al., 2019).

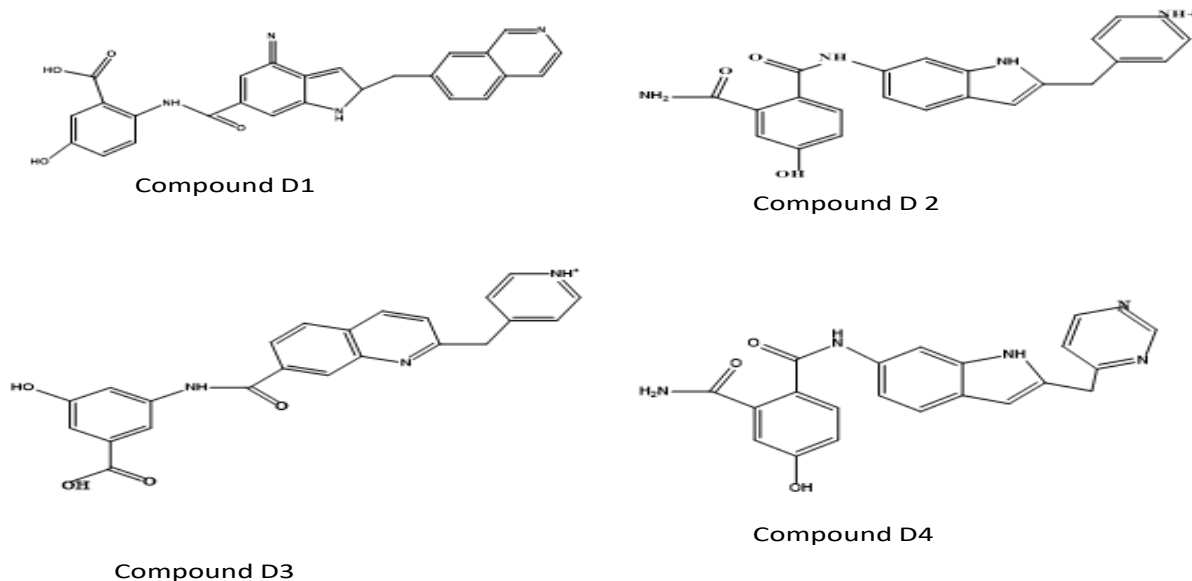


Figure 2.3: Chemical formulae of D1, D2, D3, and D4 compounds, which were developed by altering the 2-thioxothiazolidin-4-one ring

A collection of commercial chemical libraries containing more than 1.6 million compounds was assessed and tested for inhibitory action on the *Staphylococcus aureus* MurD ligase model using high throughput screening and *in vitro* validation. The compounds ranked 1 through 10 (H1 through H10) were selected for further investigation by means of binding free energy computations and the ways in which different ligands gets interacted among the amino acid residues present in the catalytic pocket. It was shown that whereas electrostatic solvation charges impeded the attachment of the ligand molecules, Van der Waals and coulomb energy are essential factors that support ligand binding (M. A. Azam & Jupudi, 2019). Compound H5 (Fig. 2.4) possessed the strongest inhibitory effect, with IC₅₀ along with MIC values in between 7 μ M

and 128 $\mu\text{g/ml}$, in that order, demonstrating the inhibitory impact upon multiple commercial strains, including *Staphylococcus aureus* NCIM 5021 and *Staphylococcus aureus* MRSA 43300. Compound H10's limited permeability into the bacterial cell may be the reason it did not show any inhibitory action against any of the strains tested. Ligand H5 stabilized the complex by forming a sequence of hydrogen bonds with Lysine19, Glutamine 23, Glycine 80, and Glycine 147 residues in addition to engaging with Lysine19 via a π -cation association (Azam & Jupudi, 2019).

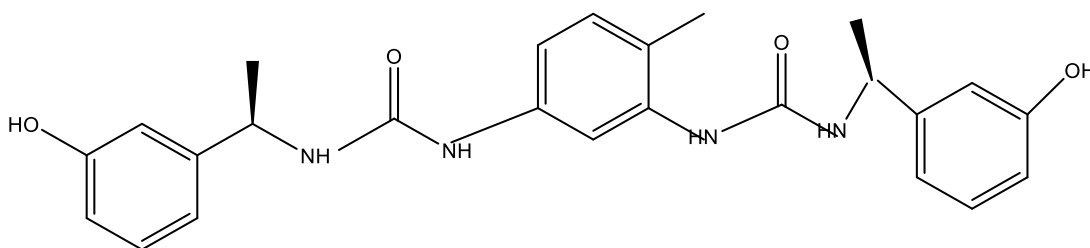


Figure 2.4. Chemical formula of inhibitor H5

Molecular modeling studies were used to dock a large number of known MurD inhibitors to the *Escherichia coli* MurD attachment point. The majority of the inhibitors studied recently displayed a common method of interaction, as demonstrated by the docking results. Major residues Threonine36, Arginine 37, Histidine 183, Lysine 319, Lysine 348, Threonine321, Serine 415, as well as Phenylalanine 422 were involved during the interaction between the inhibitor and the enzyme. It was found that non-polar interactions, such as the Van der Waals force, were important with regard to the inhibitor-protein complex's attachment and stability, whereas ionic or electrostatic interactions were only marginally significant (M. A. Azam & Jupudi, 2017) .

Based on pharmacokinetic examinations, Lipinski rule, and molecular docking, 10,344 compounds were evaluated against the *Mycobacterium TB* H37Rv 's MurD enzyme that was modelled. These compounds were taken from the Zinc and PubChem databases. MM-GBSA (molecular mechanics energies combined with generalized Born and surface area continuum solvation) being used to calculate binding free energies, and the results indicated that the top 4 compounds (ZINC11881196, ZINC12247644, ZINC14995379, and PubChem6185) had higher

values when compared with ATP. Aforementioned compounds were identified in this study as possible MurD inhibitors, and their application as therapeutic drugs can be confirmed further (Isa, 2019).

A collection of synthetic ATP-competitive inhibitors of kinase inhibitors enzyme have been evaluated against the *Escherichia coli* Mur ligases (Mur C, D, E, and F). It was possible to identify four new scaffolds that demonstrated potential for the creation of novel medications. A derivative of aza-stilbene designated as 1 (Fig. 2.5 A) was discovered to have the potential to inhibit MurD ligase (Hrast et al., 2019). Based on Nuclear magnetic resonance (NMR) spectroscopy, C-terminal domain containing the binding site for D-glutamic acid residue was detected as the position wherein incoming inhibitor binds. The substance interfered with the Leu416 methyl groups' signals and inhibited by acting with D-glutamic acid competitively. It was not dependent on the ATP-assisted enzyme closure. The IC₅₀ value of compound 1 against the MurD protein was determined to be 104 μ M. Compound 1 did not display any inhibitory action against *Staphylococcus aureus* and *Escherichia coli*. Their inadequate penetration impact may have been the cause of the above, indicating that the original compound needs to undergo additional structural changes in order to boost its inhibitory effectiveness against different category of Mur enzymes (Hrast et al., 2019).

About 6,42,759 compounds taken from the Zinc database were subjected to molecular docking as well as simulation investigations against the *Acinetobacter baumannii* MurD enzyme, which has been generated using homology modeling from *E. coli* (Protein Data Bank (ID): 4UAG) (Jha et al., 2020). ZINC19221101 and ZINC12454357 (Fig. 2.5 B) were among the most promising compounds identified for further validation; their binding free energy values were - 62.6 ± 5.6 kcal/mol and -46.1 ± 2.6 kcal/mol, respectively. According to MD modeling studies, compound ZINC19221101 interacts with the residues Asn146, Lys123, Ser124, and Ala122 through hydrogen bonds. Furthermore, it exhibited pi-pi bonding while interacting with Lysine123, Glutamine165, Lysine330, Phenylalanine434, and Tyrosine440 and displayed Vander wall bonding while interacting with residues Arginine313, Threonine332, and Lysine364 (Jha et al., 2020). Compound ZINC12454357 demonstrated interactions via hydrogen bonding towards the conserved residue Asn146 and Tyr440, Lys364, and Lys123 of the MurD

enzyme. While pi-pi interactions were generated with residues Glu165, Phe169, His191 (preserved residue), and Lys330, Van der Waals interactions were identified with residues Pro80, Gly81 (catalytically preserved residue), Ser120, Asn121, Ala122, Leu147, Gly148, Ser167, Phe434, Ser439, and Asn441 (Jha et al., 2020).

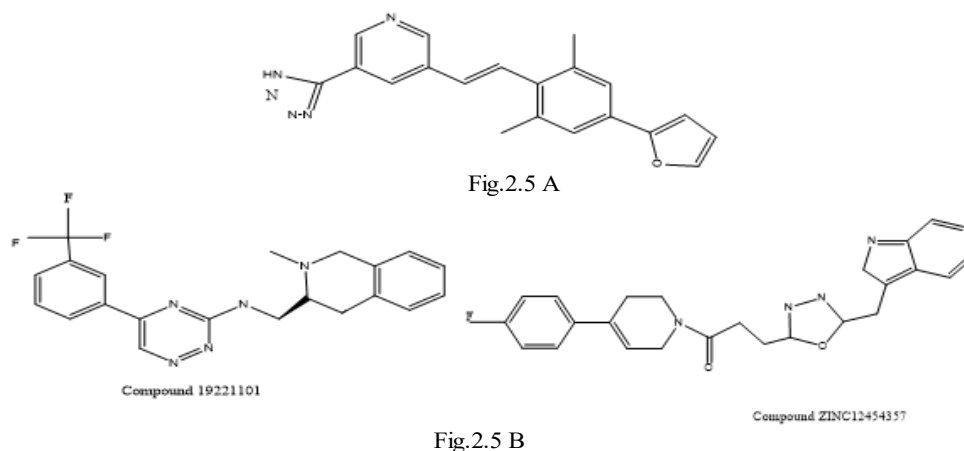


Figure 2.5: 2.5 A. Chemical formula of ATP-dependent kinase inhibitor; 2.5 B. Chemical formula of ZINC19221101 & ZINC12454357

Because fosfomycin functions as PEP's analog, it replaces PEP in the active site of the MurA enzyme by establishing a covalent link connecting a cysteine residue through process of competitive inhibition. By creating a hydrogen link between its hydroxyl group and that of UDP-N-acetylglucosamine at C-3 as well as between the drug's phosphonate oxygen and nitrogen at the amide group of UDP-N-acetylglucosamine, fosfomycin gets inserted between MurD protein and UDP-N-acetylglucosamine (Skarzynski et al., 1996) .

A series of phenoxyacetohydrazide derivatives were synthesized and evaluated against *Staphylococcus aureus* MurD (designated as 4a to 4k in Fig. 2.6 and Table 2.2). Based on studies to detect the anti-bacteriostatic activity, of molecules designated as 4a, 4j, and 4k inhibited *Staphylococcus aureus* NCIM 5022, these compounds displayed minimum inhibitory

concentration (MIC) level of 64 microgram/ml. Additionally, these compounds displayed a 128 µg/ml MIC inhibitory concentration on the MRSA strain ATCC 43300.

The compounds 4c & 4j were found to be most potent against the respective strains of *Bacillus subtilis* NCIM 2545 as well as *Klebsiella pneumoniae* NCIM 2706. Compound 4d exhibited effectiveness against the *Pseudomonas aeruginosa* strain NCIM 2036, possessing a MIC concentration of 64 µg/ml. The study revealed that compound 4k significantly inhibited *Staphylococcus aureus* MurD, yielding an IC₅₀ level of 35.80 µM. The incorporation of the SO₂ group may be the reason why derivatives of sulfonyl hydrazides have proven to be more effective than hydrazides (Jupudi et al., 2021).

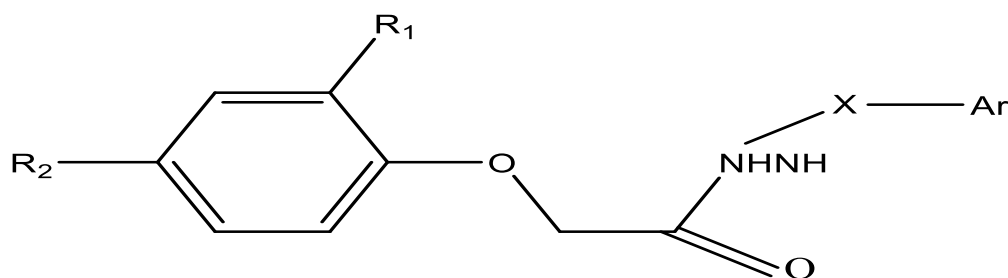


Figure 2.6: Chemical formula of phenoxyacetohydrazide ring

Cpd. marked	R1 Gp.	R2 Gp.	X Gp.	Ar Gp.
4a	-Cl	-H	>carbonyl	-2-furyl
4b	-H	-OCH ₃	>carbonyl	-2-furyl
4c	-Cl	-Cl	>carbonyl	-2-Cl-C ₆ H ₄
4d	-Cl	-Cl	>carbonyl	-3,5-diNO ₂ -C ₆ H ₃
4e	-Cl	-Cl	>carbonyl	-3-Br-C ₆ H ₄
4f	-Cl	-Cl	>carbonyl	-4-Cl-C ₆ H ₄
4g	-H	-NO ₂	>carbonyl	-2,4-di-CH ₃ O-C ₆ H ₃
4h	-H	-NO ₂	>carbonyl	-2,4-di-Cl-C ₆ H ₃
4i	-H	-OCH ₃	>carbonyl	-2-CH ₃ -C ₆ H ₄
4j	-Cl	-H	>SO ₂	-C ₆ H ₄
4k	-H	-OCH ₃	>SO ₂	-4-Cl-3-COOH-C ₆ H ₃

Table 2.2: different substituent groups joined to the parent phenoxyacetohydrazide ring to form the molecules designated 4a–4k

Using homology modeling and molecular docking, it was determined that the Van der Waals interaction, not electrostatic interactions, is the primary factor contributing to the stability of inhibitor-protein binding to MurD from *Staphylococcus aureus* (Jupudi et al., 2021).

Twenty synthesized aza-stilbene compounds were tested against *Staphylococcus aureus* Mur enzymes ligase C, Mur D, Mur E, and Mur F. The majority of these compounds possessed only little bacteriostatic activity when tested against *Staphylococcus aureus* along with *E. coli*. Two compounds, designated as 30 and 31 as shown in Figure 2.7, had modest activity *Staphylococcus aureus*, and displayed MIC levels ranging from 0.125 to 0.031 mM, against the tested bacterial strains respectively.

Based on the molecular docking investigations, it was found out that the enzyme makes numerous hydrogen bonding interactions with the tetrazole ring, whereas the enzyme makes weaker interactions with the pyridine, phenyl, and furan fractions. According to these studies, it might be necessary to make structural changes in order to improve binding affinity and inhibitory impact (Hrast et al.,2021)

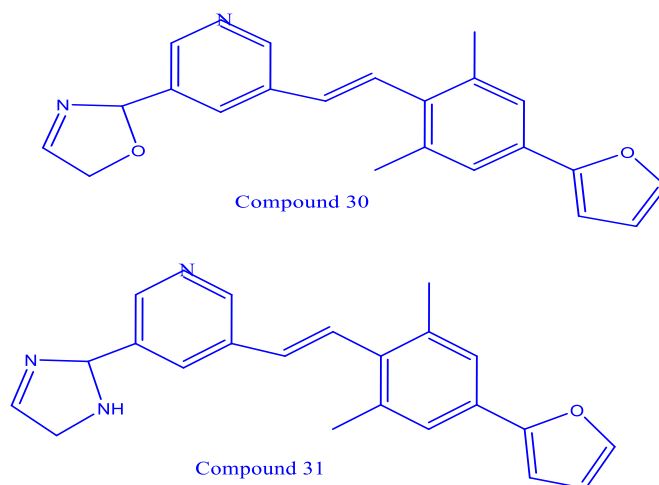


Figure 2.7 Chemical formulae of Aza-stilbene derivatives labelled as compound 30 and 31

The ChEMBL database was screened against homology-modeled Mur enzymes (Mur A, B, C, D, E, and F) of *Mycobacterium tuberculosis* (Mtb) using molecular docking and simulation studies. The compound that showed the best docking toward each of the Mtb's modeled Mur enzymes was ChEMBL446262 (Fig. 2.8). It became apparent that the compound actively formed hydrogen bonds with the enzyme's residues Serine at position 129, Arginine at 141st position Leucine at position 144, Isoleucine at 148th position, Serine 150, Glutamic acid166,

Aspartic acid at position 194, Arginine 446, and Methionine at position 448. The study recommended additional research and studies for verification to create novel inhibitors (Kumari & Subbarao, 2021).

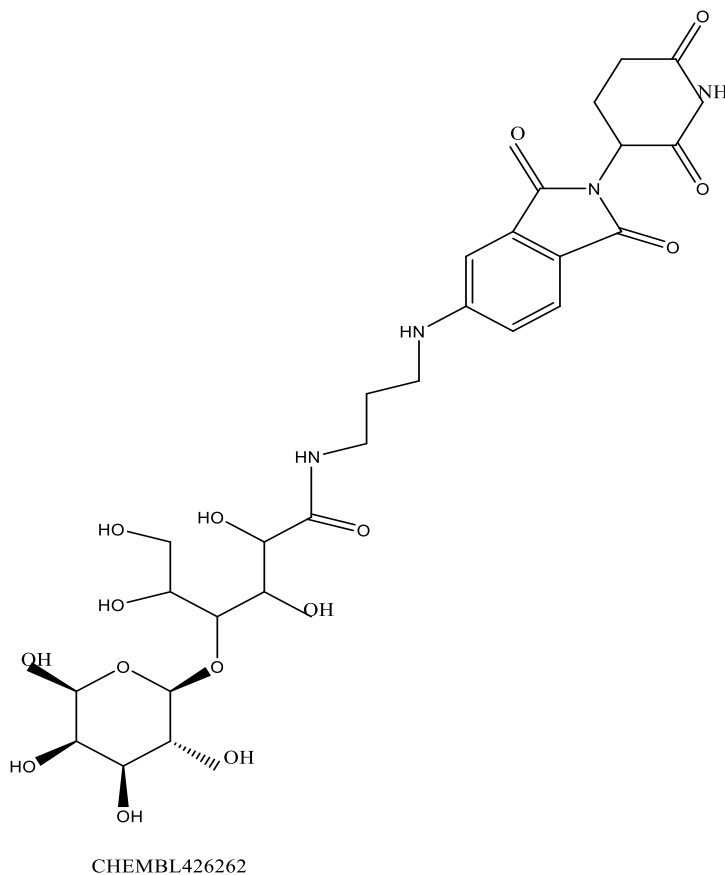


Figure 2.8 Chemical structure of compound CHEMBL426262

To explore a new class of therapeutic leads, natural product-based compounds were investigated as potential MurD inhibitors from *Acinetobacter baumannii*. Four possible compounds have been identified by flexible molecular docking screening. Three compounds, ZINC08879777, ZINC30726863, and ZINC95486217, were identified as possible *Acinetobacter baumannii* MurD binders after molecular dynamics modeling of these compounds (Tiwari et al., 2022).

It has recently been demonstrated that some bacteria, including *Xanthomonas oryzae*, use a different pathway for the synthesis of peptidoglycan. MurL, which do not exhibit similarity to

any known protein, catalyzed the epimerization of the terminal L-Glu of the MurD2 product to form UDP-MurNAc-L-Ala-D-Glu in this route. MurD2, a homolog of MurD, facilitated the attachment of L-Glu to UDP-MurNAc-L-Ala. In this study, specific inhibitors of the alternative pathway from metabolites produced from actinomycetes were studied. In the culture broth of *Micromonospora* sp. K18-0097, a novel polyketide of the oligomycin class that inhibits the MurD2 reaction was studied (Umetsu et al., 2024).

Chapter 3

Hypothesis

Hypothesis:

The ATP-dependent MurD ligases, located in the cytoplasm of bacteria is gaining attention as a drug target because of its critical function in the growth of bacteria and because it is nonexistent in humans. The MurD enzyme's catalytic mechanism and pattern of substrate binding has been elucidated by structural investigations. The mechanism of action of MurD and the other Mur ligases, like Mur C, Mur E, along with Mur F, is similar, and they share an ATP binding site that is conserved. MurD inhibitors have shown a lot of promise, but despite this, their application in research on antibacterial activity has not been substantial. The catalysis pathway of *E. coli* MurD pathway is already characterized. So, it is hypothesized that out of various new compounds from selected commercial libraries, few of these compounds may bind efficiently with the *E. coli* MurD enzyme, thereby inhibiting the catalysis step. These compounds if identified, will ultimately be used to substitute or expand the scope and use of various therapeutic agents currently available in the clinical domain as inhibitors of the MurD enzyme against various bacterial species. Predicted compound(s) will show potential *in vitro* biological activity against various bacterial species that may provide a piece of more accurate information regarding the activity of identified inhibitors against gram-positive and gram-negative bacterial species. By employing *in silico* and *in vitro* research, the data gathered from these investigations can be utilized for identifying possible inhibitors that could be developed as appropriate, strong, and targeted inhibitors of the MurD enzyme pathway, helping to overcome drug resistance and enhance therapeutic efficacy.

Chapter 4

Objectives

Objectives :

1) To identify potential compounds that could bind efficiently with *E.coli* MurD enzyme by using molecular docking .

- a) GLIDE-HTVS & Standard precision (SP) screening of libraries.
- b) GLIDE-XP screening of compounds through Extra- precision screening
- c) Molecular dynamics simulation studies and binding free energy calculation.

2). Prediction of ADMET (Absorption, Distribution, Metabolism, Excretion and Toxicity) properties of potential compounds.

3) *in vitro* assay of top two lead compounds.

- a) Antibacterial Activity Assay
- b) Determination of Minimum Inhibitory Concentration (MIC)
- c) Determination of Minimum Bactericidal Concentration (MBC)
- d) Effect of Lead Compounds on Bacterial Morphology

Chapter 5

Materials & Methods

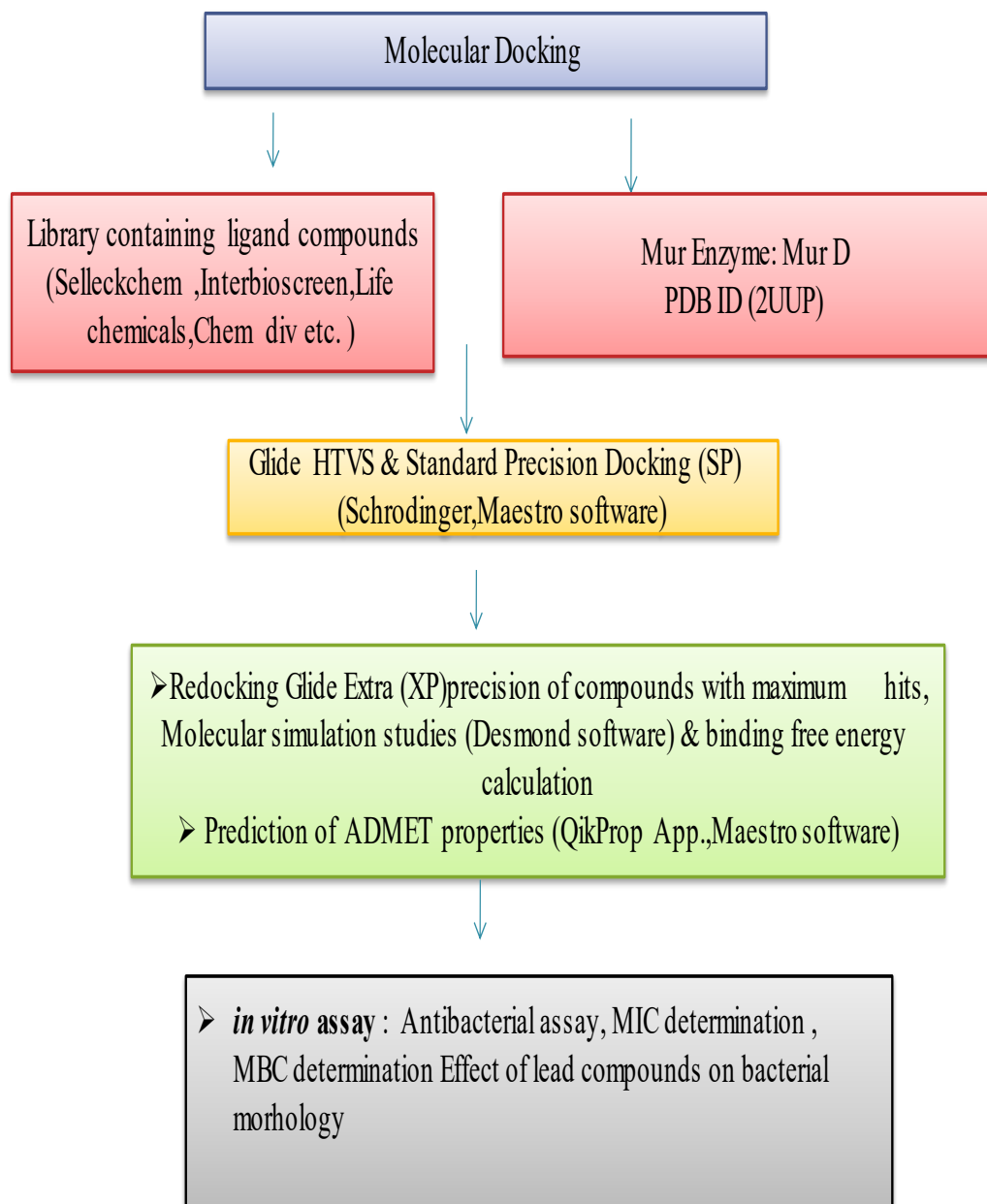


Fig 5.1 Flow chart of methodology

Materials & Methods:

The following methodology was followed to achieve the objectives

5.1.Retrieval of MurD enzyme structure and preparation for molecular docking

The X-ray crystal structure of Mur D enzyme from *E. coli* (Table 5.1) was retrieved from the Protein Data Bank (PDB) (<https://www.rcsb.org>). The PDB structure (2UUP) of *E. coli* Mur D enzyme has a resolution of 1.88 Å obtained by X-ray diffraction studies. Further, this PDB structure has no mutations in its polymer sequence, thus making it suitable for the molecular docking process (<https://www.rcsb.org>). Out of 22 crystal structures of the Mur D enzyme available in the Protein Data Bank, 14 of these are inhibitor bound. Crystal structures with PDB IDs (2UUO, 2UUP, 2VTD, 2VTE, 2JJF, 2JFG, and 2JFH) have been published by the same research group (Kotnik et al., 2007) & (Humljan et al., 2008). Therefore, the most recent publications and inhibitor-bound crystal structure were taken into account while choosing the target molecule. Using the Glide program of the Schrodinger software trial Maestro suite, the Protein Preparation Wizard tool was used to prepare the input enzyme molecule. The raw PDB structure was modified to include necessary modifications such as the elimination of heteroatoms, the addition of missing hydrogen atoms, the assignment of correct bond ordering, the removal of water molecules, the formation of disulfide bonds, the fixing of charges, and the group orientation (www.schrodinger.com).

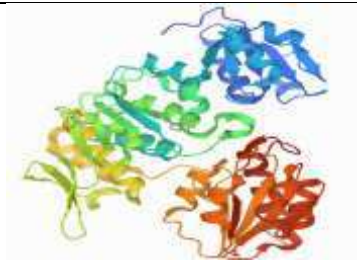
	Selected Enzyme	PDB ID	Organism	Structure
1.	Mur D	2UUP	<i>E.coli</i>	

Table 5.1: Selected enzyme target with respective PDB identification for X-ray crystal structure (<https://www.rcsb.org>)

5.2 Preparation of Ligand Molecules & Grid Generation:

Candidate ligand molecules were selected from a combination of compound libraries like Asinex (<https://www.asinex.com>), Life Chemicals (<https://lifechemicals.com>), ChemDiv (<https://www.chemdiv.com>), Enamine (<https://enamine.net/compound-libraries>), Selleckchem (<https://www.selleckchem.com>), and Interbioscreen (<https://www.ibscreen.com>). Smaller libraries like the FDA-approved Drug Library, Bioactive compound library, and natural product libraries from this broader set of libraries containing structurally diverse, medicinally active, and cell-permeable compounds which have been confirmed for their bioactivity, water-soluble and chemically stable compounds, and containing structural motifs that have been substantiated by nature for better biological response were taken into consideration to increase the chances of finding a better biological agent to act as an inhibitor against the targeted enzyme. This was done to solve the issue associated with previously discovered inhibitors not working as intended in subsequent experimental validation stages, such as instances in which they failed to pass through the bacterial cell wall and lacked any antibacterial action, etc.

The construction of ligands involved the use of the Maestro application's Ligprep module, which executed various functions including adding hydrogen atoms, fixing charges and group orientation, converting 2D to 3D, correcting bond lengths and angles, low energy structure and proper chirality, ionization states, tautomers, stereochemistries, ring conformation, etc. were integrated into ligand molecules, then optimisation and minimization in the force field Optimized Potential for Liquid Simulations (OPLS_2005) (Jorgensen et al., 1996; Shivakumar et al., 2010).

Following the completion of the ligand and enzyme preparation, the generation of the receptor-grid proceeded. Calculated on a grid by different sets of fields, the receptor's active site offers a precise scoring function with thermodynamic ideal energy. A receptor-grid file was created first, and then molecular docking was carried out.

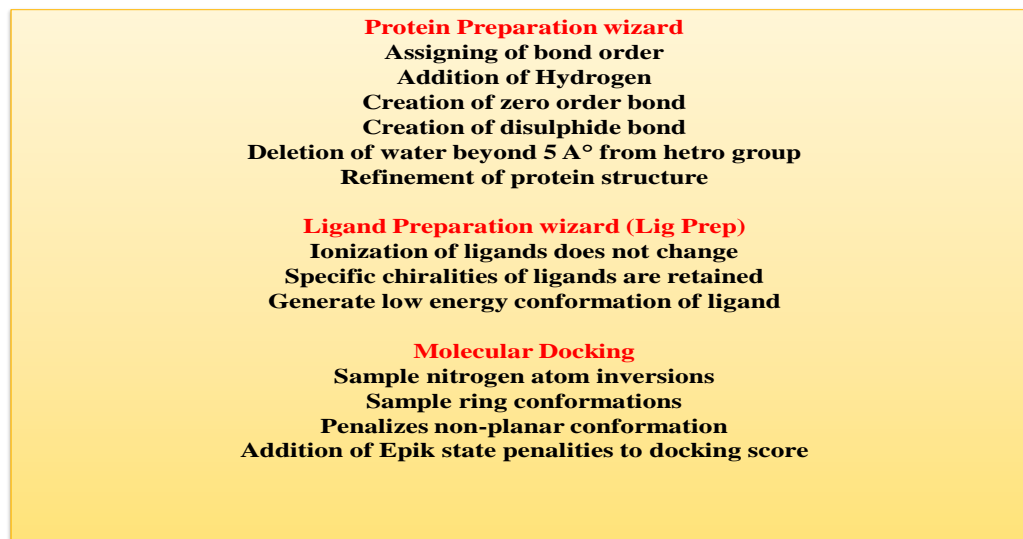
5.3 Maestro (molecular modelling environment) molecular docking; GLIDE (Grid based ligand docking with energetics) :

The grid-based ligand docking with energetics (GLIDE) application was used to perform molecular docking, and the output was expressed as G-score. The G-score is based on the empirical scoring function of non-covalent interactions and steric hindrances of buried polar groups (www.schrodinger.com). GLIDE is a multi-platform, robust, and centralized user interface that is particularly used to develop structures and to promptly and efficiently set up and tender calculations to Schrödinger's computational programs. There are mainly five types of non-covalent bonding i.e hydrogen bonds, hydrophobic forces, van der Waals forces, π - π interactions, electrostatic interactions that take place between a protein- ligand interaction (<https://en.wikipedia.org/wiki/Protein-ligand-complex>). Hydrophobic interactions prevailed in proteins and involved in protein folding and protein-ligand binding. Hydrogen bonds are formed between hydrogen atoms to an electronegative atom. Polar interactions (salt bridge) depend on the dielectric constant of the medium and the distance between the two polar groups. Van der Waals forces exist between non-polar group and in polar groups of the protein-ligand interactions. Halogen bond interactions are ascribed to the transfer of negative charge from a lewis base to a lewis acid.

5.4 GLIDE-HTVS (High-throughput virtual screening)

The advancement of genomic and proteomics approaches has led to a progressive increase in the last several decades in the finding of effective therapeutic targets. Drugs based on experimentation and computing are firmly used to identify lead compounds. The target proteins' biological function can be altered by the lead compounds. The most effective technique for quickly identifying a medication is HTVS. A computational screening technique called HTVS is widely used to screen compound library *in silico* groups. HTVS was performed by employing the GLIDE docking module of Maestro suite of Schrodinger software using OPLS _2005 force field (www.schrodinger.com, Schrödinger Release 2023-1: Glide, Schrödinger, LLC, New York, NY, 2021). Candidate ligand molecules (about 3,00,000) that were selected from a combination of compound Libraries like Asinex (<https://www.asinex.com>), Life chemicals

(<https://lifechemicals.com>), Chem Div (<https://www.chemdiv.com>), Enamine (<https://enamine.net/compound-libraries>), Selleckchem (www.selleckchem.com), Interbioscreen libraries (<https://www.ibscreen.com>) with subcategories of bioactive, FDA approved, natural, flavanoides and other highly specific inhibitor compound libraries were first docked using GLIDE-HTVS. Detailed selected parameters used for GLIDE-HTVS/XP molecular docking is represented in Fig 5.1. HTVS method was performed as it is specifically proven to discard non-binders' compounds by filtering for standard rule-of-five criteria. While molecular docking has demonstrated to be a useful tool to identify bioactive agents fast; there are still problems with the perfection and stability of scoring functions in HTVS methods. The construction of ligands were done using the Ligprep module of the Maestro application. The addition of hydrogen atoms, fixing of charges and group orientation, 2D to 3D conversion, corrected bond lengths and bond angles, low energy structure and correct chiralities, ionization states, tautomers, stereochemistry, ring conformation, and other functions were all made possible by this application for the ligand molecules. The Optimized Potential for Liquid Simulations (OPLS_2005) force field was then minimized and optimized (Jorgensen et al., 1996; Shivakumar et al., 2010; Gaur et al., 2023). Ultimately, a single conformation was created for every ligand, prepared for docking. Thus, using the relevant wizard applications, the input enzyme molecule was constructed, incorporating modifications into the original PDB structure, including the addition of hydrogen atoms, the assignment of bond orders, the formation of di-sulphide bonds, the formation of zero order bonds to metal, the fixing of charges, and the group orientation. The processes for ligand and protein preparation were completed, and then a receptor-grid file was formed. Scaling of the Van der Waal radii of receptor atoms by 1.00 Å with a partial atomic charge of 0.25 in order to execute the grid creation module was done. The receptor's active site offers a precise scoring function with thermodynamic ideal energy, which is computed using several sets of fields on a grid. Rigid receptor molecular docking with flexible ligands was done once the file for receptor-grid is created. The final energy assessment is based on the G-score. The lead molecules obtained after HTVS were then redocked with the more computationally expensive GLIDE-SP scoring functions.



35

Fig 5.1: Parameters used for GLIDE-HTVS/XP molecular docking

5.5 GLIDE- Standard Precision (SP) Docking: Following HTVS screening, the compounds were again put through a more rigorous Standard - precision (SP) screening process. Standard-precision (SP) docking is suitable for screening a large number of ligands with unknown quality. Glide SP takes roughly 10 seconds per compound to complete its comprehensive sampling, making it the ideal speed-accuracy ratio. The softer, more lenient function known as SP is effective in recognizing ligands with a moderate propensity to bind. This version is suitable for many database screening applications and aims to reduce false negatives (Friesner et al., 2004).

5.6 GLIDE Extra precision (XP)

GLIDE's XP mode employs a more exacting scoring mechanism. Only the finest ligand positions were being delineated for redocking using GLIDE-XP. The purpose of the GLIDE-XP approach is to eliminate spurious interactions between protein ligands and to improve the association between high scores and optimal binding. The final ligand compounds were subjected to molecular docking investigations using the GLIDE-XP Maestro molecular docking suite (Friesner et al., 2004; Halgren et al., 2004; Friesner et al., 2006). The compounds obtained from SP screening were then redocked into the active site of enzyme (PDB ID 2UUP) with the

more computationally expensive GLIDE-XP scoring functions. The ligands were constructed by employing the Ligprep module of the Maestro application. Ligprep carries out various ligand modifications, such as adding hydrogens, converting 2D to 3D, adjusting bond lengths and angles, low energy structure, stereochemistries, and ring conformation. Ligand performs optimally in the pH range of 7. In addition, another property like ionization remains constant, tautomers are not generated, and specific characteristics are retained; this is the default setting in the Maestro software. Subsequently, the force field optimum potential for liquid simulations (OPLS_2005) was used to assign all atom types and force field charges (Jorgensen et al., 1996; Shivakumar et al., 2010). At last, a single conformation was produced for every ligand, signifying that the molecules were prepared for docking. The chosen protein's X-ray structure was obtained from the PDB. The Maestro protein preparation wizard was being utilized to modify the raw PDB structure. Several modifications were made to the original structure of the selected protein: all water molecules were eliminated; hydrogen atoms were inserted; bond orders were assigned; di-sulfide bonds were formed; zero order bonds were created with metal; charges were fixed; and group orientations were altered. GLIDE Extra- precision (GLIDE-XP) module makes use of more stringent functions for scoring. GLIDE Extra- precision module makes use of more stringent functions for scoring. Depiction of the finest possible ligand positions can be obtained with the help of GLIDE XP. Application of GLIDE XP rules out any likelihood of false protein-ligand interactions by demonstrating a better relationship between optimum binding and quality scores (Friesner et al., 2006; Gaur et al., 2023). Docking confirmations holding least energy were chosen after docking of selected ligands into the target enzyme.

5.7 Molecular Dynamics simulation studies:

Molecular dynamics (MD) simulation offers a powerful tool for studying the dynamical properties and interactions of biomolecular complexes at the atomic level. In the present study, the dynamics as well as stability of a specific receptor-ligand complex were investigated using Desmond Molecular Dynamics simulation software, version 2021-1. The computational experiments were conducted on a high-performance Z2 TWR G4 workstation, equipped alongwith an Ubuntu 18.04.3 LTS 64-bit operating system, an Intel Core i7-9700 CPU, and an

NVIDIA Quadro P620/PCIe/SSE2 graphics processing unit. This setup provides a robust platform for conducting detailed molecular simulations, ensuring accurate and reliable results (Van Der Spoel et al., 2005). The initial preparation of the receptor-ligand complex for simulation involved the use of Desmond's system builder tool. This step included solvating the complex in an orthorhombic simulation box using the simple point-charge (SPC) explicit water model. The SPC water model is widely employed in molecular dynamics simulations due to its ability to realistically mimic the properties of water, thereby providing a more accurate simulation environment for the biomolecular complex. To simulate physiological conditions closely, the solvated complex was neutralized by adding an appropriate number of Na^+ and Cl^- counterions. Additionally, a salt concentration of 0.15 M was introduced to replicate the ionic strength typically found in biological systems. This careful preparation ensures that the simulated environment closely resembles the physiological conditions, which is crucial for obtaining biologically relevant insights from the simulation. The receptor-ligand complex was further characterized using the OPLS_3e force field, a widely recognized force field that provides high accuracy in modeling molecular interactions and energetics. The use of an explicit solvent model with SPC water molecules within the orthorhombic box is pivotal for capturing the dynamic hydration effects and solvation dynamics accurately. Following the system preparation, the Desmond Minimization protocol was applied for a duration of 100 picoseconds (ps) to relax the system, ensuring that any initial steric clashes or unfavorable conformations were resolved. Subsequent simulations ran at a constant temperature of 300 K and pressure of 1.0325 bar for 100 nanoseconds (ns).

These conditions were chosen to reflect standard biological conditions, providing a relevant context for evaluating the dynamics of the complex. The analysis of the simulation trajectory focused on the root-mean-square deviation (RMSD) fluctuations, that act as an essential indication of the complex's stability and changes in conformation over time. Furthermore, long-range electrostatic interactions were precisely calculated using the smooth particle mesh Ewald (SPME) approach, with a tolerance of $1\text{e-}09$ demonstrating a high degree of precision; short-range van der Waals and Coulomb interactions were controlled using a cutoff radius of 9.0 Å. To further dissect the interactions and dynamical behavior of the protein-ligand complex, the

Simulation Event Analysis tool of Desmond was employed (Cutinho et al., 2020) . This analysis provided detailed insights into the specific interactions stabilizing the complex, including hydrogen bonds, hydrophobic interactions, and ionic bonds, thereby enriching our understanding of the molecular basis of receptor-ligand recognition and binding. This comprehensive approach to molecular dynamics simulation underscores the utility of Desmond MD software in conjunction with advanced computational hardware for unraveling the intricate dynamics of biomolecular systems. Through careful system preparation, application of accurate force fields, and detailed analysis of simulation data, this study contributes valuable insights into the stability and interaction dynamics of the receptor-ligand complex under investigation (www.schrodinger.com).

5.8 Binding Free Energy Calculation studies:

The top virtual hit, WZB117 (S1)-2UUP, was subjected to post-simulation premier molecular mechanics generalized Born surface area (MM-GBSA) analysis using the thermal mmgbsa.py script from the Schrodinger's Prime module. For this analysis, the OPLS3e force field was employed. The Optimized Potentials for Liquid Simulations (OPLS) force field is designed to accurately model molecular interactions, including those critical for binding affinities in biological systems. The OPLS3e variant is an enhanced version that offers improved accuracy for a wide range of molecular properties, making it an excellent choice for this analysis. Additionally, the solvation effects were modeled using the VSGB (Variable Dielectric Generalized Born) solvent model. This model is designed to accurately account for the solvation energy, which is a critical component of the MM-GBSA calculation. It provides a sophisticated approach to estimating the effect of the solvent on the free energy of binding, which is essential for accurately predicting binding affinities in a biological context. Following the completion of the MD simulations, the trajectory frames were carefully selected at 1 ns interval for analysis. This sampling strategy was chosen to ensure that a representative set of configurations from the MD simulation was analyzed, covering the dynamical behavior of the complex over time.

The overall binding free energy calculated by the MM-GBSA method can be broken down into several components, reflecting different types of interactions and energies involved in the formation of the complex. The general equation for MM-GBSA calculations is given by:

$$\Delta G_{\text{bind}} = \Delta G_{\text{MM}} + \Delta G_{\text{Solv}} - T\Delta S$$

where

- ΔG_{bind} is the binding free energy of the ligand to the receptor.
- ΔG_{MM} is the gas-phase molecular mechanics energy, which includes the internal energy (E_{int}) electrostatic energy (E_{ele}) and van der Waals energy (E_{vdw})
- ΔG_{Solv} is the solvation free energy, which is further divided into polar (G_{polar}) and non-polar ($G_{\text{non-polar}}$) contributions. The polar contribution is often calculated using the Generalized Born (GB) model, and the non-polar part is typically estimated from the solvent accessible surface area (SASA).
- $T\Delta S$ represents the change in entropy upon binding at temperature T . This term is often difficult to calculate accurately and may be omitted or estimated using various approximation methods in practical MM-GBSA calculations.

5.9 Absorption, Distribution, Metabolism, Excretion and Toxicity (ADMET) studies:

Estimation of ADMET (Absorption, Distribution, Metabolism, Excretion, and Toxicity) properties of all the best-docked compounds obtained after Glide XP-docking was performed using QikProp application of Maestro.

Many compounds are not favourable during clinical trials on account of their weak ADMET properties like reduced solubility of the compound, the time needed for gastric emptying, passage time through the intestine, chemical endurance of compound inside the stomach, and the degree to which the compound is permeable into the intestinal wall which can influence the absorption of the compound after oral intake. Prediction of ADMET (Absorption, Distribution, Metabolism, Excretion, and Toxicity) properties of a compound through the use of *in silico* tools assists in getting rid of inappropriate compounds at the earlier stage of clinical trials before a lot of time and money is invested for initial screening of compounds. In this context, computer-based theoretical approaches assist as ideal options for the estimation of ADMET properties of newly selected compounds (Jorgensen & Duffy, 2002).

5.10 *in vitro* validation of lead compounds

Top two virtual hits were procured commercially, Cayman chemicals, USA (<https://www.caymanchem.com>).

Preparation of inocula

In accordance with the manufacturer's instructions, a double-strength tryptic soy broth (Sigma-Aldrich), which was then poured into test tubes in 10-milliliter portions and autoclaved. A 24-hour-old bacterial suspension grown in tryptic soy broth in a test tube was used to create a standardized inoculum of strains of bacterial culture suspensions of *Escherichia coli* (ATCC 8739), *Staphylococcus aureus* (ATCC 6538), *Pseudomonas aeruginosa* (ATCC 9027), and *Bacillus subtilis* (ATCC 6633) suspensions equivalent to 0.5 McFarland. To achieve a uniform bacterial suspension, this was mixed with the use of a vortex shaker. New, uninoculated broth was added to the mixture until the turbidity matched the 0.5 McFarland standard, or roughly 1.5×10^8 CFU/ml. 9 ml of freshly made double strength tryptic soy broth was mixed with 0.09 ml of the standardized bacterial suspension, needed to achieve a bacterial cell density of 5×10^5 CFU/ml. In line with conventional procedures, this was utilized within 30 minutes of preparation to stop a change in cell number.

5.10 (a). Antibacterial Activity Assay:

The screening of the top two compounds chosen for assessment of their antibacterial characteristics was conducted using the well-diffusion method in accordance with the established methodology (Bauer et al., 1966; CLSI, 2021).

In accordance with the manufacturer's instructions, Mueller-Hinton Agar (MHA) (Himedia Laboratories Pvt. India) was added to a sterile conical flask containing distilled water, and the mixture was heated until the MHA powder was completely dissolved. The completely clear Mueller-Hinton Agar (MHA) solution was autoclaved and later on dispensed in sterilized petri dishes (20 -25 ml) and left in a laminar airflow to solidify. Inoculum of *Escherichia coli* (ATCC 8739), *Staphylococcus aureus* (ATCC 6538), *Pseudomonas aeruginosa* (ATCC 9027), and *Bacillus subtilis* (ATCC 6633) procured commercially were seeded on newly prepared moisture-

free MHA surface. The plates were left for about 15 minutes for the agar surface to dry. After drying of agar surface, wells (6mm) were made with the help of cork borer and the wells were inoculated with the highest concentration (100 µg/ml) (50µl) of the selected virtual hits to be tested. After about 15 minutes of pre-diffusion, the plates were incubated at 37 °C for 24 hours. The mean of three duplicate measurements of the zone of clearance's diameter was used for presenting the results.

5.10 (b) Determination of Minimum Inhibitory Concentration (MIC)

The Minimum inhibitory Concentration (MIC) of each of the top two virtual hit compounds were evaluated by macrodilution method according to conventional techniques with some modifications (Andrews, 2001; EUCAST,2003; Malekinejad et al., 2012). The virtual hit compounds that were procured commercially were measured and added to DMSO to give a final concentration of 1000 µg/ml to form the stock solution. From the stock solution, different concentrations ranging from 200, 100, 80, 60, 40, 20, 10, 8 and 6 µg/ml were prepared. These concentrations were twice the final concentrations that were required, so these were mixed with an equal amount of media to get a final concentration of 100, 50, 40,30, 20, 10, 5, 4 and 3 µg/ml respectively.

MIC was conducted against *Escherichia coli* (ATCC 8739), *Staphylococcus aureus* (ATCC 6538), *Pseudomonas aeruginosa* (ATCC 9027), and *Bacillus subtilis* (ATCC 6633) (Commercially procured). Tests were performed in triplicates for each of the selected strains. 1.0 ml of diluted bacterial inoculum was added to 1.0 mL of each of the test compound dilution tube making total volume of 2 ml. For calculation of MIC, tubes were incubated at 37 °C for 24 hours. Ciprofloxacin was used as the control drug. Using spectrophotometric analysis at 600 nm, the tubes were examined to determine if any visible growth had formed throughout the incubation period. Additionally, the formula was used to determine the percentage of inhibition, and the minimum inhibitory concentration (MIC) was defined as the compound concentration at which the percentage of inhibition was greater than 95% (Wiegand et al.,2008; Akinduti et al., 2019, CLSI, 2020).

$$\text{Inhibition percentage (\%)} = 1 - \frac{\text{Test final 24} - \text{Test initial 0}}{\text{Broth final 24} - \text{Broth initial 0}} \times 100$$

Where, Test final₂₄: Absorbance of test (test compound+ bacterial cells) at 24 hours

Test initial₀: Absorbance of test (test compound+ bacterial cells) at 0 hours

Broth final₂₄: Absorbance of broth (broth + bacterial cells) at 24 hours

Broth initial₀: Absorbance of broth (broth + bacterial cells) at 0 hours (Negative Growth control)

5.10 (c) Calculation of minimum bactericidal concentration (MBC)

The MBC for the antimicrobials was determined using the dilution in broth method (CLSI, 2020). From each MIC tube and the above concentration tubes, 100 μ L of the broth was withdrawn. After that, 20–25 mL of molten Mueller-Hinton agar (cooled to 45–50°C) was poured into sterile Petri dishes containing the 100 μ L inoculum. The plates were swirled gently to mix evenly. They were incubated for 24 hours at 37 degrees Celsius, with MBC being recorded as the compound's lowest concentration at which colonies did not develop under these circumstances (Wiegand et al., 2008; CLSI, 2020).

5.10 (d) To Study the Effect of Lead Compounds on Bacterial Cell Morphology

The JEOL field emission Scanning Electron Microscope was used to examine the morphological changes in the bacteria after they were exposed to virtual lead molecules at their MIC concentrations. *Escherichia coli* (ATCC 8739), *Staphylococcus aureus* (ATCC 6538), *Pseudomonas aeruginosa* (ATCC 9027), and *Bacillus subtilis* (ATCC 6633) cells were cultured to 10^{7-8} CFU mL⁻¹ in 100 mL capacity flasks containing nutrient broth. Following the addition of lead compounds (S1 & S2) to bacterial cells at their corresponding MIC concentrations, the cells were incubated for 12 hours at 35 °C on a rotatory shaker (100 r/min). Following incubation, cells treated with lead compounds and untreated control cells were spun for 10 minutes at 5000 rpm. After three rounds of sterile PBS (1 \times) washing, the pellets were fixed for four hours at 4°C with occasional vortexing using 2.5% glutaraldehyde and 2% paraformaldehyde. Following three consecutive washes with 1 \times PBS, the cells were dehydrated for ten minutes each using an ethanol gradient (30, 50, 70, 90, and 100%). After air drying the cell biomass on glass slides, a 2

nm thin film of gold was sputter-coated. The coated samples were observed at an accelerating voltage of 10 kV using a Field emission Scanning Electron Microscope (Ahmed et al., 2020; Denney, 2019).

Analysis of Data: Significance of results was calculated by using Analysis of variance (ANOVA) by taking p value <0.05 as level of significance.

Chapter 6

Results & Discussion

Results & Discussion:

6.1 :Identification of potential lead molecules by molecular docking : High-throughput virtual screening (HTVS) , Standard Precision (SP) & XP (Extra Precision) Screening of compound libraries

The development of various compounds with potential medicinal applications has been greatly aided by the application of high-throughput virtual screening (HTVS) techniques. Millions of compounds, biological, pharmacological, or toxicological studies on these compounds can be swiftly finished by HTVS. With the help of these screening techniques, scientists can find active substances that can quickly alter a certain biomolecular route or mechanism. In molecular docking a compound with a desired chemical structure and biological activity is called a lead compound. The effectiveness of innovative drug design is largely dependent on the quality of a lead molecule, which has a direct impact on the quality of the therapeutic candidate. Virtual screening technology is a crucial research tool in lead compound discovery and optimization processes. It has the ability to separate a small number of active molecules from a vast number of small molecule candidates, reducing the number of potential targets for further experimental assays and increasing hit rate.

In this study, about 0.3 million compounds were taken from a combination of different libraries and docked into the active site of the *E. coli* MurD enzyme (PDB ID 2UUP). After the HTVS screening, the compounds were ranked according to their docking score, and the final 1367 compounds (Table. 6.1) were further docked in Glide's standard precision (SP) mode. One of the most advanced biopharmaceutical technologies is high-throughput virtual screening (HTVS), which uses computer algorithms to find biologically active compounds among massive amounts of chemical compound libraries. Furthermore, this approach frequently makes use of the prior screening of specialized libraries to evaluate their binding affinities and enhance their physicochemical characteristics (Tripathi et al., 2022).

Table 6.1: List of Lead molecules obtained after HTVS screening of various libraries

Compound ID	Glide Score	Compound ID	Glide Score
Y-39983 HCl.cdx	-7.138323	WAY-604652	-5.6915563
OG-L002.cdx	-6.677657	ALESSE (ethinyl estradiol).cdx	-5.6911585
S5409 Chelidamic acid hydrate.cdx	-6.314305	S4789 5-Acetylsalicylic acid.cdx	-5.685655
WAY-612625	-6.3654528	LM-3134 CH5138303.cdx	-5.6843136
XMD8-92.cdx	-6.2853218	vsw_1-LIGPREP-011-in.maegz:542	-5.6742348
WL-347672	-6.2080175	S3817 Harmine hydrochloride.cdx	-5.6993286
WAY-274713	-6.1922225	S4819 Saccharin.cdx	-5.6532366
S5410 Chloramphenicol sodium succinate.cdx	-6.1521563	vsw_1-LIGPREP-015-in.maegz:820	-5.6681453
TG 100713.cdx	-6.1292106	S4767 7-Hydroxy-3,4-dihydrocarbostyryl.cdx	-5.6461127
vsw_1-LIGPREP-015-in.maegz:992	-6.1032383	D-Luciferin.cdx	-5.6754142
RG108.cdx	-6.0808445	vsw_1-LIGPREP-015-in.maegz:861	-5.6333844
Methazolastone (Temozolomide).cdx	-6.0578749	S3936 7-Hydroxycarbostyryl.cdx	-5.6287837
Gemcitabine hydrochloride.cdx	-6.0484326	WAY-299598	-5.6899254
Ticarcillin sodium.cdx	-5.9871144	vsw_1-LIGPREP-011-in.maegz:574	-5.6231753
S3624 Quinolinic acid.cdx	-5.9995245	KD025 (SLx-2119).cdx	-5.6259294
S3676 Carbendazim.cdx	-6.0376672	DMXAA.cdx	-5.6050212
WAY-386549	-5.9476443	Foscarnet Sodium.cdx	-5.6004447
WAY-313101	-6.0972084	vsw_1-LIGPREP-006-in.maegz:344	-5.5914306
Taxifolin (Dihydroquercetin).cdx	-5.959297	LM-3086.cdx	-5.5839351
WAY-306077	-5.971832	WAY-341709	-5.5726561
Sodium Fluorophosphate.cdx	-5.9335207	CRT0066101.cdx	-5.575487
S3828 Orcinol glucoside.cdx	-5.909708	GDC-0068.cdx	-5.6116407
Go 6983.cdx	-5.942094	S9395 N-Benzoyl-(2R,3S)-3-phenylisoserine.cdx	-5.5629781
3-Methyladenine.cdx	-5.8950056	Bismuth subcitrate potassium.cdx	-5.5596053
BVD-523.cdx	-5.8735909	LM-3243 CRT0044876.cdx	-5.5583035
GSK2269557.cdx	-6.4818515	S3627 Tryptamine.cdx	-5.5551688
WAY-612628	-6.0911211	vsw_1-LIGPREP-015-in.maegz:809	-5.5541581
SRT2183.cdx	-5.8443813	WAY-384449	-5.912113
vsw_1-LIGPREP-006-in.maegz:426	-5.7902368	S4785 Nicotinamide N-oxide.cdx	-5.5492297
vsw_1-LIGPREP-011-in.maegz:531	-5.784928	Minocycline hydrochloride.cdx	-5.6559771
Takinib.cdx	-5.733869	vsw_1-LIGPREP-007-in.maegz:106	-5.7041409
S4717 Isatin.cdx	-5.7283831	S4799 Indole-3-acetic acid.cdx	-5.5139772
vsw_1-LIGPREP-006-in.maegz:84	-5.7354598	MK4827.cdx	-5.5105005
SSR128129E (SSR).cdx	-5.7210959	Irsogladine.cdx	-5.5104276
N6022.cdx	-5.7333011	Pioglitazone.cdx	-5.9896025
(+,-)-Octopamine hydrochloride.cdx	-5.7316933	WAY-306232	-5.5009422
WAY-235139	-5.8115139	S3693 2,6-Dihydroxypurine.cdx	-5.7394559

Compound ID	Glide Score	Compound ID	Glide Score
TAK-063.cdx	-5.49688028	LY 411575.cdx	-5.38910191
Dehydroepiandrosterone.cdx	-5.4907115	ABBV-075 (Mivebresib).cdx	-5.87698081
p276-00.cdx	-5.65108597	SB 742457.cdx	-5.3892678
CL-805459	-5.57432154	S4763 4-Hydroxychalcone.cdx	-5.38041908
Mirin.cdx	-5.55748969	S9361 Coumarin-3-carboxylic acid.cdx	-5.37642407
BI-78D3.cdx	-5.47322258	S3650 Penicillin V potassium salt.cdx	-5.37172775
vsw_1-LIGPREP-007-in.maegz:416	-5.47238375	Ellagic acid.cdx	-5.43017219
vsw_1-LIGPREP-011-in.maegz:105	-5.47238375	WAY-389361	-5.36756166
HTH-01-015.cdx	-5.47130017	Mefloquine hydrochloride.cdx	-5.36907155
GSK591 (EPZ015866, GSK3203591).cdx	-5.48448521	WAY-347144	-5.36334265
AEBSF hydrochloride .cdx	-5.46461027	vsw_1-LIGPREP-015-in.maegz:855	-5.36117002
S4719 Kynurenic acid.cdx	-5.46215808	vsw_1-LIGPREP-015-in.maegz:560	-5.37900339
Mercaptopurine.cdx	-5.57581642	Doxycycline hyclate.cdx	-5.57973042
FCE28073.cdx	-5.63823401	AZD 6482.cdx	-5.34743768
S5676 Zearalenone.cdx	-5.49075427	Piceatannol.cdx	-5.34498063
Chlortetracycline HCl.cdx	-5.64085481	vsw_1-LIGPREP-011-in.maegz:418	-5.34600271
Serotonin hydrochloride.cdx	-5.44223333	vsw_1-LIGPREP-011-in.maegz:95	-5.40885287
S5548 7-Hydroxy-4-chromone.cdx	-5.44674486	S5610 Indole-3-acetamide.cdx	-5.33618092
AS1517499.cdx	-5.4814111	vsw_1-LIGPREP-002-in.maegz:10	-5.92852545
WAY-336760	-5.45434138	vsw_1-LIGPREP-005-in.maegz:4	-5.92852545
vsw_1-LIGPREP-011-in.maegz:427	-5.44728614	WAY-626346	-5.33218491
vsw_1-LIGPREP-013-in.maegz:11	-5.44728614	S3661 2-Methoxy-1,4-naphthoquinone.cdx	-5.32866631
SecinH3.cdx	-5.4329356	Cyclocytidine hydrochloride.cdx	-5.32688774
S3754 4-Hydroxybenzoic acid.cdx	-5.42940473	Tioxolone.cdx	-5.32493844
vsw_1-LIGPREP-011-in.maegz:551	-5.44969606	WAY-308845	-5.31846801
vsw_1-LIGPREP-015-in.maegz:858	-5.44969606	Sulindac.cdx	-5.31737523
S3632 Trichloroisocyanuric acid.cdx	-5.42687265	Floxuridine.cdx	-5.34372804
S5159 Doxycycline.cdx	-5.65902434	S3800 Lycorine hydrochloride.cdx	-5.34516638
WAY-302734	-5.42159219	S3683 Methylmalonate.cdx	-5.32746253
Triflusal.cdx	-5.41216878	WAY-345462	-5.3096398
WAY-385023	-5.41187248	S3903 Lycorine.cdx	-5.34024221
WAY-333718	-5.40924083	vsw_1-LIGPREP-015-in.maegz:795	-5.30698661
Azlocillin sodium salt.cdx	-5.40820525	Torin 2.cdx	-5.3820781
CL-420396	-5.46239635	S4117.cdx	-5.75675677
WAY-627522	-5.44735668	S3968 Histamine.cdx	-5.75675677
S3947 Hydroumbellic acid.cdx	-5.3972788	Phloretin.cdx	-5.69298407
WAY-300430	-5.3906467	Mecarbinat.cdx	-5.29606077

Compound ID	Glide Score	Compound ID	Glide Score
S3799 Gentisic acid.cdx	-5.29414	vsw_1-LIGPREP-011-in.maegz:572	-5.18727929
WAY-608219	-5.29066175	WAY-357954	-6.07861373
WAY-271396	-5.284578	WAY-346647	-5.18338653
S5160 4-Methoxysalicylic acid.cdx	-5.28286545	S4739 Oxyresveratrol.cdx	-5.1808241
PF477736.cdx	-5.39293992	vsw_1-LIGPREP-015-in.maegz:789	-5.18049705
WAY-308352	-5.2769176	Methacycline hydrochloride.cdx	-5.46698262
Sarafloxacin hydrochloride.cdx	-5.33703279	amoxicillin.cdx	-5.36846606
S5557 Aklomide.cdx	-5.26158952	S5127 Spiculispore Acid.cdx	-5.17618015
WAY-308518	-5.26002374	WAY-307770	-5.17037032
WAY-613356	-5.25658806	Cysteamine HCl.cdx	-5.19203337
BLZ945.cdx	-5.26361686	LDN-212854.cdx	-5.17572093
EX527.cdx	-5.24449109	Hypoxanthine.cdx	-5.47933847
pim inhibitor I(SMI-4a).cdx	-5.30115922	vsw_1-LIGPREP-008-in.maegz:102	-5.16829412
UM171.cdx	-5.24726125	BAY 1895344.cdx	-5.70440546
vsw_1-LIGPREP-006-in.maegz:347	-5.25926803	XL019.cdx	-5.21258841
WAY-304753	-5.66087128	S9374 2',5'-Dihydroxyacetophenone.cdx	-6.53160976
vsw_1-LIGPREP-015-in.maegz:95	-5.24052044	S5505 2'-deoxyuridine.cdx	-5.16272235
S4801 6-Chloropurine.cdx	-5.49820316	S5226 L-carnosine.cdx	-5.9104632
S4946 2,3-Dihydroxybenzoic acid.cdx	-5.23281429	Glimepiride.cdx	-5.1842389
ALVESCO (ciclesonide).cdx	-5.23123174	Clodronate disodium.cdx	-5.16384148
WAY-625855	-5.23077265	937174-76-0.cdx	-5.15026851
S5051 Pipemidic acid.cdx	-5.27731527	WAY-389511	-5.1498239
ACTRON (ketoprofen).cdx	-5.2283302	vsw_1-LIGPREP-015-in.maegz:582	-5.13947982
PP2.cdx	-5.22555687	WAY-303885	-5.13847313
S3904 Isoimperatorin.cdx	-5.22464043	WAY-612666	-5.13762383
S4722 (+)-Catechin.cdx	-5.22257249	WL-309836	-5.14013567
A-966492.cdx	-5.49391546	CID755673.cdx	-5.13684055
vsw_1-LIGPREP-007-in.maegz:98	-5.21821386	S3691 4-Chlorosalicylic acid.cdx	-5.13010676
PP121.cdx	-5.21546006	WAY-327114	-5.3057803
PIK-294.cdx	-5.21394635	WAY-613212	-5.12824248
S4809 3-Indolepropionic acid.cdx	-5.214382	CID16020046 (CID 16020046).cdx	-5.53572224
WAY-633385	-5.20744379	WAY-309377	-5.13209154
vsw_1-LIGPREP-008-in.maegz:123	-5.20656369	Aloperine.cdx	-5.13303163
MYDRIACYL (tropicamide).cdx	-5.21089036	WAY-334111	-5.45174028
EPZ015666.cdx	-5.21565842	vsw_1-LIGPREP-011-in.maegz:813	-5.12221878
Lonidamine.cdx	-5.19307772	5-HTP.cdx	-5.11610129
PK11007.cdx	-5.19127644	vsw_1-LIGPREP-011-in.maegz:109	-5.111889

Compound ID	Glide Score	Compound ID	Glide Score
FPH2 (BRD-9424).cdx	-5.10995866	Oxfendazole.cdx	-5.25260788
L-Adrenaline.cdx	-5.12098027	S5317 UK 5099.cdx	-5.05154221
vsw_1-LIGPREP-008-in.maegz:109	-5.10852308	vsw_1-LIGPREP-015-in.maegz:867	-5.08872014
AG-490.cdx	-5.37734043	Paeonol.cdx	-5.25375127
WAY-352459	-5.10565767	SNX2112.cdx	-5.04977256
S4747 Jervine.cdx	-5.10541374	Lithocholic acid.cdx	-5.0534403
mepiroxol.cdx	-5.1046778	WAY-305569	-5.05208777
S5500 Amodiaquine hydrochloride.cdx	-5.69808703	EAI045.cdx	-5.05322396
vsw_1-LIGPREP-015-in.maegz:585	-5.10310139	WAY-630390	-5.0353008
S9003 (R)-(-)-Mandelic acid.cdx	-5.10247269	vsw_1-LIGPREP-015-in.maegz:551	-5.20605496
AS252424.cdx	-5.16102722	Ethamsylate.cdx	-5.03512379
GDC-0032 (RG-7604).cdx	-5.11588465	WAY-324207	-5.03346111
WAY-324683	-5.09794864	PF-06840003.cdx	-5.03906145
10-Hydroxycamptothecin.cdx	-5.09263806	S4781 Xanthoxylene.cdx	-5.29411177
Dihydromyricetin.cdx	-5.11935642	ifenprodil tartrate.cdx	-5.02301522
Methoxsalen.cdx	-5.08483182	WAY-299744-A	-5.61240426
vsw_1-LIGPREP-006-in.maegz:119	-5.122789	BI-D1870.cdx	-5.0527528
S3742 Cholic acid.cdx	-5.08678027	S4774 Xanthurenic Acid.cdx	-5.12706516
vsw_1-LIGPREP-011-in.maegz:559	-5.16656062	WAY-307691	-5.01458248
vsw_1-LIGPREP-015-in.maegz:572	-5.09514446	WAY-325350	-5.01208188
Uracil.cdx	-5.1295208	PRT-060318 (PRT318).cdx	-5.01191684
Mizoribine.cdx	-5.08745871	vsw_1-LIGPREP-015-in.maegz:104	-5.01532501
Zonisamide.cdx	-5.07592297	DEMADEX (torsemide).cdx	-5.43524598
Dinitolmide.cdx	-5.07407483	vsw_1-LIGPREP-011-in.maegz:416	-5.01013888
vsw_1-LIGPREP-007-in.maegz:119	-5.06900626	S5575 2-Benzoxazolinone.cdx	-5.01181673
TPCA-1.cdx	-5.06085307	Golgicide A.cdx	-5.04815649
vsw_1-LIGPREP-006-in.maegz:121	-5.06031284	WAY-296514	-5.00482234
S5601 Balofloxacin Dihydrate.cdx	-5.15663184	Shikimic acid.cdx	-5.00269375
S3858 Lawsone.cdx	-5.05727755	vsw_1-LIGPREP-006-in.maegz:104	-4.9963102
WAY-309235-A	-5.35933236	NMS-E973.cdx	-5.29681593
vsw_1-LIGPREP-004-in.maegz:85	-5.05719081	vsw_1-LIGPREP-006-in.maegz:102	-4.99515522
vsw_1-LIGPREP-007-in.maegz:148	-5.05719081	vsw_1-LIGPREP-015-in.maegz:548	-4.99515522
vsw_1-LIGPREP-011-in.maegz:782	-5.05719081	vsw_1-LIGPREP-008-in.maegz:114	-5.05915368
Olopatadine HCl.cdx	-5.05576009	Terbutaline sulfate.cdx	-5.00586653
GSK2879552.cdx	-5.1296599	Verinurad (RDEA3170).cdx	-5.02685714
Zoxazolamine.cdx	-5.05359147	vsw_1-LIGPREP-015-in.maegz:550	-4.99161846
WAY-320725	-5.0524484	WAY-625069	-4.98849469

Compound ID	Glide Score	Compound ID	Glide Score
S4884 Trans-Zeatin.cdx	-5.00871047	vsw_1-LIGPREP-011-in.maegz:560	-4.93014212
Myricetin.cdx	-5.02221559	vsw_1-LIGPREP-015-in.maegz:345	-4.93014212
Licochalcone A.cdx	-5.05364289	vsw_1-LIGPREP-015-in.maegz:647	-4.93014212
WAY-341921	-4.98225781	vsw_1-LIGPREP-011-in.maegz:96	-4.92975368
Nadifloxacin.cdx	-5.10366389	WAY-386884	-4.92901729
vsw_1-LIGPREP-015-in.maegz:852	-4.98022145	S3911 Veratramine.cdx	-4.92997973
WAY-307655	-4.97864013	vsw_1-LIGPREP-011-in.maegz:583	-4.92793305
Azaguanine-8.cdx	-6.18277481	S5023 Nadolol.cdx	-4.92796484
Isoprenaline hydrochloride.cdx	-4.97700578	RIMADYL (carprofen).cdx	-4.92624982
Climbazole.cdx	-5.02826341	WAY-299219	-4.92493007
P505-15.cdx	-4.96624823	BS-181.cdx	-4.92419594
Splitomicin.cdx	-4.96200707	Tranexamic acid.cdx	-4.9229499
Clofibric acid.cdx	-4.96124867	Ampicillin sodium.cdx	-5.14869623
S5211 4-Aminosalicylic acid.cdx	-4.9597244	ACTIN-N (nitrofurazone).cdx	-4.91981879
vsw_1-LIGPREP-011-in.maegz:790	-4.97479035	CCT245737.cdx	-5.45016612
Phenytoin sodium.cdx	-5.02926698	WAY-308859	-4.91746441
ORY-1001.cdx	-5.0000958	Coelenterazine.cdx	-4.92239354
S4784 Phloracetophenone.cdx	-5.0978798	LF3.cdx	-4.94253619
Kinetin.cdx	-4.96460072	SCH727965.cdx	-4.90891796
WAY-629120	-4.94446474	WAY-634700	-4.90837356
untitled.cdx	-5.35385468	S4833 Cefoxitin sodium.cdx	-4.90762905
WAY-229350	-4.9431379	OTS514.cdx	-4.90686293
TAK-659.cdx	-4.94241149	WAY-381809-A	-4.90918157
vsw_1-LIGPREP-015-in.maegz:118	-5.39815609	WAY-336578	-4.90562751
AMG-517.cdx	-4.94363385	WAY-247613	-4.90158007
vsw_1-LIGPREP-008-in.maegz:124	-5.06883225	GF 109203X(G 6850).cdx	-4.93543691
Biochanin A.cdx	-4.96410747	vsw_1-LIGPREP-015-in.maegz:112	-4.90044814
NU1025.cdx	-4.93875087	Voxtalisib (XL765, SAR245409).cdx	-5.31031827
Aloe-emodin.cdx	-4.93813356	S3942 Cardamonin.cdx	-5.25536698
WAY-639038	-4.93763737	WAY-347184	-4.89843516
ly404039.cdx	-5.1758664	WAY-326335	-4.89884571
SHP099.cdx	-4.94051	S3953 L-Lysine hydrochloride.cdx	-4.89351266
Sclareolide.cdx	-4.9364399	S5630 L-lysine.cdx	-4.89351266
AS604850.cdx	-4.99970263	WAY-352198	-4.89319756
vsw_1-LIGPREP-007-in.maegz:10	-4.93410264	vsw_1-LIGPREP-011-in.maegz:110	-4.89128824
vsw_1-LIGPREP-011-in.maegz:419	-4.93410264	vsw_1-LIGPREP-015-in.maegz:563	-4.93820333
vsw_1-LIGPREP-015-in.maegz:573	-5.10431373	vsw_1-LIGPREP-015-in.maegz:648	-4.93820333

Compound ID	Glide Score	Compound ID	Glide Score
S3665 Trolox.cdx	-4.88854875	A 922500.cdx	-4.85252359
S4586 4-Chloro-DL-phenylalanine.cdx	-4.88790505	WAY-648679	-4.84731174
LM-3282 MPI-0479605.cdx	-4.88567078	NVP-BVU972.cdx	-4.85246619
METI-DERM (prednisolone).cdx	-4.88269996	CP-724,714.cdx	-4.84556542
WAY-601882	-4.88240059	vsw_1-LIGPREP-006-in.maegz:99	-4.86916105
6H05.cdx	-4.90133443	Go6976.cdx	-4.84470596
bms-707035.cdx	-4.93477186	dynasore .cdx	-5.12309342
Synephrine hydrochloride.cdx	-4.89093975	Sodium picosulfate.cdx	-4.85556218
WAY-305552	-4.87908716	S9428 Brazilin.cdx	-4.9478183
Trelagliptin.cdx	-4.87885567	S4610 Mebendazole.cdx	-5.50062744
XMD8-87.cdx	-4.93452016	S2501 Pyrantel pamoate.cdx	-4.8415235
WAY-305391	-4.88490133	Yohimbine hydrochloride.cdx	-4.86565975
AZD7762.cdx	-4.87485043	AZD5363.cdx	-5.28733346
GI-526726	-4.8736011	WAY-643199	-4.83930742
vsw_1-LIGPREP-011-in.maegz:556	-4.87289753	S3898 Hydroxy Camptothecine.cdx	-4.8459318
vsw_1-LIGPREP-015-in.maegz:108	-4.87289753	WAY-642468	-4.83850815
ON123300.cdx	-5.48935554	S4606 Glutathione.cdx	-4.84303415
WAY-329626	-4.87112211	vsw_1-LIGPREP-007-in.maegz:105	-4.83004167
ABT-888(Veliparib).cdx	-5.51431385	S9251 Oxypeucedanin.cdx	-4.82692621
vsw_1-LIGPREP-015-in.maegz:578	-4.86987013	WAY-323423	-4.8328551
WAY-321433	-4.86962474	WAY-273428	-4.84704912
vsw_1-LIGPREP-011-in.maegz:97	-4.86947546	WAY-616773	-4.82567428
WAY-359060	-4.868418	WAY-657956	-4.82531357
WAY-326492	-4.8682884	Dehydroacetic acid.cdx	-4.84143659
WAY-305923	-4.94210621	WAY-656883	-4.83037077
S5237 Dihydroartemisinin acid.cdx	-4.86812572	Carsalam.cdx	-4.82019721
WAY-384811	-4.86242611	Xanthone.cdx	-4.81889204
CP 673451.cdx	-4.87174543	S5333 Sulbenicillin Sodium.cdx	-4.81824557
vsw_1-LIGPREP-006-in.maegz:105	-4.85770533	1.cdx	-4.81730382
S9438 Isosakuranetin.cdx	-4.87551176	WAY-389982	-4.81517149
S3879 kaempferide.cdx	-4.88572071	Adrucil (Fluorouracil).cdx	-5.01442281
Daphnetin.cdx	-4.87476619	Butein.cdx	-5.09100182
S3866 Galanthamine.cdx	-4.87248633	WAY-301515	-4.81367893
WAY-340898	-4.92721064	OSI-027.cdx	-4.81202927
WAY-605051	-4.85517812	S4715 Benzamide.cdx	-4.80543868
WAY-643862	-4.85910982	KX2-391.cdx	-4.8596249
vsw_1-LIGPREP-011-in.maegz:586	-4.85348361	AT7519.cdx	-5.21436321

Compound ID	Glide Score	Compound ID	Glide Score
AT7519 HCl.cdx	-5.21436321	Chrysophanic acid.cdx	-4.76804662
vsw_1-LIGPREP-004-in.maegz:148	-4.80345033	S3945 L-Cycloserine.cdx	-5.01445396
vsw_1-LIGPREP-008-in.maegz:101	-4.80195957	Oxacillin sodium monohydrate.cdx	-4.76737687
S4761 Thymoquinone.cdx	-4.80136423	IOX2.cdx	-4.86356125
S4749 Citalopram HBr.cdx	-4.80209987	PENETREX (enoxacin).cdx	-4.81210782
WAY-352532	-4.80005795	vsw_1-LIGPREP-008-in.maegz:107	-4.76489456
WAY-237727	-4.79996944	CETACORT (hydrocortisone).cdx	-4.76476182
S9440 Naringenin chalcone.cdx	-5.35724735	vsw_1-LIGPREP-007-in.maegz:100	-4.78563177
S4766 Gibberellic acid.cdx	-4.79827542	WAY-276831	-4.76279598
XEN445.cdx	-4.79793496	SKI II (SphK-I2).cdx	-4.76264662
WAY-385813	-4.79724134	GSK1265744.cdx	-5.37550098
GNE-317.cdx	-4.79401317	3PO.cdx	-4.75812235
Linagliptin.cdx	-4.79307379	Hydroxychloroquine sulfate.cdx	-4.80667243
S5173 2'-Hydroxy-4'-methylacetophenone.cdx	-4.91007599	WAY-304514	-4.75622221
Ganetespib(STA-9090).cdx	-4.79782078	vsw_1-LIGPREP-006-in.maegz:96	-4.77272861
vsw_1-LIGPREP-015-in.maegz:856	-4.79052675	Quercetin.cdx	-4.78509266
Dexamethasone.cdx	-4.78553371	vsw_1-LIGPREP-015-in.maegz:561	-5.22320658
ZM306416.cdx	-4.78492047	dihydroartemisinin.cdx	-4.75282437
Dopamine hydrochloride.cdx	-4.78317645	WAY-384178	-4.74828905
S3941 Pinocembrin.cdx	-4.80128091	Bindarit.cdx	-4.74624966
Erdosteine.cdx	-4.78240546	TCID.cdx	-4.74499627
CL-417716	-4.86918405	GSK2801.cdx	-4.74497615
S9092 Norisoboldine.cdx	-4.81614713	WAY-616062	-4.74269316
vsw_1-LIGPREP-015-in.maegz:531	-4.97999013	STF-31.cdx	-4.7397152
WAY-272651	-4.78031273	WAY-347742	-4.73893189
WAY-635250	-4.78023275	SB-269970 HCl.cdx	-4.74614085
S9380 5,7-Dihydroxy-4-methylcoumarin.cdx	-4.84230505	WAY-307597	-4.73834187
LY2811376.cdx	-4.8151061	S3625 Tyramine.cdx	-4.73788881
S5286 Ramatroban.cdx	-4.77996089	WAY-303558	-4.74365902
Kaempferol.cdx	-4.81005159	S9442 Bergaptol.cdx	-4.92592802
WAY-331439	-4.77695577	Skp2 inhibitor C1 (SKPin C1).cdx	-4.73108758
WAY-269431	-4.77681285	Chlorzoxazone.cdx	-4.76196251
S5168 Anthraquinone.cdx	-4.77547876	Naringenin.cdx	-4.74544631
WAY-113767	-4.77334788	S4246.cdx	-4.75584261
S4710 Picolinamide.cdx	-4.77326104	BAY-61-3606.cdx	-4.75671775
RITA (NSC 652287).cdx	-4.77234488	WAY-305911	-5.15440278
vsw_1-LIGPREP-015-in.maegz:417	-4.77005229	S4783 Benzyl isothiocyanate.cdx	-4.83359281

Compound ID	Glide Score	Compound ID	Glide Score
WAY-309523-A	-4.7260087	WAY-359135	-4.6843922
EPI-001.cdx	-4.72415458	vsw_1-LIGPREP-007-in.maegz:387	-4.71389413
CC-122.cdx	-4.72384537	vsw_1-LIGPREP-008-in.maegz:104	-4.68298671
Amiloride hydrochloride dihydrate.cdx	-4.7244323	WAY-388117	-4.68205575
WAY-324849	-4.722015	WAY-337131	-4.69193148
Palonosetron HCl.cdx	-4.72102077	vsw_1-LIGPREP-015-in.maegz:422	-4.81768432
WAY-383501	-4.71915194	CP21R7 (CP21).cdx	-4.68700954
WAY-601880	-4.71812825	S3651 4-Amino-5-imidazolecarboxamide.cdx	-4.99954495
WAY-382527	-4.71782307	WAY-330793	-4.67541654
AZD1080.cdx	-5.03343479	JNJ-7706621.cdx	-4.67267921
NAQUIVAL (trichlormethiazide).cdx	-5.3439566	S9359 Anthraquinone-2-carboxylic Acid.cdx	-4.67225403
IPA-3.cdx	-4.7250486	WAY-630009	-4.78334792
AG14361.cdx	-4.807241	Rufinamide.cdx	-4.67042992
S9364 6-Hydroxycoumarin.cdx	-4.70951559	S5166 Benzoyleneurea.cdx	-4.67632596
vsw_1-LIGPREP-011-in.maegz:417	-4.84835621	SU6656.cdx	-4.66892985
Gramine.cdx	-4.72417459	vsw_1-LIGPREP-015-in.maegz:863	-4.66580236
LY2109761.cdx	-4.77141298	S3939 4'-Methoxyresveratrol.cdx	-4.6695047
(R)-Nepicastat HCL(RS-25560-198).cdx	-5.07244801	S9228 Schisandrin C.cdx	-4.66241195
S4894 D-Glucurone.cdx	-4.70799485	WAY-386031	-4.6618407
WAY-325898	-4.78698608	WAY-383468	-4.66161666
VGX-1027.cdx	-4.70161923	UPF-1069.cdx	-4.66113251
vsw_1-LIGPREP-015-in.maegz:961	-4.70040012	WAY-323401	-4.66031963
WAY-606601	-4.94329176	S4750 Sulfacetamide sodium salt hydrate.cdx	-4.67757385
S3698 Nortriptyline (hydrochloride).cdx	-4.70035189	WAY-346373	-4.7921764
S9107 Glycitein.cdx	-4.70746846	S3621 Pazufloxacin (mesylate).cdx	-4.76867928
vsw_1-LIGPREP-004-in.maegz:99	-4.69837625	S3989 L-Hisidine.cdx	-5.11186774
WAY-351402	-4.69640698	WAY-355031	-4.65324847
WAY-606496	-4.69616883	abt-751.cdx	-4.65306044
WAY-625727	-4.69306552	WAY-323095	-4.64872856
UMI-77 .cdx	-4.84450799	NLG-919.cdx	-4.82207683
WAY-601527	-4.6915947	vsw_1-LIGPREP-004-in.maegz:115	-4.64620969
Adenosine Dialdehyde (ADOX).cdx	-4.72651137	vsw_1-LIGPREP-015-in.maegz:419	-4.64620969
Hematoxylin.cdx	-4.80905864	S5031 Sulfaquinoxaline sodium.cdx	-4.92446178
WAY-221951	-4.6894427	vsw_1-LIGPREP-006-in.maegz:120	-4.66904441
URB597.cdx	-4.68834954	sp600125.cdx	-4.64436303
WAY-320546-A	-4.6894634	ENMD-2076.cdx	-4.95836305
WAY-332548	-4.68990498	WAY-303778	-4.6469563

Compound ID	Glide Score	Compound ID	Glide Score
Celastrol.cdx	-4.64762712	WAY-659163	-4.76916391
S3629 Syringic acid.cdx	-4.63446147	vsw_1-LIGPREP-007-in.maegz:406	-4.66730668
Bromodeoxyuridine.cdx	-4.68025312	S4969 Tropine.cdx	-4.60244238
WAY-307791	-4.63349661	WAY-657436	-4.6012749
WP1066.cdx	-4.63451401	A 205804.cdx	-4.59973906
S9179 Catharanthine hemitartrate.cdx	-4.82002488	WAY-307237-A	-4.60442001
Cryptotanshinone.cdx	-4.62960131	S3795 Phloretic acid.cdx	-4.59771589
WAY-624461	-4.62862533	WAY-384181	-4.59719263
S5711 Deracoxib.cdx	-4.62905653	Diclazuril.cdx	-4.99381602
Cinchophen.cdx	-4.62882286	Danofloxacin mesylate.cdx	-4.75734401
WAY-383479	-4.62645132	WAY-604481	-4.59573222
vsw_1-LIGPREP-015-in.maegz:874	-4.62454141	WAY-345999	-4.59533996
vsw_1-LIGPREP-007-in.maegz:96	-4.62373777	S4590 Dithranol.cdx	-4.59482828
Cyromazine.cdx	-4.62924507	CL-426691	-4.63283431
WAY-302510	-4.66493224	LGK-974.cdx	-4.6085667
WAY-623751	-4.62321298	Melphalan.cdx	-4.59303389
WAY-272666	-4.62144333	Bepotastine besilate.cdx	-4.59777342
Pravastatin sodium.cdx	-4.62326024	WAY-351626	-4.59268262
Chloroxylenol.cdx	-4.62038307	vsw_1-LIGPREP-015-in.maegz:817	-4.58985156
S4863 4-Hydroxyphenylacetic acid.cdx	-4.61860593	WAY-337998	-4.62488256
S5541 Dimetridazole.cdx	-4.61619286	vsw_1-LIGPREP-011-in.maegz:576	-4.61433414
AZD3759.cdx	-4.92988425	vsw_1-LIGPREP-011-in.maegz:650	-4.81203651
WAY-633981	-4.70682808	vsw_1-LIGPREP-015-in.maegz:10	-4.81203651
WAY-341446	-4.61379319	AZ628.cdx	-4.58852311
S4769 L-5-Hydroxytryptophan.cdx	-4.61330192	WAY-600.cdx	-4.65692039
vsw_1-LIGPREP-015-in.maegz:554	-4.61404599	WAY-629296	-4.58666496
NPS-2143.cdx	-4.61849874	S5603 5-Bromocytosine.cdx	-4.5891897
Besifloxacin HCl.cdx	-4.67656996	VER-49009.cdx	-5.12469618
PYRAZINAMIDE (pyrazinamide).cdx	-4.60977179	WAY-642047	-4.58522053
vsw_1-LIGPREP-006-in.maegz:101	-4.61263955	S9205 Hydroxygenkwanin.cdx	-4.58482168
vsw_1-LIGPREP-006-in.maegz:415	-4.61263955	WAY-384659	-4.66701286
vsw_1-LIGPREP-011-in.maegz:547	-4.61263955	WAY-627930	-4.68709252
vsw_1-LIGPREP-011-in.maegz:554	-4.60773195	WAY-346583	-4.57932689
vsw_1-LIGPREP-015-in.maegz:416	-4.60773195	WAY-337265	-4.57861067
vsw_1-LIGPREP-015-in.maegz:955	-4.60773195	Verubecestat (MK-8931).cdx	-4.59882385
S5307 2'-deoxy-2'-fluoro-2'-C-methyluridine.cdx	-4.60935321	WAY-330577	-4.57634837
LY2874455.cdx	-4.60592425	WAY-305334	-4.63089225

Compound ID	Glide Score	Compound ID	Glide Score
10058-F4.cdx	-5.15452386	vsw_1-LIGPREP-011-in.maegz:553	-4.53993928
WAY-389574	-4.5761019	S9291 Isopimpinellin.cdx	-4.53721374
GDC-0879.cdx	-4.57859236	S5512 Juglone.cdx	-4.55244913
vsw_1-LIGPREP-007-in.maegz:102	-4.57271666	SGC2085.cdx	-4.64547203
CHENIX (chenodiol).cdx	-4.57388725	S4869 Sulfamethoxazole sodium.cdx	-4.54324587
vsw_1-LIGPREP-015-in.maegz:541	-4.56637538	WAY-333361	-4.53332357
S4936 Antiarol.cdx	-4.56511801	vsw_1-LIGPREP-006-in.maegz:108	-4.53296893
EXJADE (deferasirox).cdx	-4.56967183	WAY-306938	-4.53264086
Fisetin.cdx	-4.59286535	S9272 Koumine.cdx	-4.53255637
WAY-623531	-4.56173376	WAY-611601	-4.53076024
WAY-302117	-4.56161265	S5010 Indometacin Sodium.cdx	-4.53081078
WAY-278430	-4.56115723	Tamibarotene.cdx	-4.5285463
S5128 Orsellinic acid ethyl ester.cdx	-4.60093231	FH535.cdx	-4.88102647
ARRY-380 (ONT-380, Irbinetinib).cdx	-5.02367287	vsw_1-LIGPREP-011-in.maegz:112	-4.57996184
vsw_1-LIGPREP-011-in.maegz:795	-4.55993932	WAY-326257	-4.52766761
vsw_1-LIGPREP-008-in.maegz:110	-4.56952107	WAY-308293	-4.52538098
Labetalol hydrochloride.cdx	-4.58492935	Dimesna.cdx	-4.52478788
2-D08.cdx	-4.56231169	S3702 Dihydrothymine.cdx	-4.52267814
vsw_1-LIGPREP-008-in.maegz:10	-4.55542209	vsw_1-LIGPREP-011-in.maegz:555	-4.51901587
vsw_1-LIGPREP-015-in.maegz:564	-4.55542209	WAY-309382	-4.51822799
Marbofloxacin.cdx	-4.61164155	Tranilast.cdx	-4.51480971
SP2509.cdx	-4.58680491	WAY-614321	-4.51414854
Broxyquinoline.cdx	-4.6018258	CZC24832.cdx	-4.51398324
vsw_1-LIGPREP-011-in.maegz:102	-4.55228954	WAY-327809	-4.51759362
4SC-202.cdx	-4.55135535	S9315 Praeruptorin A.cdx	-4.51146287
PF 3716556.cdx	-5.02489028	WAY-271196	-4.54925832
vsw_1-LIGPREP-011-in.maegz:647	-4.55029135	S4574 Piperazine.cdx	-4.52294784
vsw_1-LIGPREP-015-in.maegz:557	-4.55029135	Levosulpiride.cdx	-4.50886803
WAY-348213	-4.54751303	WAY-324781	-4.51269783
PF-06463922.cdx	-4.88364025	WAY-347993	-4.50828885
S4778 o-Veratraldehyde.cdx	-4.54743622	AZD1981.cdx	-4.50726555
Necrostatin-1.cdx	-4.54702304	WAY-325619	-4.50606582
vsw_1-LIGPREP-008-in.maegz:122	-4.55556201	A-366.cdx	-4.5053926
S4963 Purpurin.cdx	-4.65794501	S4804 1-Naphthyl acetate.cdx	-4.50516555
WAY-272676	-4.54356983	PP442.cdx	-4.50504095
WAY-325091	-4.54054227	vsw_1-LIGPREP-006-in.maegz:127	-4.56091871
vsw_1-LIGPREP-004-in.maegz:106	-4.53993928	vsw_1-LIGPREP-008-in.maegz:13	-4.56091871

Compound ID	Glide Score	Compound ID	Glide Score
vsw_1-LIGPREP-015-in.maegz:151	-4.56091871	Genistein.cdx	-4.48714161
Dapivirine.cdx	-4.50456701	vsw_1-LIGPREP-006-in.maegz:100	-4.90917822
S4861 Oxindole.cdx	-4.49688927	vsw_1-LIGPREP-011-in.maegz:814	-4.64985071
WAY-386646	-4.5118671	AMINOPHYLLINE (aminophylline).cdx	-4.49249402
WAY-307439	-4.49449566	PROFENAL (suprofen).cdx	-4.45934456
NEVIRAPINE (nevirapine).cdx	-4.49370945	WAY-277378	-4.66741833
WAY-390008	-4.49362537	Latrepirdine.cdx	-4.53567079
vsw_1-LIGPREP-015-in.maegz:798	-4.49517853	azd6244.cdx	-4.46386937
vsw_1-LIGPREP-015-in.maegz:807	-4.69554683	WAY-614277	-4.47272373
GNF-5.cdx	-4.48852524	vsw_1-LIGPREP-015-in.maegz:110	-4.54319239
ARQ 092.cdx	-4.5133403	vsw_1-LIGPREP-007-in.maegz:157	-4.45203323
S4634 SULFADIAZINE SODIUM.cdx	-4.64321939	WAY-351979	-4.45180952
WAY-335432	-4.55656998	CATAFLAM (diclofenac potassium).cdx	-4.45246581
vsw_1-LIGPREP-006-in.maegz:85	-4.48476648	Evista (Raloxifene Hydrochloride).cdx	-4.46582494
WAY-302823	-4.69930668	WAY-310989	-4.4672006
CB-5083.cdx	-4.48402458	S4582 Eflornithine hydrochloride hydrate.cdx	-4.72870685
WAY-384609	-4.483818	Cl-amidine.cdx	-4.93639166
SB239063.cdx	-4.51450001	BMS265246.cdx	-4.44399889
vsw_1-LIGPREP-011-in.maegz:644	-4.48299691	WAY-381805	-5.44447047
Ciprofibrate.cdx	-4.48257254	S9020 Dihydratanshinone I.cdx	-4.44294143
Apoptosis Activator II.cdx	-4.48221257	SULFADIAZINE (sulfadiazine).cdx	-4.59800517
Tenalisib (RP6530).cdx	-4.5017714	Sulphadimethoxine.cdx	-4.57698035
LY3023414.cdx	-4.47804415	Danthron.cdx	-4.44045254
WAY-311599	-4.90326257	WAY-348569	-4.46583938
vsw_1-LIGPREP-006-in.maegz:114	-4.4754255	vsw_1-LIGPREP-015-in.maegz:555	-4.44136422
KPT-330.cdx	-4.47147151	vsw_1-LIGPREP-008-in.maegz:151	-4.43649528
WAY-330860	-4.47590008	vsw_1-LIGPREP-011-in.maegz:789	-4.47120688
ADL5859.cdx	-4.47078877	Kartogenin.cdx	-4.43259719
WAY-337770	-4.46996356	TWS119.cdx	-4.43231531
MK-8245.cdx	-4.4704787	Sodium ascorbate.cdx	-4.43270012
WAY-642085	-4.46939061	WAY-114700	-4.43131381
WAY-302425	-4.4809389	vsw_1-LIGPREP-015-in.maegz:960	-4.43985481
Rosiglitazone maleate.cdx	-5.80119263	Ciclopirox.cdx	-4.42814726
WAY-348393	-4.46686894	E-64c (Loxistatin Acid).cdx	-4.42784347
vsw_1-LIGPREP-007-in.maegz:107	-4.49526891	Dovitinib Lactate.cdx	-4.65051736
WAY-269433	-4.46395081	Betamipron.cdx	-4.42761069
AZ 960.cdx	-4.74147297	GSK2656157.cdx	-4.43236908

Compound ID	Glide Score	Compound ID	Glide Score
WAY-642438	-4.4254498	vsw_1-LIGPREP-006-in.maegz:115	-4.99330182
S4559 Cloxiquine.cdx	-4.49385655	vsw_1-LIGPREP-015-in.maegz:124	-4.41517565
Doxofylline.cdx	-4.42475506	CHIR-99021 (CT99021) hcl.cdx	-4.9044431
ARQ-197.cdx	-4.48771582	vsw_1-LIGPREP-011-in.maegz:802	-4.40305817
Scopine.cdx	-4.75799582	Baicalein.cdx	-4.4537018
WAY-627929	-4.47433831	S4953 Usnic acid.cdx	-5.32518907
vsw_1-LIGPREP-015-in.maegz:530	-4.4579942	procodazole.cdx	-4.44162347
vsw_1-LIGPREP-015-in.maegz:556	-4.42375012	WAY-299622	-4.4120619
S4599 Benzyl benzoate.cdx	-4.42265933	WAY-626487	-4.39655528
S5446 2-Chloro-1-(4-fluorobenzyl)benzimidazole.cdx	-4.42096079	vsw_1-LIGPREP-015-in.maegz:566	-4.45394203
IQ-1.cdx	-4.50578859	vsw_1-LIGPREP-015-in.maegz:801	-4.45394203
JIB04 (NSC693627).cdx	-4.41967661	WAY-325131	-4.41455438
WAY-614930	-4.41852761	S3692 N-Ethylmaleimide.cdx	-4.39387523
WAY-388100	-4.41807372	TMP195.cdx	-4.3937572
vsw_1-LIGPREP-015-in.maegz:421	-4.4169375	WAY-646502	-5.27397803
WAY-345925	-4.41916797	vsw_1-LIGPREP-001-in.maegz:10	-4.45801131
vsw_1-LIGPREP-015-in.maegz:876	-4.41637686	Aceclidine Hydrochloride.cdx	-4.39315266
WAY-612005	-4.41600615	vsw_1-LIGPREP-006-in.maegz:110	-4.39179229
vsw_1-LIGPREP-008-in.maegz:98	-4.41594791	vsw_1-LIGPREP-007-in.maegz:417	-4.39179229
vsw_1-LIGPREP-007-in.maegz:112	-4.41502577	S5578 Cadaverine.cdx	-4.39179229
WAY-323928	-4.41581996	WAY-321215	-4.39149283
vsw_1-LIGPREP-015-in.maegz:877	-4.41802218	WAY-383247	-4.39069524
CP868569.cdx	-4.42841998	WAY-628395	-4.60564949
CH5126766 (RO5126766).cdx	-4.8657199	WAY-311621	-4.38974754
WAY-602544	-4.41259832	vsw_1-LIGPREP-004-in.maegz:149	-4.40984055
TSU-68 (SU6668).cdx	-4.41321864	vsw_1-LIGPREP-011-in.maegz:792	-4.40984055
WAY-625114	-4.41139085	vsw_1-LIGPREP-015-in.maegz:544	-4.40984055
WAY-604346	-4.41117988	AZD2281.cdx	-4.38873721
vsw_1-LIGPREP-008-in.maegz:117	-4.4110016	Pilocarpine HCl.cdx	-4.58273021
Y-27632 2HCL.cdx	-4.41060338	WAY-240321	-4.38836314
prasugrel.cdx	-4.63652249	WZB117.cdx	-4.38762058
S3940 3'-Hydroxypterostilbene.cdx	-4.40992613	WAY-346250	-4.38719254
Tasquinimod .cdx	-4.50852233	S 38093.cdx	-4.38749215
WAY-304820	-4.40824858	WAY-329501	-4.38429838
WAY-303536-A	-4.53153455	S9375 2'-Hydroxyacetophenone.cdx	-5.25645189
LJI308.cdx	-4.8666571	HJC0152.cdx	-4.38771166
AZD1208.cdx	-4.46136554	CC-930.cdx	-4.38624004

Compound ID	Glide Score	Compound ID	Glide Score
Cilostazol.cdx	-4.3808388	SGX-523 .cdx	-4.34882676
WAY-331407	-4.38247071	NSC697923.cdx	-4.34691448
Riociguat(BAY 63-2521).cdx	-4.38275013	WAY-382680	-4.34669945
WAY-323934	-4.38043607	S4793 Cedryl acetate.cdx	-4.34654452
Creatinine.cdx	-4.37888663	WAY-327891	-4.35804312
vsw_1-LIGPREP-007-in.maegz:150	-4.3843481	BKM-120.cdx	-4.34411095
WAY-306112	-4.37856374	OAC1.cdx	-4.71893615
Homatropine bromide.cdx	-4.37725455	WAY-384035	-4.33936046
WAY-631071	-4.3769063	S3980 Pyridoxine.cdx	-4.56309504
BMS863233.cdx	-4.75746496	S5060 Metadoxine.cdx	-4.56309504
SULLA (sulfameter).cdx	-4.75044423	WAY-604503	-4.33886185
S9240 Isofraxidin.cdx	-4.38488526	WAY-240561	-4.33688902
vsw_1-LIGPREP-015-in.maegz:347	-4.45349616	S4580 Hydroquinone.cdx	-4.3348331
GSK2141795.cdx	-4.37354365	vsw_1-LIGPREP-008-in.maegz:345	-4.36401825
Ethacridine lactate monohydrate.cdx	-4.37124523	vsw_1-LIGPREP-015-in.maegz:558	-4.36401825
E-64.cdx	-4.37022983	S9233 Imperialine.cdx	-4.34497543
WAY-624113	-4.37021211	WAY-631007	-4.33326493
ronidazole.cdx	-4.36850398	WAY-332724	-4.33324274
WAY-322960	-4.36722552	7,8-Dihydroxyflavone.cdx	-4.35583401
vsw_1-LIGPREP-007-in.maegz:120	-4.37716092	TDZD-8.cdx	-4.33260506
Nicotinamide.cdx	-4.36539254	CX-4945.cdx	-4.33247927
Pefloxacin mesylate.cdx	-4.52549838	WAY-305231	-4.33152856
BAY 73-4506.cdx	-4.36519297	S4780 7-Methoxy-4-methylcoumarin.cdx	-4.33100855
S4649 Atipamezole hydrochloride.cdx	-4.45142651	GSK-LSD1 dihydrochloride.cdx	-4.70942977
WAY-347315	-4.36240691	BDA-366.cdx	-4.34552247
WAY-630557	-4.3663673	Tubercidin.cdx	-4.33077353
WAY-236488	-4.36060397	LDC000067.cdx	-4.32920804
WAY-324212	-4.76090021	WAY-302404	-4.32898811
vsw_1-LIGPREP-007-in.maegz:91	-4.47650776	AG-879.cdx	-4.33669731
S3674 Levamlodipine.cdx	-4.36343804	Artemisinin.cdx	-4.32850215
vsw_1-LIGPREP-008-in.maegz:148	-4.3581523	vsw_1-LIGPREP-011-in.maegz:584	-4.32663711
BFH772.cdx	-4.35722343	WAY-643352	-4.32660489
A-674563.cdx	-4.37758558	olsalazine sodium.cdx	-4.32600175
S9500 Valbenazine tosylate.cdx	-4.60258904	S3820 Dehydroevodiamine hydrochloride.cdx	-4.32433928
WAY-624696	-4.35259861	XMD16-5.cdx	-4.48888095
WAY-612430	-4.3491103	WAY-311539	-4.33688982
PQ 401.cdx	-4.64574127	WAY-340674	-4.32349707

Compound ID	Glide Score	Compound ID	Glide Score
vsw_1-LIGPREP-011-in.maegz:561	-4.94819938	LCI699.cdx	-4.38799049
S4585 Succinylsulfathiazole.cdx	-4.61857765	8-OH-DPAT (8-Hydroxy-DPAT).cdx	-4.29208722
WAY-626271	-4.32218175	Felodipine.cdx	-4.29197101
Daprodustat (GSK1278863).cdx	-4.32236263	S9162 Rubimallin.cdx	-4.32183961
vsw_1-LIGPREP-007-in.maegz:425	-4.32657731	WAY-303506-A	-4.49305962
WAY-627937	-4.32002075	FR 180204.cdx	-4.29149516
WAY-629128	-4.37389513	WAY-325177	-4.29074106
WAY-620263	-4.37966513	WAY-642747	-4.35040069
METOLAZONE (metolazone).cdx	-4.31912925	vsw_1-LIGPREP-007-in.maegz:104	-4.28938594
WAY-340247	-4.35261031	vsw_1-LIGPREP-011-in.maegz:541	-4.29046779
VE-822.cdx	-4.331126	SF1670 (PTEN inhibitor).cdx	-4.28777356
WAY-306136	-4.31230813	WAY-304853	-4.28553958
vsw_1-LIGPREP-004-in.maegz:122	-4.30965617	Dyngo-4a.cdx	-4.90236884
S9321 Topotecan.cdx	-4.31040512	WAY-297616	-4.28443026
WAY-601822	-4.3091306	vsw_1-LIGPREP-008-in.maegz:150	-4.28917892
WAY-634087	-4.30886215	vsw_1-LIGPREP-011-in.maegz:118	-4.28917892
WAY-347774	-4.9571122	WAY-271914	-4.48201732
ML130.cdx	-4.30721274	WAY-359150	-4.2962703
A769662.cdx	-4.3076549	INDOCIN (indomethacin).cdx	-4.28195725
Rosiglitazone hydrochloride.cdx	-4.8737599	WAY-303055	-4.27834031
WAY-630231	-4.30792589	GDC-0084.cdx	-4.27745024
Cyclamic acid.cdx	-4.30456081	E7449.cdx	-4.71635358
WAY-301456	-4.30259032	vsw_1-LIGPREP-015-in.maegz:890	-4.28183013
S3892 Isopsoralen.cdx	-4.30224352	S5277 INCB032304.cdx	-4.27592531
BRL54443.cdx	-4.30106482	WAY-325330	-4.27868722
WAY-631921	-4.30041523	Flavopiridol hydrochloride.cdx	-4.31072536
BILTRICIDE (praziquantel).cdx	-4.29862084	P005091(P5091) .cdx	-4.27156337
TAK-700.cdx	-4.40832102	INCB28060.cdx	-4.27691194
S3610 Cordycepin.cdx	-4.29771441	Naltrexone hydrochloride.cdx	-4.31879346
S9053 Irisfloreantin.cdx	-4.29577365	vsw_1-LIGPREP-004-in.maegz:107	-4.27033697
vsw_1-LIGPREP-015-in.maegz:121	-4.32787019	WAY-633284	-4.26848217
Primaquine diphosphate.cdx	-4.29482481	Nitrendipine.cdx	-4.26822091
WAY-297436	-4.29418453	SB225002.cdx	-4.27081052
WAY-323395	-4.93466941	vsw_1-LIGPREP-004-in.maegz:124	-4.26636594
vsw_1-LIGPREP-008-in.maegz:344	-4.29331527	WAY-649338	-4.33736333
vsw_1-LIGPREP-011-in.maegz:99	-4.29331527	vsw_1-LIGPREP-007-in.maegz:97	-4.47827592
WAY-633376	-4.29423265	S5153 Tetrahydroberberine.cdx	-4.34301889

Compound ID	Glide Score	Compound ID	Glide Score
WAY-305333	-4.58269364	S4990 TBHQ.cdx	-4.23747492
vsw_1-LIGPREP-015-in.maegz:794	-4.26836239	WAY-275580	-4.26120801
Azacyclonol.cdx	-4.26465538	WAY-359213	-4.23654636
vsw_1-LIGPREP-011-in.maegz:817	-4.26346046	S9100 Fraxinellone.cdx	-4.23596929
Adiphenine hydrochloride.cdx	-4.28368043	vsw_1-LIGPREP-015-in.maegz:815	-4.23529146
WAY-633483	-4.26073393	CYT 387.cdx	-4.23515682
S5616 4-Methylcatechol.cdx	-4.26123031	INK 128.cdx	-4.23503504
WAY-631665	-4.25955023	BIIB021 (CNF2024).cdx	-4.27856429
WAY-332446	-4.25865178	WAY-353222	-4.23361316
3-TYP.cdx	-4.67180411	WAY-358718	-4.23319256
WAY-327447	-4.68258215	WAY-604491	-4.26964197
CL-832195	-4.25741384	SN-38.cdx	-4.23617649
CL-900704	-4.43868834	Mianserin hydrochloride.cdx	-4.37989876
Mequinol.cdx	-4.25625412	S4856 Iproniazid.cdx	-4.23029051
WAY-644916	-4.25589585	Adrenalone hydrochloride.cdx	-4.37771929
Luliconazole.cdx	-4.25400928	NVP-TAE226.cdx	-4.22753116
CNX-774.cdx	-4.26492598	WAY-303599	-4.227284
Naloxone HCL.cdx	-4.37192841	WAY-305009	-4.22675789
WAY-239137	-4.25221902	(-)-MK 801 maleate.cdx	-4.29521486
WAY-631177	-4.25202728	vsw_1-LIGPREP-011-in.maegz:122	-4.2294146
S3862 Gallic acid trimethyl ether.cdx	-4.25270688	BIO (6-bromindirubin-3-oxime).cdx	-4.22350686
Nisoldipine.cdx	-4.25144507	WAY-309080	-4.22283025
Atglistatin.cdx	-4.25469174	S9387 Maackiain.cdx	-4.22178533
(+)-Usniacin.cdx	-5.06687316	WAY-628112	-4.22082318
Cladribine.cdx	-4.24779695	CAY10505.cdx	-4.27583289
ino-1001.cdx	-4.2472422	WAY-628153	-4.22031786
Hydroxyurea.cdx	-4.2548249	WAY-631305	-4.22016109
WL-144324	-4.24536319	vsw_1-LIGPREP-006-in.maegz:425	-4.2197511
Sodium valproate.cdx	-4.24730782	LDC4297 (LDC044297).cdx	-4.21788771
WAY-632882	-4.24498719	S3764 Isoferulic Acid.cdx	-4.21775287
SB207499.cdx	-4.24412957	WYE-176082	-4.21644531
Cytisine.cdx	-4.24315088	S3952 3,4-Dihydroxybenzaldehyde.cdx	-4.3234209
WAY-307488	-4.32362389	S9065 Songorine.cdx	-4.21547486
RO9021.cdx	-4.30432293	WAY-300320	-4.21479516
WAY-333062	-4.24097801	WAY-325694	-4.22452897
Sulfadoxine.cdx	-4.39207771	WAY-611819	-4.21315563
3-Indolebutyric acid.cdx	-4.24218113	vsw_1-LIGPREP-004-in.maegz:116	-4.21286624

Compound ID	Glide Score	Compound ID	Glide Score
S9336 Ethyl Coumarin-3-carboxylate.cdx	-4.2116787	Omeprazole.cdx	-4.28431603
KENACORT (triamcinolone).cdx	-4.21156202	RILUZOLE (riluzole).cdx	-4.19093358
S5394 Tizoxanide.cdx	-4.37809145	Halofuginone.cdx	-4.19986008
WAY-602296	-4.21083942	WAY-324897	-4.38084731
S9258 (+)-Isocorynoline.cdx	-4.24749816	WAY-302430	-4.73701383
WAY-302073	-4.53828617	S5531 Doripenem.cdx	-4.58606147
WAY-385457	-4.21537897	S3859 Vanillyl Alcohol.cdx	-4.1865193
S4897 Nortropine Hydrochloride.cdx	-4.20949876	S9094 Pogostone.cdx	-4.18920626
LM-3093 AZD9291.cdx	-4.21705566	WAY-308881	-4.18565176
vsw_1-LIGPREP-015-in.maegz:107	-4.20933496	vsw_1-LIGPREP-008-in.maegz:113	-4.20766794
WAY-628675	-4.20787324	vsw_1-LIGPREP-015-in.maegz:796	-4.20766794
DAPT.cdx	-4.20779249	SL327.cdx	-4.59626698
WAY-303766	-4.20742201	S9421 Demethylnobiletin.cdx	-4.18556389
S5493 Atropine sulfate.cdx	-4.20945169	Nocodazole.cdx	-4.65089007
vsw_1-LIGPREP-015-in.maegz:85	-4.22928213	S4777 Plumbagin.cdx	-4.19189454
vsw_1-LIGPREP-006-in.maegz:106	-4.20675218	Hesperetin.cdx	-4.1996047
piromidic acid.cdx	-4.23651874	WAY-310759	-4.18110629
vsw_1-LIGPREP-008-in.maegz:100	-4.29515242	WAY-324199	-4.18167096
vsw_1-LIGPREP-015-in.maegz:546	-4.29515242	BAY57-1293.cdx	-4.19727838
WAY-300598	-4.20632983	WAY-646107	-4.18087122
vsw_1-LIGPREP-011-in.maegz:557	-4.23552299	WAY-383585	-4.18053465
S4831 Piperonyl butoxide.cdx	-4.20307772	WAY-628285	-4.17964038
WAY-304138	-4.20277211	WAY-303139	-4.20632055
WAY-622187	-4.20252536	S4898 Sulfalazine sodium.cdx	-4.31878983
WAY-232366	-4.20065932	WAY-312438	-4.17728639
WAY-307977	-4.20231424	ZM241385.cdx	-4.17686413
WAY-648211	-4.19933675	S4636 Teneligliptin hydrobromide.cdx	-4.30229166
brefeldin A.cdx	-4.1988109	WAY-217565	-4.17604525
WAY-307495	-4.19822668	S3745 Balsalazide disodium.cdx	-4.17720069
Donepezil HCl.cdx	-4.20079151	WAY-306168	-4.17562987
S5225 Boldenone.cdx	-4.19502123	WAY-325688	-4.1737102
Albendazole oxide.cdx	-4.39551019	S9121 Irgenin.cdx	-4.19731673
S4985 Dimethyl-4-Hydroxyisophthalate.cdx	-4.27765844	S9176 Pimpinellin.cdx	-4.17241673
S4942 4-Hydroxy-3,5-dimethoxybenzyl alcohol.cdx	-4.19421768	SCR7.cdx	-4.17865788
WAY-302520	-4.19169499	P529.cdx	-4.17045816
WAY-271562	-4.19164259	S5291 Sulfisomidin.cdx	-4.30446457
Isosorbide.cdx	-4.19134595	vsw_1-LIGPREP-011-in.maegz:426	-4.1697909

Compound ID	Glide Score	Compound ID	Glide Score
WAY-391805	-4.16592873	vsw_1-LIGPREP-004-in.maegz:101	-4.13624381
WAY-352145	-4.1656449	AT9283.cdx	-5.53391739
WAY-645401	-4.1726075	LM-3053 SKLB1002.cdx	-4.13484838
S5640 Ethyl caffeate.cdx	-4.16654178	WAY-276413	-4.1390761
WAY-643997	-4.16391742	LANIAZID (isoniazid).cdx	-4.13357186
vsw_1-LIGPREP-004-in.maegz:114	-4.16273824	CC-115.cdx	-4.17483604
WAY-389133	-4.16256456	KRN633.cdx	-4.1316701
WAY-632144	-4.16207878	Bithionol.cdx	-4.52042711
Chk2 Inhibitor II (BML-277).cdx	-4.58675987	PF-06405761.cdx	-4.13198453
WAY-631009	-4.8322817	Piperlongumine.cdx	-4.13043439
S3804 Alpha-Mangostin.cdx	-4.3256176	WAY-639952	-4.12928517
WAY-309420	-4.15503749	WAY-624111	-4.12899659
PIK 293.cdx	-4.1551821	WAY-380365	-4.1285192
WL-139277	-4.18762014	WAY-354835	-4.1315221
CL-380504	-4.14884271	WAY-628715	-4.78802628
isoxicam.cdx	-4.14994712	WAY-645841	-4.12737198
Oltipraz.cdx	-4.148133	WAY-613351	-4.36368034
S9123 Eriodictyol.cdx	-4.1660736	WAY-308963	-4.12645031
S9378 4',5-Dihydroxyflavone.cdx	-4.14771261	S3709 Furagin.cdx	-4.21371811
CP-690550 citrate.cdx	-4.1586373	vsw_1-LIGPREP-011-in.maegz:565	-4.12289698
Artemether.cdx	-4.14684054	WAY-654383	-4.12189055
WAY-386897	-4.20978597	vsw_1-LIGPREP-006-in.maegz:416	-4.12161824
vsw_1-LIGPREP-008-in.maegz:96	-4.14611772	WAY-631805	-4.12040683
vsw_1-LIGPREP-011-in.maegz:413	-4.14611772	WAY-351817	-4.11545121
vsw_1-LIGPREP-012-in.maegz:9	-4.14611772	Isoliquiritigenin.cdx	-4.39234384
MK8745.cdx	-4.50369475	S9070 Isoxanthohumol.cdx	-4.11280926
WAY-335612	-4.68982969	S5651 Dexrazoxane.cdx	-4.72044229
vsw_1-LIGPREP-011-in.maegz:124	-4.1448857	WAY-626189	-4.11046975
S3877 Lysionotin.cdx	-4.17544039	S9080 Anhydroicaritin.cdx	-4.12610541
S4701 2-Deoxy-D-glucose.cdx	-4.14164938	WAY-309041	-4.10981509
aminacrine.cdx	-4.14135491	WAY-346670	-4.11460338
WAY-299348	-4.14051713	vsw_1-LIGPREP-015-in.maegz:96	-4.10837104
S5243 Ruxolitinib Phosphate.cdx	-4.14049712	WAY-628123	-4.10633661
WAY-384686	-4.14022342	Nabumetone.cdx	-4.10575104
WAY-303731	-4.15793766	S4765 Syringaldehyde.cdx	-4.19493036
S9328 5,6,7-Trimethoxyflavone.cdx	-4.13771494	WAY-600748	-4.10511827
WAY-603781	-4.1360439	VUF 10166.cdx	-4.17730847

Compound ID	Glide Score	Compound ID	Glide Score
IC261.cdx	-4.10276827	RG2833 (RGFP109).cdx	-4.07898829
WAY-326753	-4.42797406	Iloperidone.cdx	-4.08967158
WAY-614431	-4.10238664	WAY-339297	-4.07632967
PF-543 .cdx	-4.10671598	vsw_1-LIGPREP-015-in.maegz:547	-4.35298375
WAY-627079	-4.10111638	Buspirone hydrochloride.cdx	-4.40513911
vsw_1-LIGPREP-015-in.maegz:584	-4.09962794	SB415286.cdx	-4.86081238
CHIBROXIN (norfloxacin).cdx	-5.20319616	WAY-380360	-4.07418163
vsw_1-LIGPREP-015-in.maegz:84	-4.09853847	WAY-339380	-4.07383014
ACETADOTE (acetylcysteine).cdx	-4.09848914	LM10.cdx	-4.07528735
S3778 Patchouli alcohol.cdx	-4.0984833	WAY-305329	-4.07290192
vsw_1-LIGPREP-011-in.maegz:705	-4.09883621	S4630 Diazoxide.cdx	-4.08060978
vsw_1-LIGPREP-015-in.maegz:827	-4.09883621	WAY-326424	-4.1718916
S4617 Dextromethorphan hydrobromide hydrate.cdx	-4.10138413	WAY-347992	-4.07243376
AZD8330.cdx	-4.09628985	WAY-350434	-4.1215262
MENADIONE (menadione).cdx	-4.09622367	WAY-383514	-4.08248475
AZD9496.cdx	-4.34476199	vsw_1-LIGPREP-008-in.maegz:99	-4.29336658
S4601 5-Chloro-8-hydroxy-7-iodoquinoline.cdx	-4.27540137	vsw_1-LIGPREP-015-in.maegz:792	-4.29336658
PMSF.cdx	-4.09294435	vsw_1-LIGPREP-015-in.maegz:853	-4.29336658
WAY-383719	-4.11473683	S4728 3,3'-Diindolylmethane.cdx	-4.07063525
WAY-659200	-4.09175086	Budesonide.cdx	-4.0702096
WAY-353748	-4.0931155	vsw_1-LIGPREP-015-in.maegz:780	-4.07060754
S3759 Norcantharidin.cdx	-4.08984319	WAY-645857	-4.06944627
WAY-323015	-4.0893362	Toltrazuril.cdx	-4.73511434
Megestrol Acetate.cdx	-4.08657524	Tetrahydropapaverine hydrochloride.cdx	-4.08153406
Altretamine.cdx	-4.13461147	WAY-307854	-4.10585351
Artesunate.cdx	-4.08550834	vsw_1-LIGPREP-008-in.maegz:346	-4.18412329
WAY-634864	-4.0843289	LOZOL (indapamide).cdx	-4.06924674
vsw_1-LIGPREP-006-in.maegz:116	-4.08389168	T0070907.cdx	-4.06645765
vsw_1-LIGPREP-008-in.maegz:111	-4.0832145	WAY-301806	-4.08154604
HIVID (zalcitabine).cdx	-4.08228448	GW788388(1).cdx	-4.46895819
WAY-337064	-4.49269375	WAY-310476	-4.3096403
S3991 Ketoisophorone.cdx	-4.08144964	WAY-645927	-4.05661587
3BDO.cdx	-4.07990398	WAY-336367	-4.05409338
Nitrofurantoin.cdx	-4.15055494	WAY-311525	-4.47311614
WAY-631971	-4.07799341	WAY-385707	-4.05879261
WAY-647228	-4.07794631	S3848 Hydroxytyrosol Acetate.cdx	-4.05424647
WAY-388436	-4.10381815	WAY-307900	-5.06373969

Compound ID	Glide Score
AZD3839.cdx	-4.08154336
Methylthiouracil.cdx	-4.09394836
MINTEZOL (thiabendazole).cdx	-4.05272607
S4714 (-)-Menthol.cdx	-4.05209673
WAY-311644	-4.07744073
PHA-793887.cdx	-4.46730977
S9360 4-Hydroxyquinazoline.cdx	-4.0944008
S4736 Trapidil.cdx	-4.049899
vsw_1-LIGPREP-011-in.maegz:816	-4.04767073
S9384 Sophocarpine Monohydrate.cdx	-4.04774233
MSC2530818.cdx	-4.06192506
WAY-303109	-4.04949106
WAY-119580	-4.04189101
WAY-329190	-4.04153112
LY315920.cdx	-4.03839452
WAY-297187	-4.03753389
WAY-629056	-4.03720614
Tizanidine hydrochloride.cdx	-4.87337411
VS-5584 (SB2343).cdx	-4.03625311
YU238259.cdx	-4.03548777
Biotin.cdx	-4.03821774
vsw_1-LIGPREP-006-in.maegz:148	-4.4119405
WAY-238384	-4.0337252
WAY-634712	-4.03346349
S5629 L-Proline.cdx	-4.03174071
WAY-234115	-4.03153388
WAY-351099	-4.03125117
S3978 5-Phenyl-2,4-pentadienoic acid.cdx	-4.03147745
K-Ras(G12C) inhibitor 6.cdx	-4.03023163
Apocynin (acetovanillone).cdx	-4.06540783
WAY-312716	-4.02704518
BSI-201.cdx	-4.02634568
vsw_1-LIGPREP-011-415	-4.0249616
TH287.cdx	-4.34976084
S4685 Efavirenz.cdx	-4.02415446
S5628 L-Valine.cdx	-4.02382131
Alogliptin(SYR-322).cdx	-4.02349934

A sampling strategy based on anchor and refined growth is employed by the SP mode. For XP (extra precision) docking, the finalized 680 compounds (Table. 6.2) obtained after standard precision (SP) mode were taken for docking. Protein-ligand docking is an important method for studying and properly comprehending protein-ligand interactions. Drug design methodologies frequently involve docking to aid the design of potentially active leads, among other phases. Finding the ideal ligand poses and correctly assessing the relative docking propensities of several ligands are crucial (Elokely et al., 2013).

Standard precision screening, often used in computational drug discovery, refers to a high-throughput, relatively fast approach to virtually screen a library of compounds to identify potential binders or inhibitors of a target protein. The primary purpose is to filter large numbers of compounds efficiently to focus on promising candidates before moving to more resource-intensive techniques, like high-precision screening or experimental validation. In standard precision screening, molecular docking algorithms predict the preferred orientation of small molecules (ligands) within a target protein's binding site (Meng et al., 2011). Algorithms typically use simplified scoring functions, which balance computational speed and binding affinity prediction accuracy. Software tools like Schrödinger's Glide provide a standard precision mode designed to efficiently score large libraries with reliable results for lead identification and rank ordering Standard Precision vs. High Precision (XP) Screening (Schrödinger, LLC. 2021). Molecular docking programs are used for structure-based virtual screening. There are currently a lot of these docking programs accessible, and choosing one is challenging if one is unaware of the features or effectiveness of each program. An explosion of new approaches is occurring in the field of machine learning for drug discovery. These approaches are often based on easily computed basic physicochemical properties like solubility or general drug likeness. In contrast, molecular docking is a method that is widely used in drug discovery to estimate binding affinities (García-Ortegón, et al., 2022).

Table 6.2: List of Lead molecules obtained after SP (Standard-Precision) screening

Compound ID	Docking score	Compound ID	Docking score
TWS119.cdx	-7.30357545	PF477736.cdx	-6.06296969
S3799 Gentisic acid.cdx	-6.97344194	MK4827.cdx	-6.06109413
vsw_1-LIGPREP-015-in.maegz:992	-6.85893294	WAY-247613	-6.06093545
UM171.cdx	-6.82123093	WAY-271396	-6.04842392
vsw_1-LIGPREP-015-in.maegz:876	-6.78237459	WAY-604491	-6.04036849
S5610 Indole-3-acetamide.cdx	-6.76213464	Hesperetin.cdx	-6.03350758
ALESSE (ethinyl estradiol).cdx	-6.64766465	S3624 Quinolinic acid.cdx	-6.02439162
OG-L002.cdx	-6.64388933	vsw_1-LIGPREP-015-in.maegz:861	-6.01959638
S4785 Nicotinamide N-oxide.cdx	-6.62275989	WAY-601822	-6.0194429
S5676 Zearalenone.cdx	-6.60615469	S3903 Lycorine.cdx	-5.99781948
vsw_1-LIGPREP-004-in.maegz:99	-6.56298898	S3800 Lycorine hydrochloride.cdx	-5.99618257
S9374 2',5'-Dihydroxyacetophenone.cdx	-6.55921491	CP868569.cdx	-5.98820837
WAY-631071	-6.54893615	IOX2.cdx	-5.98523721
S9428 Brazilin.cdx	-6.49656755	vsw_1-LIGPREP-011-in.maegz:789	-5.97758482
vsw_1-LIGPREP-006-in.maegz:105	-6.4722437	Dihydromyricetin.cdx	-5.95620245
vsw_1-LIGPREP-007-in.maegz:106	-6.43835377	S3936 7-Hydroxycarbostryl.cdx	-5.95328879
N6022.cdx	-6.42446145	ALVESCO (ciclesonide).cdx	-5.9455827
SCH727965.cdx	-6.41484093	S9123 Eriodictyol.cdx	-5.94405094
URB597.cdx	-6.38737827	3PO.cdx	-5.93623706
S4767 7-Hydroxy-3,4-dihydrocarbostryl.cdx	-6.34949289	PIK-294.cdx	-5.91596707
S4722 (+)-Catechin.cdx	-6.34207873	Tioxolone.cdx	-5.91034806
Azlocillin sodium salt.cdx	-6.33440041	S4719 Kynurenic acid.cdx	-5.90968555
AZD5363.cdx	-6.319438	Ticarcillin sodium.cdx	-5.90394523
NU1025.cdx	-6.31090383	Bismuth subcitrate potassium.cdx	-5.90224165
PP121.cdx	-6.30849516	vsw_1-LIGPREP-015-in.maegz:852	-5.90221493
(+,-)-Octopamine hydrochloride.cdx	-6.30145413	vsw_1-LIGPREP-006-in.maegz:120	-5.8839824
WAY-612625	-6.28119901	A769662.cdx	-5.88292076
WZB117.cdx	-6.27735391	Doxofylline.cdx	-5.87794984
CB-5083.cdx	-6.2280268	vsw_1-LIGPREP-015-in.maegz:531	-5.87101698
S5409 Chelidamic acid hydrate.cdx	-6.22750583	10-Hydroxycamptothecin.cdx	-5.86894266
TG 100713.cdx	-6.21798549	untitled.cdx	-5.8660641
Y-39983 HCl.cdx	-6.21581006	S3898 Hydroxy Camptothecine.cdx	-5.86426362
XL019.cdx	-6.19852198	WAY-302823	-5.86214559
S9361 Coumarin-3-carboxylic acid.cdx	-6.17213039	WAY-304138	-5.85222808
Hematoxylin.cdx	-6.148236	AMINOPHYLLINE (aminophylline).cdx	-5.84953399
Linagliptin.cdx	-6.13511417	WAY-308352	-5.8469019
BFH772.cdx	-6.10822283	vsw_1-LIGPREP-015-in.maegz:820	-5.84492533

Compound ID	Docking score	Compound ID	Docking score
AZD7762.cdx	-6.09781775	AZ628.cdx	-5.8334557
Daphnetin.cdx	-6.08594284	vsw_1-LIGPREP-007-in.maegz:416	-5.83177282
Diclazuril.cdx	-6.07515782	vsw_1-LIGPREP-011-in.maegz:105	-5.83177282
WAY-612628	-6.06998	vsw_1-LIGPREP-011-in.maegz:531	-5.83091974
WAY-300430	-5.82607432	AMG-517.cdx	-5.62772448
Go 6983.cdx	-5.81021355	WAY-326492	-5.62322183
vsw_1-LIGPREP-011-in.maegz:790	-5.80492648	S4799 Indole-3-acetic acid.cdx	-5.61917849
CID755673.cdx	-5.80408143	WAY-336578	-5.61908525
Nitrofurantoin.cdx	-5.80113148	HTH-01-015.cdx	-5.61516063
vsw_1-LIGPREP-015-in.maegz:104	-5.79971393	vsw_1-LIGPREP-006-in.maegz:108	-5.61328905
S5410 Chloramphenicol sodium succinate.cdx	-5.79762747	WAY-301515	-5.60295865
WAY-306938	-5.79288904	WAY-308845	-5.60133449
WAY-648679	-5.79139982	vsw_1-LIGPREP-015-in.maegz:961	-5.59936672
vsw_1-LIGPREP-011-in.maegz:97	-5.7857433	vsw_1-LIGPREP-011-in.maegz:542	-5.59594632
S9240 Isofraxidin.cdx	-5.77973931	vsw_1-LIGPREP-015-in.maegz:855	-5.58459737
S5548 7-Hydroxy-4-chromone.cdx	-5.76087496	EPI-001.cdx	-5.57853111
Ethamsylate.cdx	-5.74689372	Irsogladine.cdx	-5.57483075
S9395 N-Benzoyl-(2R,3S)-3-phenylisoserine.cdx	-5.74545218	S4784 Phloracetophenone.cdx	-5.57242299
S4809 3-Indolepropionic acid.cdx	-5.73544298	Mecarbinat.cdx	-5.57121501
S4717 Isatin.cdx	-5.72928171	CL-420396	-5.56941945
WAY-331439	-5.72893738	WAY-628395	-5.56618544
S5226 L-carnosine.cdx	-5.72200408	WAY-337131	-5.56555207
WAY-627522	-5.71712671	Piceatannol.cdx	-5.5628371
Gemcitabine hydrochloride.cdx	-5.70767263	LY 411575.cdx	-5.54644811
Synephrine hydrochloride.cdx	-5.7065239	CL-380504	-5.54294615
S3683 Methylmalonate.cdx	-5.70460084	Cyclamic acid.cdx	-5.5381779
S4739 Oxyresveratrol.cdx	-5.70373468	S4789 5-Acetylsalicylic acid.cdx	-5.5329127
LM-3134 CH5138303.cdx	-5.6954386	mepiroxol.cdx	-5.52862406
S4819 Saccharin.cdx	-5.68813066	vsw_1-LIGPREP-015-in.maegz:874	-5.5207145
Floxuridine.cdx	-5.68758246	Ganetespib(STA-9090).cdx	-5.51444444
vsw_1-LIGPREP-015-in.maegz:530	-5.68653127	S5711 Deracoxib.cdx	-5.51409382
Besifloxacin HCl.cdx	-5.67506678	Sodium Fluorophosphate.cdx	-5.51179825
OTS514.cdx	-5.67127526	YU238259.cdx	-5.50900784
RG108.cdx	-5.67073184	HIVID (zalcitabine).cdx	-5.50791004
WAY-628123	-5.67040885	S4780 7-Methoxy-4-methylcoumarin.cdx	-5.50790643
S3676 Carbendazim.cdx	-5.66895899	SB 742457.cdx	-5.50047349
vsw_1-LIGPREP-015-in.maegz:877	-5.66767354	S4774 Xanthurenic Acid.cdx	-5.49804689
S5225 Boldenone.cdx	-5.66258534	WAY-306112	-5.49751984

Compound ID	Docking score	Compound ID	Docking score
ARRY-380 (ONT-380, Irbinitinib).cdx	-5.65835041	vsw_1-LIGPREP-015-in.maegz:795	-5.49644401
Torin 2.cdx	-5.65639677	WAY-336760	-5.49453471
IPA-3.cdx	-5.6559793	vsw_1-LIGPREP-011-in.maegz:95	-5.49141075
WAY-633483	-5.65109049	WAY-347315	-5.48609068
PK11007.cdx	-5.64176873	TPCA-1.cdx	-5.48516588
Methoxsalen.cdx	-5.63105449	vsw_1-LIGPREP-011-in.maegz:644	-5.48176901
S3862 Gallic acid trimethyl ether.cdx	-5.62886521	WAY-345925	-5.4807496
BRL54443.cdx	-5.47891042	vsw_1-LIGPREP-008-in.maegz:109	-5.38133189
GSK2141795.cdx	-5.47586114	S4894 D-Glucurone.cdx	-5.38054989
p276-00.cdx	-5.47316751	WAY-324207	-5.37783894
Levosulpiride.cdx	-5.46109586	S4685 Efavirenz.cdx	-5.37775013
KD025 (SLx-2119).cdx	-5.46073847	Adrucil (Fluorouracil).cdx	-5.37725435
vsw_1-LIGPREP-007-in.maegz:98	-5.4593877	Cladribine.cdx	-5.37659307
WAY-333718	-5.4592322	7,8-Dihydroxyflavone.cdx	-5.37530715
WAY-309377	-5.45859877	WAY-339380	-5.3740999
Serotonin hydrochloride.cdx	-5.45764343	BS-181.cdx	-5.37221562
WAY-631009	-5.45436226	CID16020046 (CID 16020046).cdx	-5.36292049
WAY-355031	-5.45302698	WAY-330577	-5.36164952
KENACORT (triamcinolone).cdx	-5.45227852	WAY-633284	-5.36069509
S4763 4-Hydroxychalcone.cdx	-5.44299972	vsw_1-LIGPREP-006-in.maegz:104	-5.36027137
XMD8-92.cdx	-5.43714908	WAY-310759	-5.36020866
FR 180204.cdx	-5.43452884	ino-1001.cdx	-5.35865882
Nadifloxacin.cdx	-5.43184274	Cinchophen.cdx	-5.35863216
BAY-61-3606.cdx	-5.42527613	vsw_1-LIGPREP-011-in.maegz:427	-5.35776418
Ampicillin sodium.cdx	-5.4245778	vsw_1-LIGPREP-013-in.maegz:11	-5.35776418
WAY-323095	-5.41871389	S9070 Isoxanthohumol.cdx	-5.35313006
P505-15.cdx	-5.41658754	WAY-340674	-5.35142343
vsw_1-LIGPREP-006-in.maegz:99	-5.41455365	Myricetin.cdx	-5.34945124
2-D08.cdx	-5.41350817	WAY-616773	-5.34884468
vsw_1-LIGPREP-006-in.maegz:344	-5.41129481	Necrostatin-1.cdx	-5.34781467
vsw_1-LIGPREP-015-in.maegz:798	-5.41000174	WAY-337265	-5.34728255
LY3023414.cdx	-5.40421448	WAY-386549	-5.345221
SRT2183.cdx	-5.40250236	LM-3243 CRT0044876.cdx	-5.3423041
Shikimic acid.cdx	-5.40224219	Alogliptin(SYR-322).cdx	-5.34027323
WAY-311525	-5.4013152	WAY-385023	-5.33904448
WAY-322960	-5.40098859	Doxycycline hyclate.cdx	-5.33514442
S3947 Hydroumbellic acid.cdx	-5.40059751	S5333 Sulbenicillin Sodium.cdx	-5.33385697

Compound ID	Docking score	Compound ID	Docking score
WAY-276413	-5.39695255	Cysteamine HCl.cdx	-5.33144894
S4630 Diazoxide.cdx	-5.39491424	vsw_1-LIGPREP-004-in.maegz:148	-5.32666378
WAY-307854	-5.39437127	ronidazole.cdx	-5.32623032
WAY-659163	-5.39255943	S3858 Lawsone.cdx	-5.32592102
vsw_1-LIGPREP-006-in.maegz:119	-5.39062926	EAI045.cdx	-5.32255574
WAY-345462	-5.38868851	WAY-389361	-5.32239024
amoxicillin.cdx	-5.38847607	WAY-358718	-5.32108106
WAY-306232	-5.38808614	S3627 Tryptamine.cdx	-5.31990801
AZD 6482.cdx	-5.38695342	Trelagliptin.cdx	-5.31973678
PP2.cdx	-5.3858771	vsw_1-LIGPREP-011-in.maegz:416	-5.31628627
vsw_1-LIGPREP-015-in.maegz:107	-5.38339909	abt-751.cdx	-5.3140872
Bromodeoxyuridine.cdx	-5.31392865	S5023 Nadolol.cdx	-5.21444993
vsw_1-LIGPREP-008-in.maegz:148	-5.30725595	S3879 kaempferide.cdx	-5.2137248
ifenprodil tartrate.cdx	-5.30526683	WAY-323401	-5.21129616
S3629 Syringic acid.cdx	-5.30395092	WAY-643997	-5.20916802
WAY-346373	-5.30090404	WYE-176082	-5.20801097
WAY-606601	-5.30075419	Bindarit.cdx	-5.20732064
WAY-623751	-5.29741812	vsw_1-LIGPREP-002-in.maegz:10	-5.20619219
WAY-299598	-5.29698763	vsw_1-LIGPREP-005-in.maegz:4	-5.20619219
S5160 4-Methoxysalicylic acid.cdx	-5.29499784	Fisetin.cdx	-5.20588383
S3754 4-Hydroxybenzoic acid.cdx	-5.29376297	S5500 Amodiaquine hydrochloride.cdx	-5.20513546
WAY-659200	-5.29232332	vsw_1-LIGPREP-007-in.maegz:105	-5.20417805
WAY-306077	-5.28829983	Naringenin.cdx	-5.20356939
Clodronate disodium.cdx	-5.28049433	WAY-626346	-5.20130952
S5211 4-Aminosalicylic acid.cdx	-5.27954455	WAY-326335	-5.19691528
WAY-324683	-5.27714198	WAY-119580	-5.19542101
Phloretin.cdx	-5.2752928	WAY-606496	-5.18584211
BI-78D3.cdx	-5.27018987	aminacrine.cdx	-5.18291214
vsw_1-LIGPREP-015-in.maegz:856	-5.26753606	S3742 Cholic acid.cdx	-5.18257379
S3942 Cardamonin.cdx	-5.26483575	WL-309836	-5.17763761
vsw_1-LIGPREP-008-in.maegz:117	-5.26420392	S3859 Vanillyl Alcohol.cdx	-5.17740703
Foscarnet Sodium.cdx	-5.26174497	WAY-633981	-5.17729932
Mizoribine.cdx	-5.25359854	ly404039.cdx	-5.1691809
Carsalam.cdx	-5.25259365	S9378 4',5-Dihydroxyflavone.cdx	-5.16914064
S4765 Syringaldehyde.cdx	-5.24916795	S3674 Levamlodipine.cdx	-5.16871372
SN-38.cdx	-5.24401347	WAY-302734	-5.16502692
Chlortetracycline HCl.cdx	-5.24374226	WAY-303055	-5.16458692

Compound ID	Docking score	Compound ID	Docking score
MYDRIACYL (tropicamide).cdx	-5.24244647	Mefloquine hydrochloride.cdx	-5.16287115
S4884 Trans-Zeatin.cdx	-5.24069652	S4117.cdx	-5.16226028
WAY-631305	-5.23925507	S3968 Histamine.cdx	-5.16205614
CP 673451.cdx	-5.23682209	S4946 2,3-Dihydroxybenzoic acid.cdx	-5.16172447
vsw_1-LIGPREP-011-in.maegz:813	-5.2360524	vsw_1-LIGPREP-006-in.maegz:84	-5.16139144
CATAFLAM (diclofenac potassium).cdx	-5.23593343	Kaempferol.cdx	-5.16004495
ABBV-075 (Mivebresib).cdx	-5.23021024	WAY-321433	-5.15934866
S9364 6-Hydroxycoumarin.cdx	-5.22877039	AZD3839.cdx	-5.15676105
vsw_1-LIGPREP-011-in.maegz:109	-5.22523088	vsw_1-LIGPREP-007-in.maegz:119	-5.15496421
GSK591 (EPZ015866, GSK3203591).cdx	-5.22519084	Ethacridine lactate monohydrate.cdx	-5.15376993
WAY-299744-A	-5.22446446	L-Adrenaline.cdx	-5.15130427
Tasquinimod .cdx	-5.22310943	WAY-389574	-5.15038449
D-Luciferin.cdx	-5.22212113	Splitomicin.cdx	-5.14912509
Baicalein.cdx	-5.2209696	METI-DERM (prednisolone).cdx	-5.14742964
Dexamethasone.cdx	-5.21524996	Dinitolmide.cdx	-5.08292422
S5575 2-Benzoxazolinone.cdx	-5.14599574	vsw_1-LIGPREP-015-in.maegz:582	-5.08089162
S3625 Tyramine.cdx	-5.14562477	WAY-329190	-5.08003526
WAY-384686	-5.14513422	WAY-353748	-5.0798933
LY315920.cdx	-5.14453642	WAY-229350	-5.07763142
PF-06840003.cdx	-5.14286219	CNX-774.cdx	-5.07747778
WAY-604503	-5.142461	WAY-324849	-5.07704653
S4749 Citalopram HBr.cdx	-5.14221972	GF 109203X(G 6850).cdx	-5.07542599
S5159 Doxycycline.cdx	-5.14136567	S9328 5,6,7-Trimethoxyflavone.cdx	-5.07363979
Phenytoin sodium.cdx	-5.1399454	S3691 4-Chlorosalicylic acid.cdx	-5.07359509
Dopamine hydrochloride.cdx	-5.13802955	WAY-646107	-5.07356333
WAY-307597	-5.13685454	WAY-305923	-5.06537322
WAY-324781	-5.13573163	Methazolastone (Temozolomide).cdx	-5.0607754
XEN445.cdx	-5.13525536	Artesunate.cdx	-5.06059506
Pioglitazone.cdx	-5.127911	WAY-628715	-5.05948808
Lonidamine.cdx	-5.12674367	Ellagic acid.cdx	-5.05914547
S4747 Jervine.cdx	-5.12482055	S9291 Isopimpinellin.cdx	-5.05899933
SecinH3.cdx	-5.12374025	GNE-317.cdx	-5.05814135
S9205 Hydroxygenkwanin.cdx	-5.12083479	WAY-382527	-5.05810231
vsw_1-LIGPREP-011-in.maegz:124	-5.11586746	Hypoxanthine.cdx	-5.05712649
PF-543 .cdx	-5.11390099	AEBSF hydrochloride .cdx	-5.05376439
vsw_1-LIGPREP-007-in.maegz:387	-5.11329787	S3945 L-Cycloserine.cdx	-5.05368246
vsw_1-LIGPREP-015-in.maegz:96	-5.10459801	bms-707035.cdx	-5.05003668

Compound ID	Docking score	Compound ID	Docking score
Rosiglitazone hydrochloride.cdx	-5.10429335	vsw_1-LIGPREP-006-in.maegz:114	-5.04695251
937174-76-0.cdx	-5.10195172	WAY-308859	-5.04655316
vsw_1-LIGPREP-008-in.maegz:114	-5.09968877	vsw_1-LIGPREP-006-in.maegz:347	-5.04548832
WAY-308518	-5.09931113	vsw_1-LIGPREP-015-in.maegz:563	-5.04500152
WAY-296514	-5.09796488	vsw_1-LIGPREP-015-in.maegz:648	-5.04500152
WAY-648211	-5.09698019	Apoptosis Activator II.cdx	-5.04439281
Rosiglitazone maleate.cdx	-5.09545617	vsw_1-LIGPREP-015-in.maegz:572	-5.0437222
S4804 1-Naphthyl acetate.cdx	-5.09438391	WAY-235139	-5.04299455
WAY-341921	-5.09300314	WAY-656883	-5.04198308
WAY-600.cdx	-5.09226762	S5317 UK 5099.cdx	-5.03960424
Mirin.cdx	-5.09206086	vsw_1-LIGPREP-008-in.maegz:102	-5.03867807
S4833 Cefoxitin sodium.cdx	-5.08899928	DMXAA.cdx	-5.03838904
Primaquine diphosphate.cdx	-5.08733847	vsw_1-LIGPREP-011-in.maegz:102	-5.03835437
vsw_1-LIGPREP-007-in.maegz:104	-5.08696399	S5166 Benzoyleneurea.cdx	-5.03773798
CL-417716	-5.08565867	S4736 Trapidil.cdx	-5.03500325
S5286 Ramatroban.cdx	-5.08345595	SGC2085.cdx	-5.03284263
olsalazine sodium.cdx	-5.08334109	XMD8-87.cdx	-5.03131977
Dinitolmide.cdx	-5.08292422	S3665 Trolox.cdx	-5.02959098

In some phases of the drug development process, FDA approved medications screening method is more efficient in terms of time and resources than laboratory testing. Most of the compounds obtained after HTVS and final SP screening were from the subcategory of Bioactive and FDA approved drugs. These compounds comprised mostly cell-permeable, medicinally active, molecules that have a variety of structural features. Clinical trials have verified their safety and bioactivity. Also, natural products and chemotherapeutic compounds were among the final lead molecules obtained after the initial HTVS and final SP screening. Extra Precision (XP) screening is a higher accuracy form of molecular docking, typically used in computational drug discovery to refine the results obtained from Standard Precision (SP) screening. XP screening applies more stringent criteria and advanced scoring functions to predict binding affinities and interactions between ligands and target proteins (Halgren et al., 2004). XP screening aims to reduce false positives by applying stricter scoring parameters, thus enhancing the confidence in predicted binding poses. The scoring function in XP screening incorporates more detailed physics-based

terms to assess binding affinity, like hydrophobic enclosure and desolvation effects, which help in identifying true high-affinity binders with greater accuracy. By incorporating additional structural and chemical evaluations, XP screening reduces the number of non-specific or weak-binding compounds, allowing for more focused downstream testing. XP screening uses advanced algorithms and a more refined scoring function compared to standard precision (SP) screening. Schrödinger's Glide XP module includes terms to assess hydrophobic interactions, hydrogen-bonding networks, and penalties for ligand strain. In contrast to SP mode, which is more forgiving, XP mode penalizes infractions such as insufficient solvation. XP scoring penalizes non-ideal interactions, such as inappropriate hydrogen bonds or buried polar groups, which may lead to energetically unfavorable binding (Schrödinger, LLC. 2021). Conversely, it rewards favorable, specific interactions that contribute to tighter binding. After XP screening, among the top 400 compounds, the top 20 were further selected based on the Glide-score for their *in silico* potential compound. The XP Glide scoring function relies heavily on the enforcement of physical chemistry principles, which makes it more important to prepare proteins and ligands appropriately than it is for many other scoring systems (Friesner et al., 2006). In structure-based drug development efforts, virtual screening theoretically offers an effective way to lead discovery. Through the process of docking an extensive library of substances into one or more target receptor high resolution structures, it is possible to identify and evaluate potentially active compounds through experimental means. In lead optimization, docking techniques are also utilized to estimate the binding affinities and forecast the structures of protein-ligand complexes. Sufficient accuracy in predicting binding mode and binding affinity is necessary for both applications (Repasky et al., 2012). Docking of *E. coli* MurD (PDB ID: 2UUP) displayed hydrogen bond, pi-cation, Pi-Pi stacking, and salt bridge interactions as the main forces of stabilization between the ligand molecule and the enzyme. Four virtual hits, S1, S4, S7, and S8, displayed hydrogen bonding interactions with the lysine residue at position 115. Virtual hits S1 and S7 displayed hydrogen bonding interactions with LYS139. Virtual hits S1, S2, S3, and S9 also interacted with LYS348 through hydrogen bonding interactions within the catalytic pocket of the enzyme. Virtual hits S1, S4, and S8 also interacted with the serine residue at position 415. Five virtual hits (S1, S4, S6, S8, and S10) also displayed interactions with HIE183 residue. The top 20 compounds (Table 6.3) displayed a XP glide-score (G-score) from -9.013 to -6.311

kcal/mol. Most of the virtual lead molecules obtained after XP- screening displayed higher G-score than the control molecules available in Pubchem database as MurD inhibitors therefore the lowest G-score among the virtual hits was –6.311, which was therefore considered as a cut-off threshold to filter promising virtual leads as indicated in the G-scores represented in (Table 6.3).

Table 6.3 Lead molecules obtained after XP screening studies

	Compound ID	Glide gscore
MurD Inhibitors (Controls) https://pubchem.ncbi.nlm.nih.gov	CID84973005	-6.372
	CID25181430	-5.878
	CID84973004	-4.726
	CID84972996	-2.444
Top 20 virtual hits obtained after XP screening	WZB117.cdx	-9.013
	EPZ015666.cdx	-7.882
	SCH727965.cdx	-7.633
	Phloretin.cdx	-7.923
	S9428 Brazilin.cdx	-7.462
	CRT0066101.cdx	-7.132
	EPI-001.cdx	-6.904
	TWS119.cdx	-6.86
	UM171.cdx	-6.703
	CP868569.cdx	-6.459
	TAK-659.cdx	-6.408
	AZD7762.cdx	-6.402
	S9395 N-Benzoyl-(2R,3S)-3-phenylisoserine.cdx	-6.359
	WAY-631305	-6.35
	S5159 Doxycycline.cdx	-6.581
	WAY-333718	-6.347
	S4722 (+)-Catechin.cdx	-6.343
	KENACORT (triamcinolone).cdx	-6.311
	CNX-774.cdx	-6.315
	Floxuridine.cdx	-6.471

To illustrate the binding mode, compounds S1, S2, and S3 were analyzed. The compound S1 (WZB117) interacted with the active site residues of the protein through four hydrogen bond interactions and one each of pi-pi stacking and pi-cation interactions. The hydroxyl group of one of

the hydroxyphenyl rings was involved in a hydrogen bonding interaction with the polar serine residue at position 415. The carbonyl oxygen of this ring also established back-bone hydrogen bond interactions with positively charged lysine residue at position 348. The other hydroxyphenyl ring established a pi-cation interaction with lysine residue at position 348, while its hydroxyl group and carbonyl oxygen established hydrogen bond interactions with lysine 319 and back-bone H-bond interactions with HIE 183 and LYS115, respectively. One of the phenyl rings of this compound with a substituted fluorine atom displayed a pi-pi stacking interaction with the hydrophobic Phenylalanine161 residue, which further stabilizes the compound S1 within the enzyme's catalytic pocket (Fig. 6.1a & 6.1b).

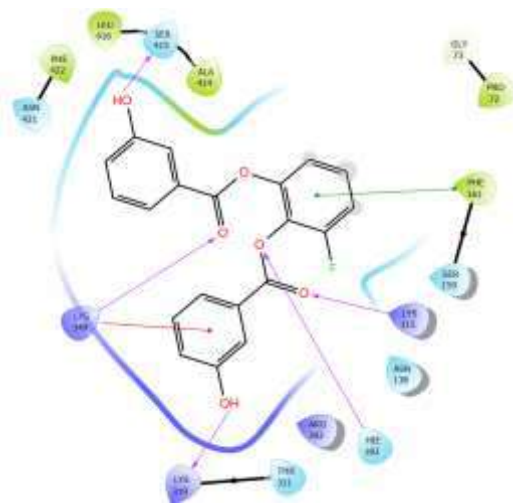


Fig.6.1a

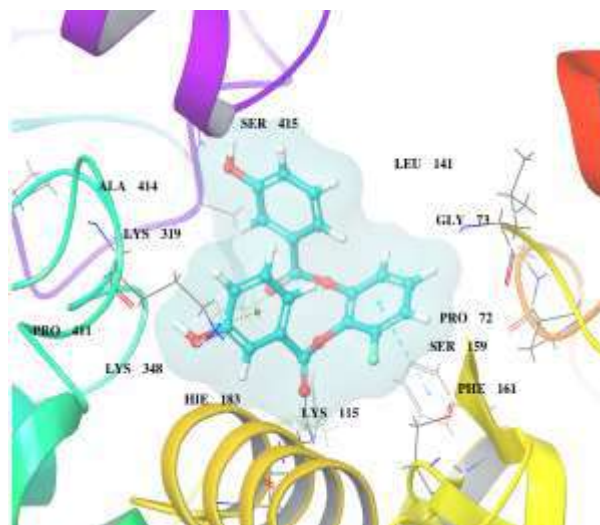


Fig. 6.1b

Figure 6.1: Fig 6.1a: Ligand interaction diagram of virtual hit S1 (WZB117) with MurD (2UUP); Fig 6.1b: Ribbon presentation diagram of MurD (2UUP)-S1 (WZB117) complex

The docked pose of compound S2 (EPZ015666) displayed that the compound interacted within the active site of protein 2UUP (Mur D) with a total of five hydrogen bonds. The Asparagine 138 amino acid is involved in two hydrogen bonding interactions with the compound, and it was also

involved in a back-bone hydrogen bonding interaction along with Lysine 348 and Phenylalanine 422 amino acid residues (Fig 6.2a and 6.2b)

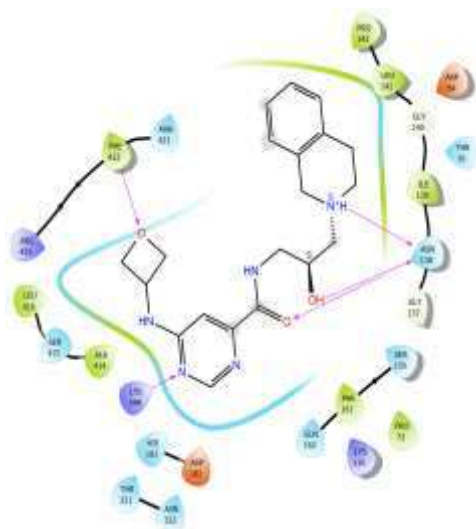


Fig.6.2a

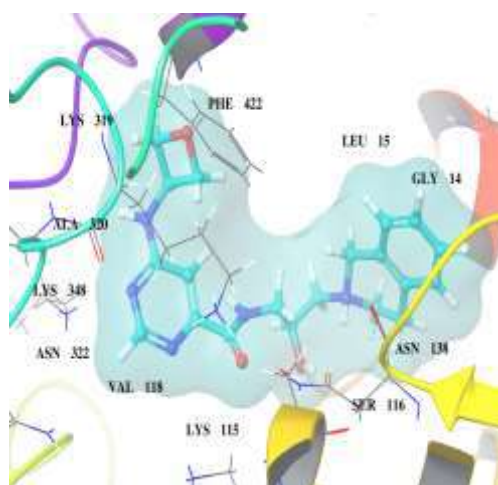


Fig. 6. 2b

Figure 6.2.: Fig 6.2a: Ligand interaction diagram of virtual hit S2 (EPZ015666) with MurD (2UUP); Fig 6.2b: Ribbon presentation of the MurD (2UUP)-S2 (EPZ015666) complex

The docking pose of compound S3 (SCH727965) displayed three hydrogen bonding interactions and two salt bridge interactions with the residues present within the catalytic pocket of the MurD enzyme (2UUP). Asparagine residue at position 138 established hydrogen bonding interactions with the compound S3, while Lysine residue at position 348 and Serine 159 amino acid residues established back-bone hydrogen bonding interactions with the compound. Aspartic acid 185 and Arginine residue at 186 positions were involved with salt bridge interactions with the compound S3, further stabilizing it within the catalytic pocket of the enzyme (Fig 6.3a and 6.3b).

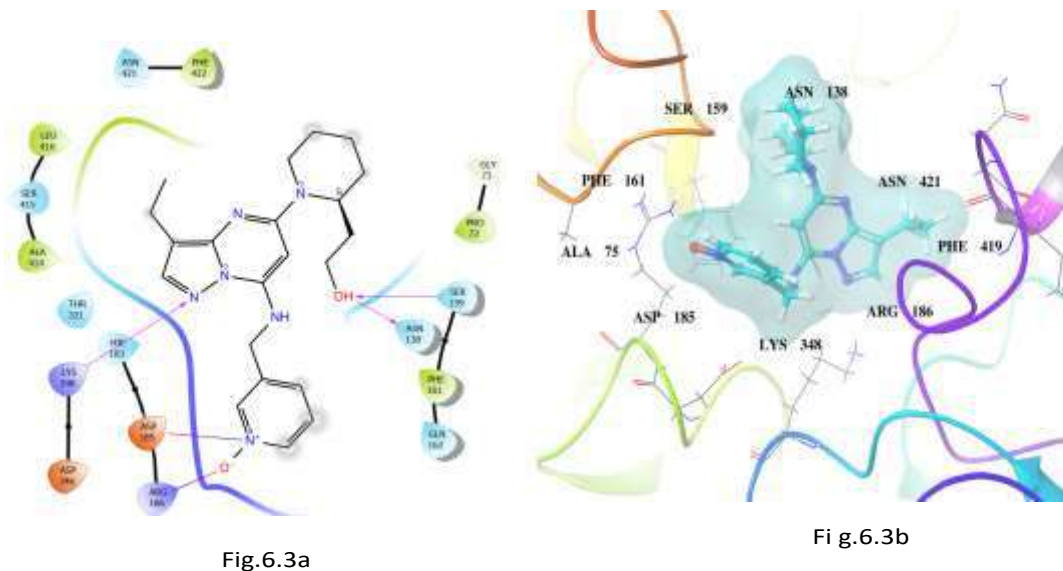


Figure 6.3: Fig 6.3a: Ligand interaction diagram of compound S3(SCH727965) with MurD (2UUP); Fig 6.3b: Ribbon presentation of MurD (2UUP) –S3 (SCH727965) complex

The docking pose of compound S4 (Phloretin) displayed six hydrogen bonding interactions and one pi cation interaction with the residues located within the catalytic pocket of the MurD enzyme (2UUP). Glutamine residue at position 157 established back hydrogen bonding interactions with the compound S4, at the same time Serine residue at position 112 and Asparagine 182 amino acid residues also established back-bone hydrogen bonding interactions with the compound S4. The compound also established hydrogen bonding interactions with HIE 183 residue and Serine 415 residue. Serine residue at 415 position was also involved with back-bone hydrogen bonding interaction and the Lysine 115 residue also displayed pi-cation interaction with the compound S4, further stabilizing it within the catalytic pocket of the enzyme (Fig 6.4 a and 6.4 b).

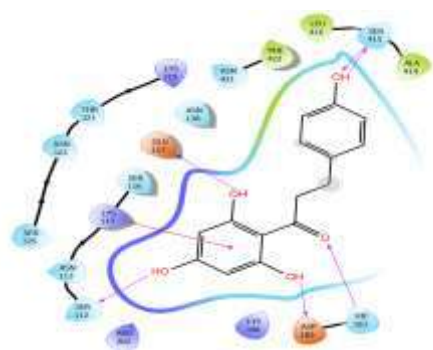


Fig.6. 4a

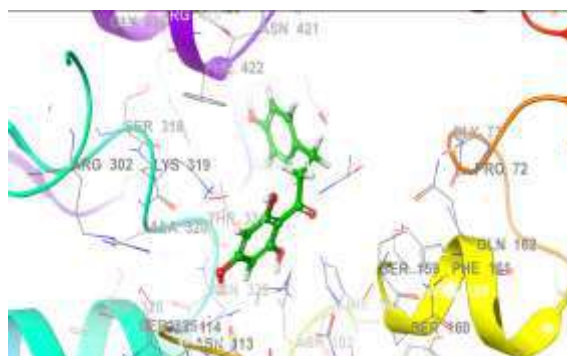


Fig.6. 4b

Figure 6.4: Fig 6.4 a: Ligand interaction diagram of compound S4 (Phloretin) with MurD (2UUP); Fig 6.4b: Ribbon presentation of MurD (2UUP) –S4 (Phloretin) complex

The compound S5 (Brazilin) displayed four hydrogen bond interactions and a pi-pi stacking interaction with the amino acid residues within the catalytic pocket of the MurD enzyme. The Aspartic acid residue at position 185 was involved with a hydrogen bonding interaction with the compound S5 along with Glycine 73 and Asparagine 138 residues establishing a hydrogen bond interaction each. Arginine at position 186 also displayed back-bone hydrogen bonding interaction with the compound S5. The phenylalanine residue 161 also established pi-pi stacking interaction with the central phenyl ring (Fig 6.5a & 6.5b).

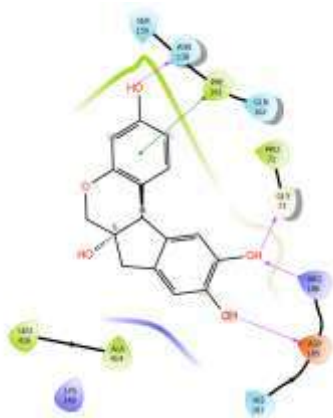


Fig.6. 5a

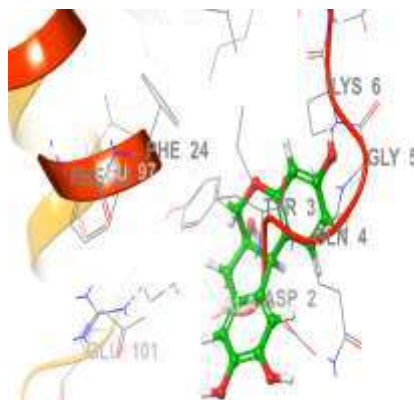


Fig. 6.5b

Figure 6.5: 6.5a: Ligand interaction diagram of compound S5 (S9428 Brazilin) with MurD (2UUP); 6.5b: Ribbon presentation of MurD (2UUP) –S5 (S9428 Brazilin) complex

The docking pose of compound S6 (CRT0066101) displayed three hydrogen bonding interactions and a pi-pi stacking interaction with the residues present within the catalytic pocket of the MurD enzyme (2UUP). Threonine residue at position 16 established hydrogen bonding interactions with the compound S6, while Glycine residue at position 137 and Aspartic acid 138 amino acid residues established back-bone hydrogen bonding interactions with the compound S6. HIE 183 residue was involved with pi-pi stacking interactions with the compound S6, further stabilizing it within the catalytic pocket of the enzyme (Fig 6.6a and 6.6b).



The docked pose of compound S7 (EPI-001) displayed that the compound interacted within the active site of protein 2UUP (Mur D) with a total of five hydrogen bonding interactions and a pi-pi stacking interaction. The Lysine 115, Lysine 319 and Aspartic acid residue at position 185 were involved in one hydrogen bonding interaction each with the compound, while Lysine at position 319 and Serine residue at position 112 also established a back-bone hydrogen bonding interaction. The compound also established a pi-pi stacking interaction with the phenylalanine residue Phenylalanine (PHE) residue at position 161 (Fig 6.7a and 6.7b).

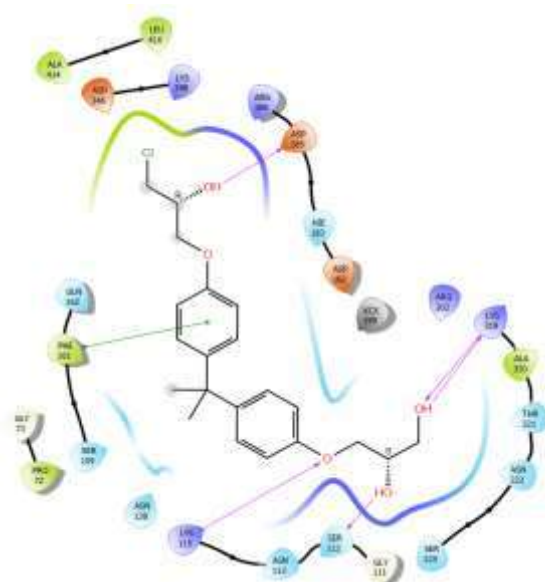


Fig.6.7a

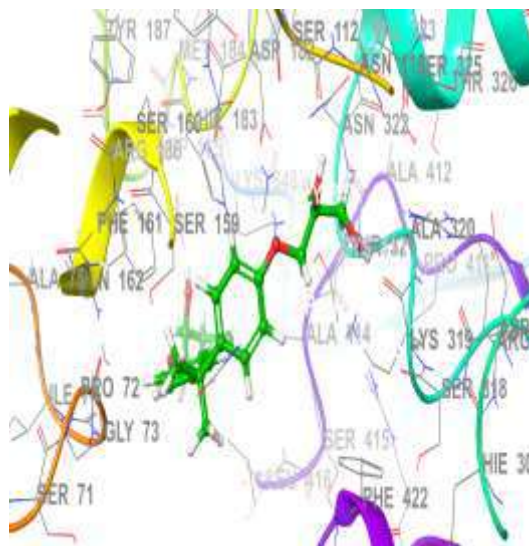


Fig.6.7b

Figure 6.7: Fig. 6.7a: Ligand interaction diagram of compound S7 (EPI-001) with MurD (2UUP) Fig 6.7b: Ribbon presentation of MurD (2UUP) –S7 (EPI-001) complex

The docking pose of compound S8 (TWS119) displayed three hydrogen bonding interactions and a pi- pi stacking interaction with the residues present within the catalytic pocket of the MurD enzyme (2UUP). Lysine residue at position 115 established hydrogen bonding interactions with the compound S8, while Serine residue at position 415 and HIE 183 amino acid residues established one hydrogen bonding interaction each with the compound S8. Phenylalanine (PHE) 422 residue was involved with pi- pi stacking interactions with the compound S8, further stabilizing it within the catalytic pocket of the enzyme (Fig 6.8a and 6.8b).

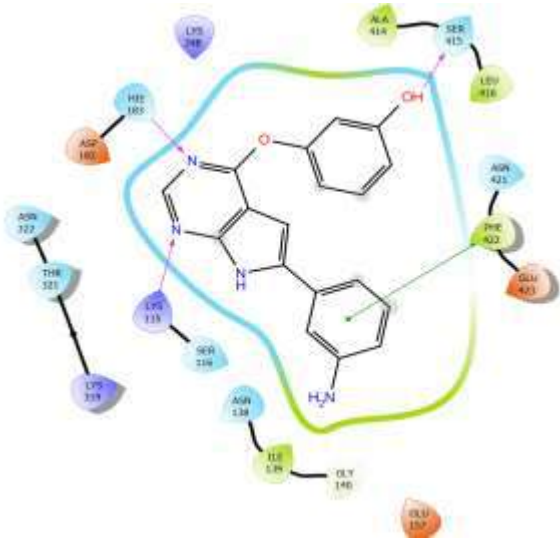


Fig.6.8a

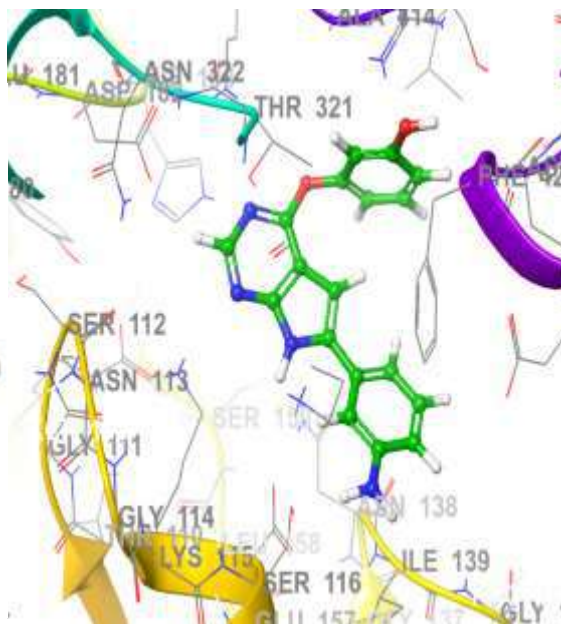


Fig.6.8b

Figure 6.8: Fig 6.8a:Ligand interaction diagram of compound S8 (TWS119) with MurD (2UUP); Fig 6.8b: Ribbon presentation of MurD (2UUP) –S8 (TWS119) complex

The docking pose of compound S9 (UM171) displayed one hydrogen bonding interaction, one pi-pi stacking interaction, one pi-cation interaction and a salt bridge interaction with the residues present within the catalytic pocket of the MurD enzyme (2UUP). The Lysine residue at position 348 established pi-cation interaction with the compound S9, while Phenylalanine residue at position 161 established pi-pi stacking interactions and the compound was involved with a back hydrogen bond and a salt bridge interaction with the Aspartic acid residue at position 185 (Fig. 6.9 a and 6.9b).

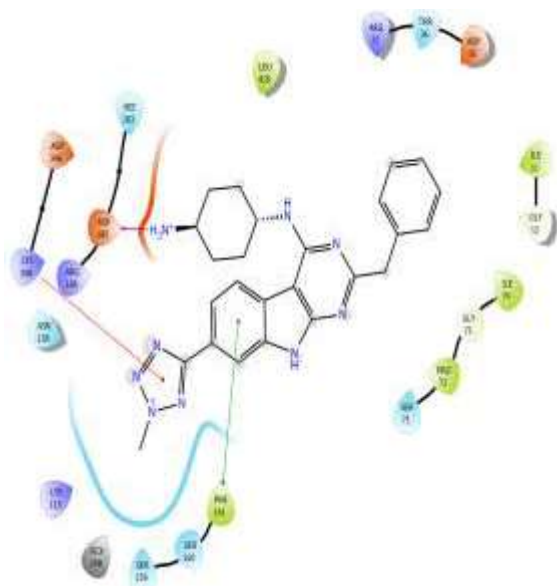


Fig.6.9a

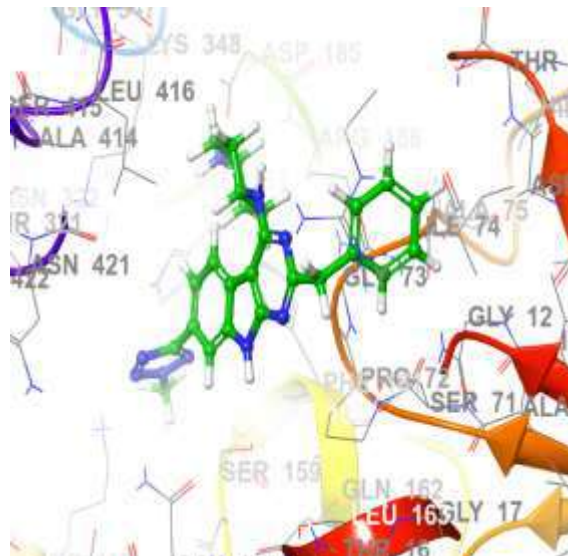


Fig.6.9b

Figure 6.9: Fig 6.9a:Ligand interaction diagram of compound S9 (UM171) with MurD (2UUP);Fig 6. 9b: Ribbon presentation of MurD (2UUP) –S9 (UM171) complex

The docking pose of compound S10 (CP868569) displayed that the compound interacted with four hydrogen bonds one each with residues Glycine at position 140, Asparagine at position 138, Glycine at position 137 and a backbone hydrogen bonding interaction with HIE183 (Fig 6.10a and 6.10b).

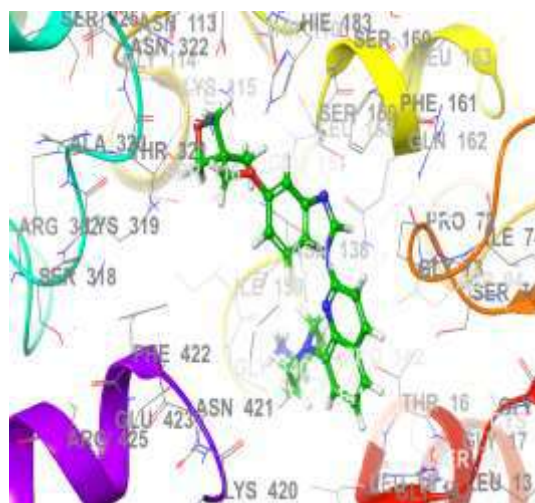


Fig.6.10 b

Figure 6.10: Fig 6.10a:Ligand interaction diagram of compound S10 (CP868569) with MurD (2UUP); Fig6.10b: Ribbon presentation of MurD (2UUP) –S10 (CP868569) complex

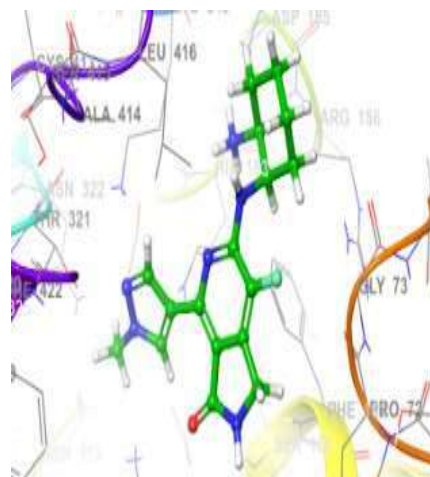


Fig. 6.11 b

Figure 6.11: Fig 6.11a: Ligand interaction diagram of compound S11 (TAK-659) with MurD (2UUP); Fig 6.11b: Ribbon presentation of MurD (2UUP) –S11 (TAK-659) complex

The docking pose of compound S11 (TAK-659) displayed two hydrogen bonding interaction, two pi-pi stacking interaction, one back hydrogen bonding interaction and a salt bridge interaction with the residues present within the catalytic pocket of the MurD enzyme (2UUP). The compound S11 forms a pi-pi stacking interaction with the Histidine183 and Phenylalanine residue at position 161. The compound interacts with the Aspartic acid residue at position 185 with the help of a salt bridge interaction. Hydrogen bond interactions are also displayed with Asparagine residue at position 138 Aspartic acid residue at position 185. The compound was also involved with a back hydrogen bond with the Threonine residue at position 321 and Asparagine 138 residue (Fig 6.11a and 6.11b).

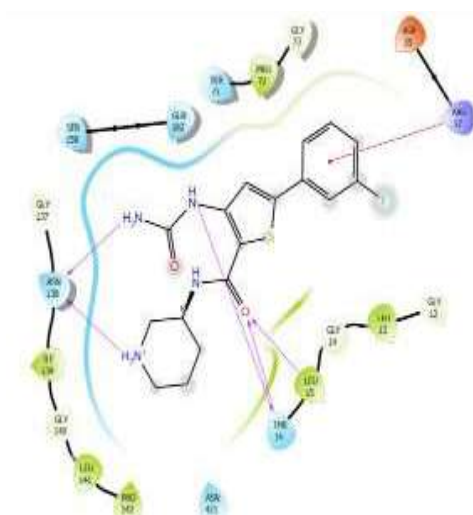


Fig. 6.12 a

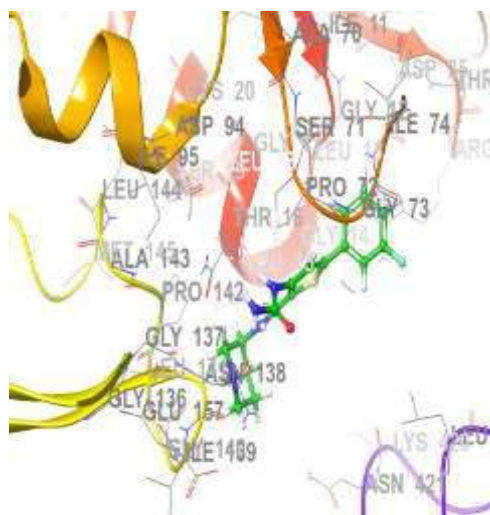


Fig. 6.12 b

58

Figure 6.12: Fig 6.12a:Ligand interaction diagram of compound S12 (AZD7762) with MurD (2UUP) ; Fig 6.12b: Ribbon presentation of MurD (2UUP) –S12 (AZD7762) complex

The docking pose of compound S12 (AZD7762) displayed the interaction of compound with Arginine residue at position 37 with a pi-cation interaction, hydrogen bonding interaction with Threonine 16 and Asparagine138 residue. Also, back hydrogen bonding interactions is displayed with Threonine at 16 position and Leucine 15 residue (Fig 6.12a and 6.12b).

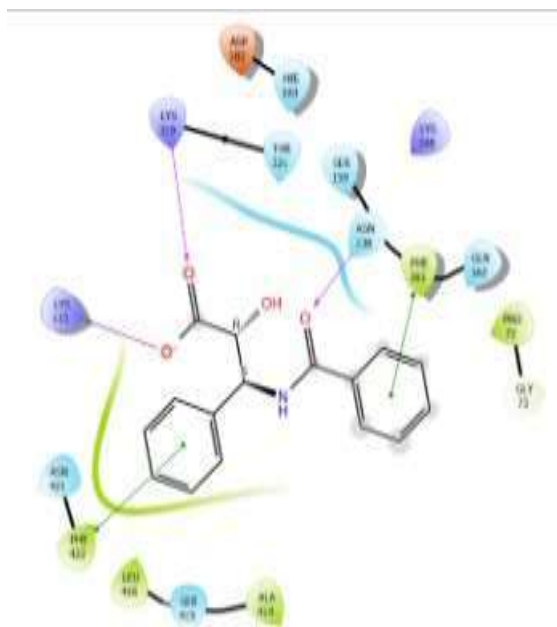


Fig.6.13 a

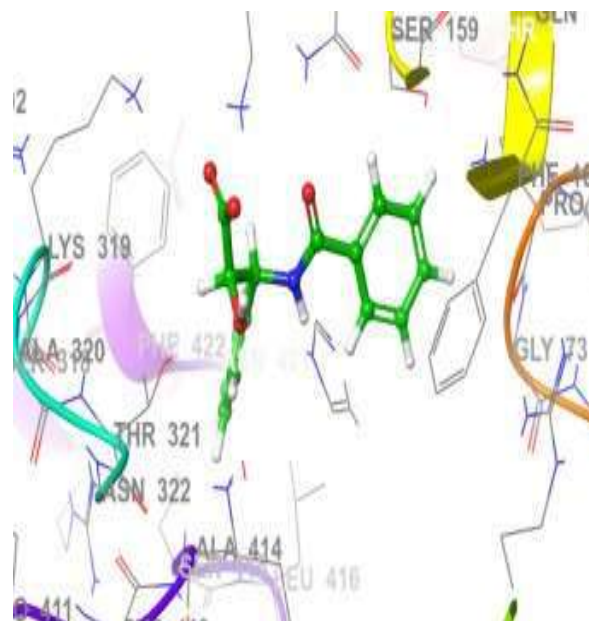


Fig.6.13 b

Figure 6.13: Fig 6.13a:Ligand interaction diagram of compound S13 (S9395 N-Benzoyl-(2R,3S)-3-phenylisoserine) with MurD (2UUP); Fig 6.13b: Ribbon presentation of MurD (2UUP) –S13 (S9395 N-Benzoyl-(2R,3S)-3-phenylisoserine) complex

The docking pose of compound S13 displayed two back-bone hydrogen bonding interaction, two pi-pi stacking interaction, and a salt bridge interaction with the residues present within the catalytic pocket of the MurD enzyme (2UUP). It established pi-pi stacking interaction one each with Phenylalanine residue at position 422 and 161. The compound also displayed back hydrogen bonding interaction with Lysine 319 and Asparagine residue at position 138. A salt bridge interaction was established with Lysine residue at position 115 (Fig 6.13a and 6.13b).

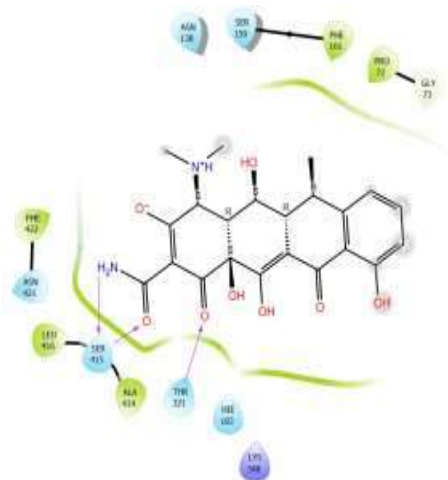


Fig.6.14 a

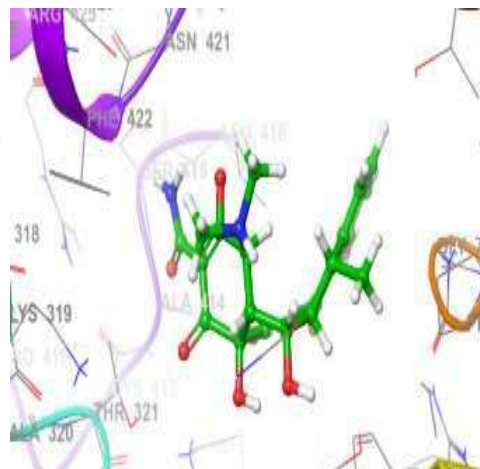


Fig. 6.14 b

Figure 6.14: Fig 6.14a:Ligand interaction diagram of compound S14 (S9395 N-Benzoyl-(2R,3S)-3-phenylisoserine) with MurD (2UUP); Fig 6.14b: Ribbon presentation of MurD (2UUP) –S14 (S9395 N-Benzoyl-(2R,3S)-3-phenylisoserine) complex

The docking pose of compound S14 displayed that the compound interacted with the residues present in the catalytic pocket of enzyme 2UUP with a hydrogen bond interaction with hydrogen bond interaction with Serine residue at position 415 and back hydrogen bond interaction with Serine 415 and and Threonine at position 321 (Fig 6.14a and 6.14b).

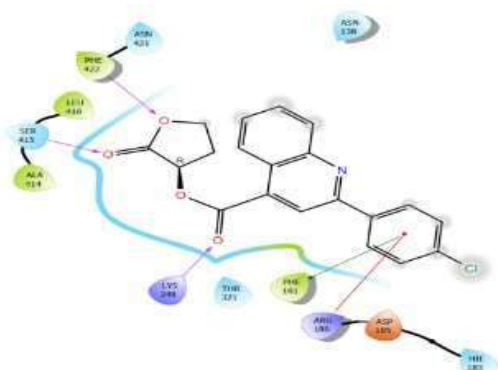


Fig.6.15 a

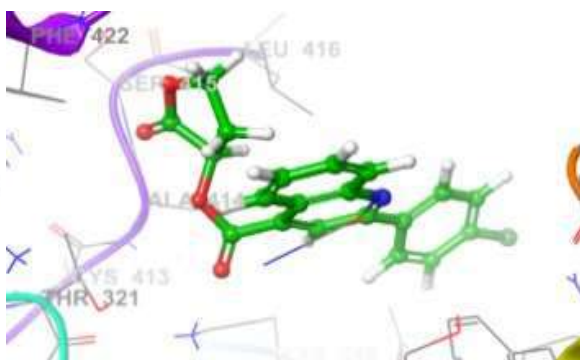


Fig. 6.15 b

Figure 6.15: Fig 6.15a:Ligand interaction diagram of compound S15 (631305) with MurD (2UUP); Fig 6.15b: Ribbon presentation of MurD (2UUP) –S15 (631305) complex

The docking pose of compound S15 (631305) displayed that the compound interacted with three hydrogen bonding interactions, a pi- cation interaction and a pi- pi stacking interaction with the residues present within the catalytic pocket of the MurD enzyme (2UUP). The compound displayed hydrogen bonding interaction with Serine 415, Phenylalanine 422 and Lysine residue at position 348, a pi-pi stacking interaction with phenylalanine 161 and a pi cation interaction with Arginine 186 (Fig 6.15a and 6.15b).

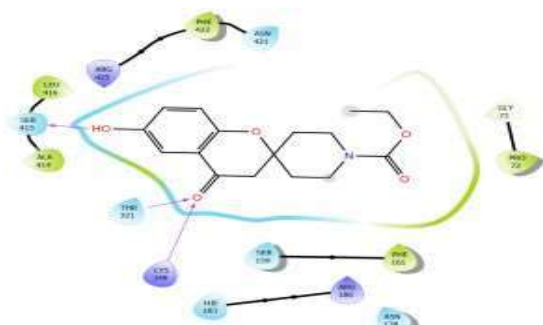


Fig. 6.16 a

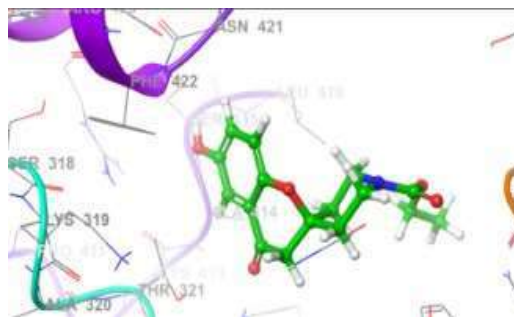


Fig. 6.16 b

Figure 6.16: Fig 6.16a: Ligand interaction diagram of compound S16 (333718) with MurD (2UUP); Fig 6.16b: Ribbon presentation of MurD (2UUP) –S16 (333718) complex

The docked pose of compound S16 (333718) interacted within the active site of protein 2UUP (Mur D) with a total of three hydrogen bonds. The compound interacted with Serine 415 residue with a hydrogen bonding interaction and was involved with back hydrogen bonding interaction Threonine 321 and Lysine at position 348 (Fig 6.16a and 6.16b)

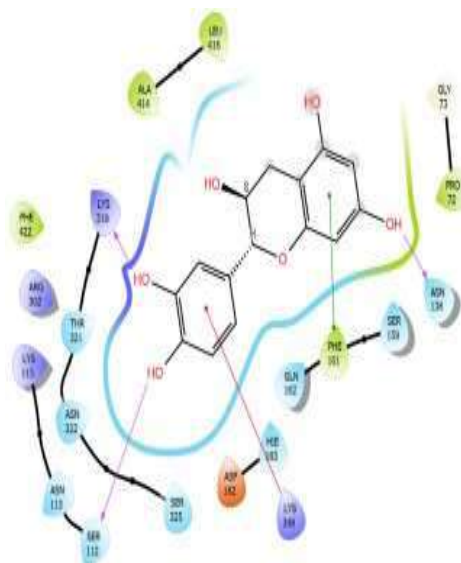


Fig.6.17 a

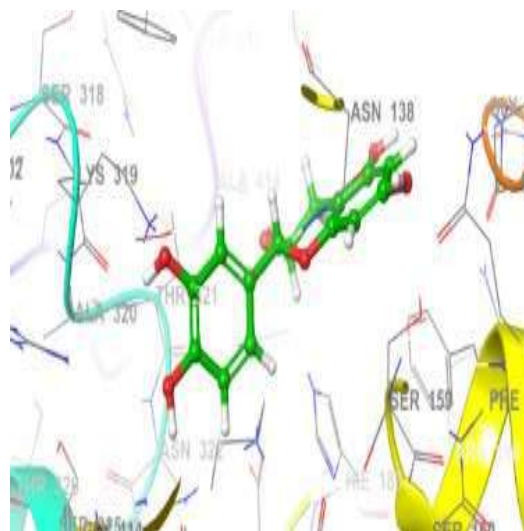


Fig. 6.17 b

Figure 6.17: Fig. 6.17a:Ligand interaction diagram of compound S17 (S4722) with MurD (2UUP); Fig 6.17b: Ribbon presentation of MurD (2UUP) –S17 (S4722) complex

The docking pose of compound S17 (S4722) displayed three hydrogen bonding interactions with Lysine 319, Serine 112 and Asparagine residue at position 138. It was also involved with a pi-cation interaction with Lysine at position 348 and a pi-pi stacking interaction with the Phenylalanine residue at position 161 present within the catalytic pocket of the MurD enzyme (2UUP) (Fig 6.17a and 6.17b).

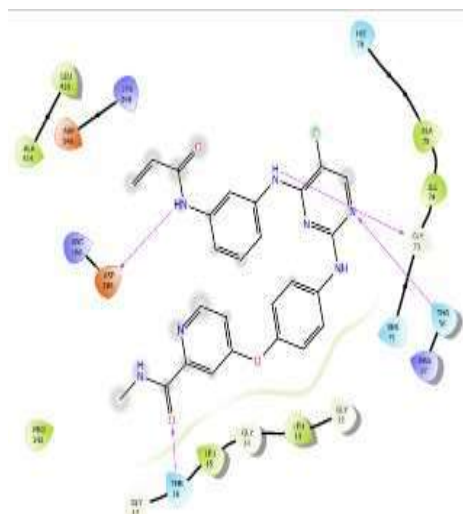


Fig. 6.18 a

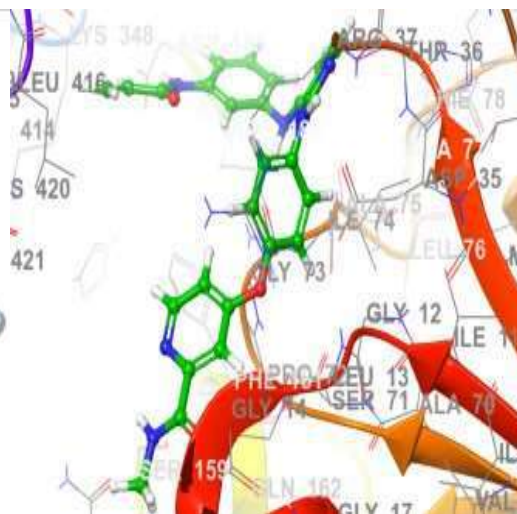


Fig. 6.18 b

Figure 6.18: Fig.6.18a:Ligand interaction diagram of compound S18 (CNX-774) with MurD (2UUP); Fig.6.18b: Ribbon presentation of MurD (2UUP) –S18 (CNX-774) complex

The docking pose of compound S18 (CNX-774) displayed two hydrogen bonding interactions with Asparagine 185 residue and Glycine 73 residue. The compound S18 also displayed back hydrogen bond interactions with Threonine residues at position 16 and 36 present within the catalytic pocket of the MurD enzyme (2UUP) (Fig 6.18a and 6.18b).

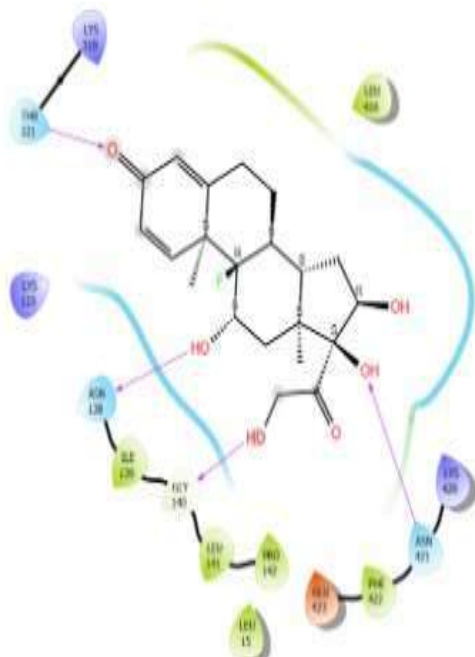


Fig. 6.19 a

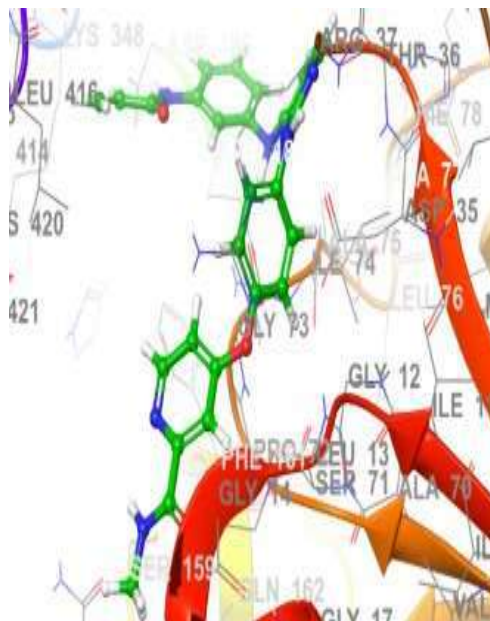


Fig. 6.19 b

Figure 6.19: Fig. 6.19a: Ligand interaction diagram of compound S19 (KENACORT (triamcinolone)) with MurD (2UUP); Fig. 6.19b: Ribbon presentation of MurD (2UUP) –S19 (KENACORT (triamcinolone)) complex

The docking pose of compound S19 (KENACORT (triamcinolone)) displayed two hydrogen bonding interactions with Asparagine residue at position 138 and Glycine 140 residue. It was also involved with back hydrogen bonding interactions with Threonine 321 and Asparagine residue at position 421 (Fig 6.19a and 6.19b).

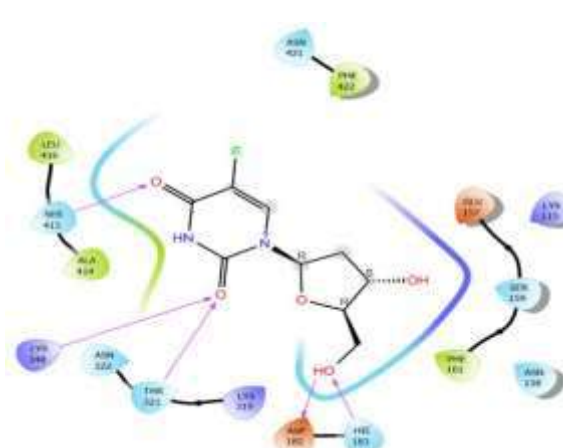


Fig. 20a

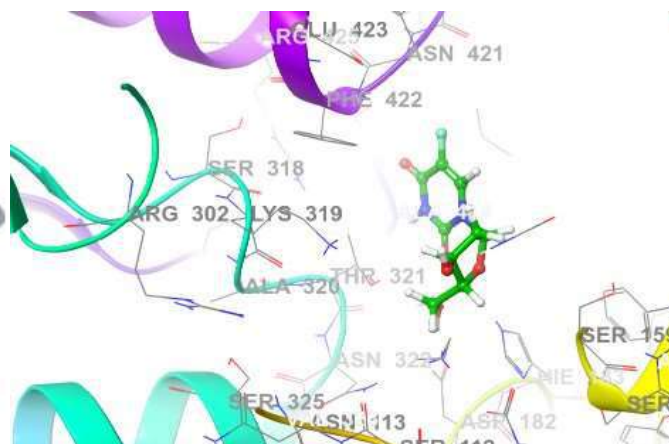


Fig. 20b

Figure 6.20: Fig.6.20a:Ligand interaction diagram of compound S20 (Floxuridine) with MurD (2UUP); Fig.6.20b: Ribbon presentation of MurD (2UUP) –S20 (Floxuridine) complex

The docked pose of compound S20 (Floxuridine) interacted within the active site of protein 2UUP (Mur D) with a total of 5 hydrogen bonds. The compound interacted with Serine 415, Lysine 348, Threonine 321, Aspartic acid 182 and Histidine 183 residue with a hydrogen bonding interaction each (Fig. 6.20a and 6.20b).

The docked ligand reproduced the key hydrogen bonds, hydrophobic contacts, and salt bridges with catalytic site residues seen in the 2UUP crystal ligand, occupied the same binding pocket orientation, and maintained interactions critical for MurD inhibition, confirming the docking accuracy. The amino acids present in the binding site of phospho-MurNAc-L-Ala-D-Glu that is the intermediate product during the catalysis of MurD enzyme consists of residues Leucine 15, Threonine 16, Asparagine 138, Glutamine 162, Lysine 348, Threonine 321, Serine 415 and Phenylalanine 422 (Turk et al., 2009). In contrast to alternative techniques for docking ligands to the three-dimensional structure of a recognized protein receptor, Glide approximates a thorough, methodical exploration of the docked ligand's conformational, orientational, and positional space. In this search, torsionally flexible energy optimization is carried out for a few hundred surviving candidate poses on an OPLS-AA nonbonded potential grid after an initial rough positioning and scoring phase that significantly reduces the search space (Friesner et al., 2004). In the study using novel Pyridin-2-yl-Carbamodithioates as inhibitors of MurD enzyme of *E.*

coli, the van der Waals interactions were also found to be the main interactions during binding of the inhibitors against *E. coli* MurD enzyme as found out by XP-screening and calculation of binding free energies studies (Azam et al., 2020). Interaction of the lead molecules with the residues present within the binding region of the *E. coli* MurD enzyme was found to be driven by strong hydrogen bond interactions in agreement with earlier studies (Azam et al., 2017). The types of various interactions that each virtual hit makes with the residues in the catalytic region of the enzyme have been depicted in Table 6.4.

Table 6.4: Extra- precision docking scores of top 20 virtual hits against MurD (2UUP) enzyme target

Vital Hits	Compound name/Molecule ID	Glide Score	Glide E-model	Type of Interactions
S1	WZB117	-9.013	-71.473	H-bond,Pi-cation,Pi-Pi stacking
S2	EPZ015666	-7.882	-59.621	H-bond
S3	SCH727965	-7.633	-57.272	H-bond,Salt-bridge
S4	Phloretin	-7.923	-52.169	H-bond,Pi-cation
S5	S9428 Brazilin	-7.357	-48.294	H-bond,Pi-Pi stacking
S6	CRT0066101	-7.126	-50.295	H-bond,Pi-Pi stacking
S7	EPI-001	-6.904	-62.614	H-bond,Pi-Pi stacking
S8	TWS119.cdx	-6.86	-54.802	H-bond,Pi-Pi stacking
S9	UM171	-6.696	-66.658	H-bond,Pi-Pi stacking,Pi-cation,salt bridge
S10	CP868569	-6.445	-69.073	H-bond
S11	TAK-659.cdx	-6.408	-50.498	H-bond,Pi-Pi stacking,salt bridge
S12	AZD7762.cdx	-6.402	-59.442	H-bond,Pi-cation
S13	S9395 N-Benzoyl-(2R,3S)-3-phenylisoserine.cdx	-6.359	-42.477	H-bond,Pi-Pi stacking,salt bridge
S14	S5159 Doxycycline.cdx	-6.581	-51.945	H-bond
S15	WAY-631305	-6.35	-57.885	H-bond,Pi-Pi stacking,Pi-cation
S16	WAY-333718	-6.347	-45.209	H-bond
S17	S4722 (+)-Catechin.cdx	-6.343	-49.537	H-bond,Pi-Pi stacking,Pi-cation
S18	CNX-774.cdx	-6.315	-77.671	H-bond
S19	KENACORT (triamcinolone).cdx	-6.311	-49.704	H-bond
S20	Floxuridine.cdx	-6.471	-39.03	H-bond

6.2. Molecular dynamics simulation studies

MD simulation for 100 ns was performed for the top-docked virtual hit S1. MD simulations were carried out to determine the stability of the interactions of ligand-protein docked complexes. In MD simulations, the stability of the protein (2UUP) with the bound D-Glu containing sulfonamide bound at the Mur D ligase binding site was investigated using RMSD

analysis of the protein backbone about the initial frame structure. The analysis of the RMSD offers insights into the stability and behavior of the ligand-receptor complex throughout the simulation period. The RMSD of the ligand was closely monitored to understand its dynamic changes within the binding site of the receptor. The RMSD results for the MurD Apo protein and the WZB117-Mur D Complex offer insights into their structural dynamics during MD simulations. The MurD Apo protein displays a minimum RMSD of 0.98 Å, indicating close agreement with the reference structure in specific regions. Both structures demonstrate comparable maximum RMSD values (5.49 Å for the Apo protein and 5.11 Å for the complex), highlighting areas of significant structural deviation over the course of the simulations. The average RMSD values are 3.59 Å for the Apo protein and 3.61 Å for the complex, indicating a moderate overall level of structural agreement. The RMSD value of the WZB117-MurD complex indicates fluctuations between 1 Å and 4.75 Å during the initial 50 ns. Afterward, a decrease in RMSD is observed, culminating in minor fluctuations towards the end. In the case of the Apo protein, higher fluctuations are observed in the initial phase until 35 ns, followed by a decrease in RMSD, and some minor fluctuations are noted towards the end (Fig 6.21).

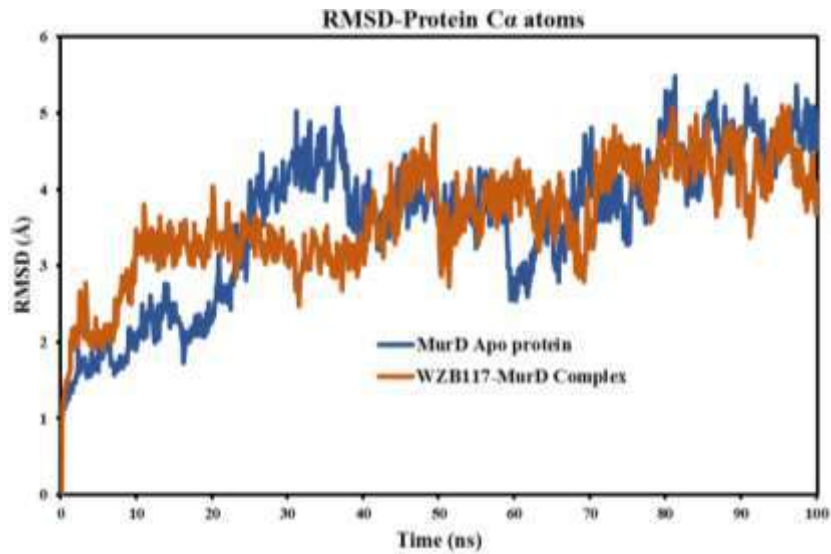


Figure 6.21: Time-dependent root mean square deviation (RMSD) of the WZB117 (S1)-Mur D complex during 100 ns of MD simulation

During the MD simulation, the RMSF analysis investigates the flexibility of individual residues within the protein-ligand interaction. Throughout the simulation, it computes the average deviation of each atom or residue from its average location. RMSF values aid in identifying regions of high flexibility (e.g., loops and turns) and low flexibility (e.g., stable secondary structures). The study sheds light on the complex's dynamic behavior and structural alterations. In the MD simulation, Compound WZB117 (S1) interacted with 40 amino acids, including Leu13(1.6Å), Leu15(2.1Å), Thr16(2.1Å), Thr36(2.1Å), Arg37(2.3Å), Ser71(1.4Å), Pro72(1.5Å), Gly73(1.8Å), Ile74(1.7Å), Ala75(1.6Å), Leu76(1.6Å), Ala77(1.9Å), His78(1.9Å), Ser112(1.0Å), Lys115(1.0Å), Asn138(1.7Å), Glu157(0.8Å), Ser159(1.1Å), Ser160(1.0Å), Phe161(1.1Å), Gln162(0.9Å), Glu164(0.8Å), Asp182(1.2Å), His183(1.1Å), Asp185(1.2Å), Arg186(1.3Å), Tyr187(1.3Å), Pro188(1.6Å), Phe189(1.5Å), Gln193(1.2Å), Kcx198(0.8Å), Lys319(1.4Å), Thr321(1.8Å), Asp346(2.3Å), Ala414(2.0Å), Ser415(2.9Å), Leu416(2.3Å), Lys420(2.5Å), Phe422(1.6Å), Glu423(1.5Å). The interaction of WZB117 (S1) with the examined residues showcases negligible RMSF values, signifying the inherent stability of the ligand within the binding site (Fig. 6.22). This observation underscores a robust and enduring binding interaction between the Mur D ligase protein and the ligand S1(WZB117).

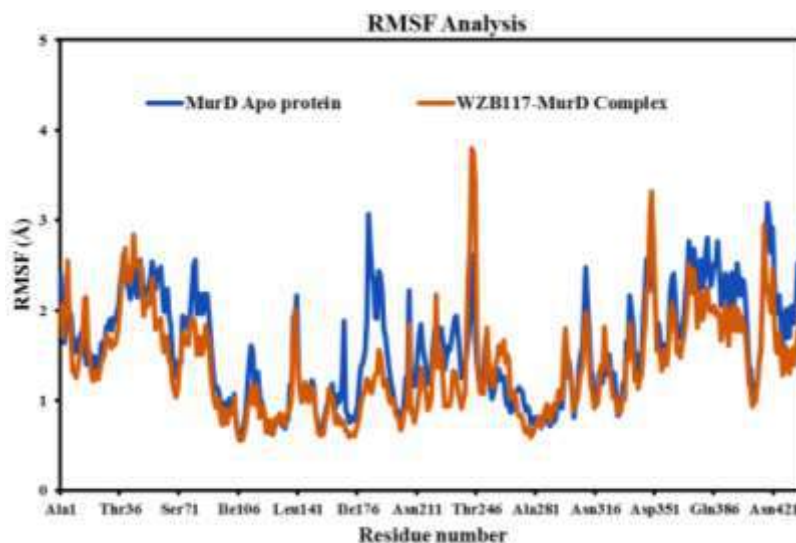


Fig 6.22: Individual amino acids Root mean square fluctuation (RMSF) plot of WZB117 (S1)-MurD complex

The interactions during the 100 ns trajectory were examined, where residue GLY73 was involved in hydrogen bond interactions with the protein. The residues GLU164 and TYR187

interacted through a water bridge interaction with the protein molecule (Fig. 6.23a). The interaction fraction of various amino acid residues has been presented in Fig. 6.23b. Similar hydrogen bond interactions were also reported during molecular dynamics evaluation of other studies (Samal et al., 2015; Wang et al., 2019). The protein-ligand interactions and plots were analyzed using the Simulation Event Analysis tool of Desmond (Cutinho et al., 2020) and the protein-ligand interactions were visualized by Maestro Visualizer using a simulation interaction diagram panel (www.schrodinger.com).

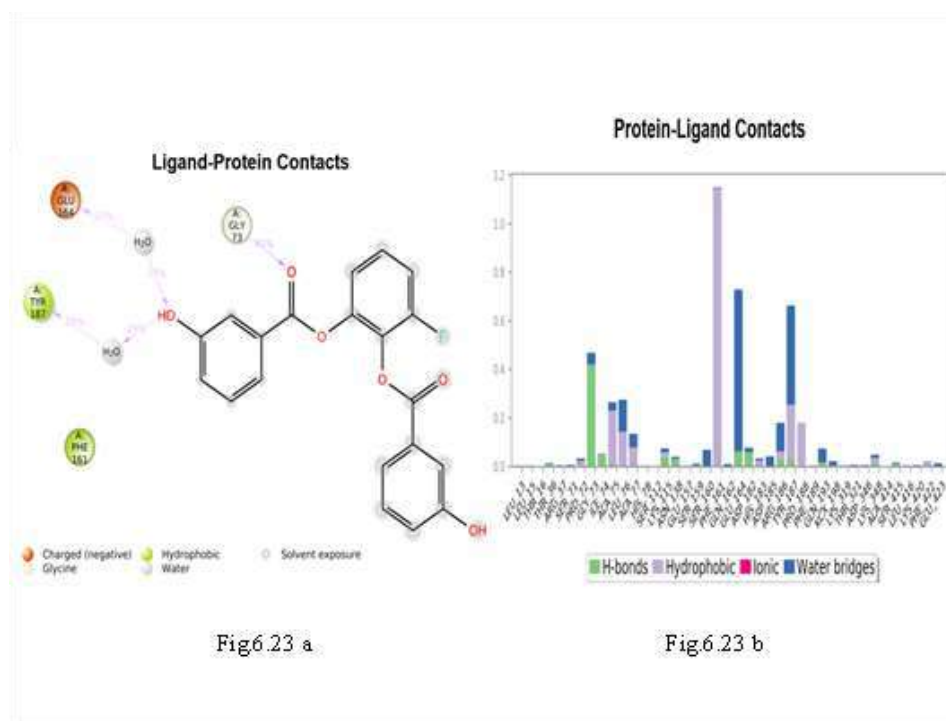


Figure 6.23 Fig 6.23a: Binding interactions of ligand (WZB117) (S1) with Mur D (2UUP) during MD Simulation of 100 ns; Fig 6.23b: Interaction fraction of various residues (WZB117 (S1)-MurD (2UUP) Complex)

6.3. Binding Free Energy Calculation studies

Binding free energy calculations are critical in molecular docking as they provide a quantitative measure of the strength and stability of interactions between a ligand (small molecule) and a target protein. This energy, often reported as the ΔG of binding, is essential in assessing the likelihood that a ligand will bind effectively to its target, which is foundational in drug discovery and rational design (Gilson et al., 2007). Binding free energy calculations estimate the affinity of a ligand for its protein target, helping to rank potential drug candidates based on their expected efficacy. Lower (more negative) binding free energies indicate stronger and more stable interactions (Mobley et al., 2009). The binding free energy profile of the protein, 2UUP (Mur D) protein, and compound S1 (WZB117) complex system was determined to display the stability of the entire system. The generation of 1-1000 frames with a 10-step sample size was used for the post-simulation MM-GBSA analysis of binding free energy (ΔG Bind) computation. The lead compound S1 (WZB117), in complex with 2UUP protein, as revealed by the dynamics studies, was the subject of 100 frames (every ns) of analysis and processing. The calculated every ns post simulation MM-GBSA binding free energy for the protein ligand complex is depicted in Table 6.5, which presents the results of the binding energy calculation for the WZB117-2UUP complex, highlighting various energy components obtained from MM-GBSA trajectories in kcal/mol. Hydrogen bonding, as indicated by ΔG Bind,_H bond, contributes -0.735 ± 0.643 kcal/mol to the overall binding energy, emphasizing the importance of specific intermolecular interactions. The calculated average ΔG Bind of the product, S1 (WZB117) in complex with the 2UUP protein, was found to be -48.701 ± 13.301 kcal/mol (Table 6.6). The non-bonded energy distribution in molecular mechanics was obtained through the high van der Waal energy (ΔG bind_vdw) of -34.590 ± 6.856 kcal/mol, lipophilic energy (ΔG Bind_Lip) of 16.730 ± 5.588 kcal/mol, and columbic (electrostatic) energy (ΔG Bind_Coul) of -10.686 ± 6.463 , which are considered the most significant contributors to the binding of compound S1 to the target 2UUP protein. The high negative values of ΔG vdW indicated hydrophilic interaction between the *E. coli* MurD (2UUP) and the inhibitor S1(WZB117) in agreement with earlier studies and the heightened negative value of ΔG bind displays that binding of the inhibitor S1 to *E. coli* MurD enzyme is guided through enthalpy in agreement with other studies (Azam et al., 2019).

Table 6.5: Binding free energy (ΔG Bind in kcal/mol) values in the WZB117-2UUP complex based on post-simulation MM-GBSA

Time (ns)	ΔG_{Bind}	$\Delta G_{\text{Bind_Coul}}$	$\Delta G_{\text{Bind_Hbond}}$	$\Delta G_{\text{Bind_Lip}}$	$\Delta G_{\text{bindsol_GB}}$	$\Delta G_{\text{bind_vdw}}$
0	-45.508	-28.285	-3.764	-12.710	30.953	-37.237
1	-40.024	-19.581	-3.271	-11.199	24.556	-28.133
2	-31.353	-31.449	-2.728	-7.197	31.078	-22.846
3	-26.768	-13.840	-1.795	-6.579	28.460	-30.098
4	-23.708	-4.600	-0.582	-8.750	15.411	-24.813
5	-32.307	-13.152	-1.023	-9.097	22.248	-30.977
6	-60.061	-15.718	-1.551	-21.676	21.188	-41.785
7	-28.352	-11.455	-1.775	-7.427	24.493	-31.088
8	-25.295	-12.645	-2.103	-6.519	24.672	-22.249
9	-22.720	-7.465	-0.871	-4.496	18.668	-22.844
10	-21.961	-5.135	-0.562	-4.388	12.140	-21.597
11	-18.914	-6.011	-0.377	-2.789	17.649	-22.459
12	-29.499	-6.449	-0.069	-8.901	18.220	-26.093
13	-28.720	-4.324	-0.346	-10.520	16.562	-24.430
14	-31.521	-10.664	-0.466	-10.358	19.888	-24.800
15	-24.351	-12.356	-0.608	-6.631	17.128	-19.010
16	-32.465	-8.483	-0.554	-8.110	10.620	-20.343
17	-19.594	-3.770	0.000	-4.605	12.706	-18.198
18	-32.647	-18.106	-0.391	-8.504	20.563	-22.347
19	-30.144	-16.460	-0.943	-9.145	17.598	-20.694
20	-31.860	-7.11602	-0.583	-8.938	11.505	-22.372
21	-33.980	-3.505	-0.371	-10.854	13.078	-29.932
22	-38.972	-10.714	-0.847	-13.079	16.757	-30.459
23	-38.231	-13.388	-0.462	-13.186	22.530	-32.416
24	-32.935	-4.639	-0.002	-13.366	14.525	-29.518
25	-39.462	-5.808	-0.269	-11.161	12.568	-29.642
26	-41.036	-16.379	-0.721	-14.523	22.319	-31.240
27	-36.605	-2.785	-0.001	-10.812	11.266	-30.158
28	-30.195	-3.800	-0.514	-8.673	9.917	-23.219
29	-27.775	-5.792	-0.023	-10.461	8.327	-23.664
30	-31.235	-6.376	-0.044	-10.848	12.574	-25.718
31	-37.070	-4.417	-0.261	-11.081	14.201	-30.466
32	-42.677	-7.183	-0.077	-16.874	14.882	-34.860
33	-33.937	-1.457	-0.089	-12.904	17.556	-33.391
34	-46.338	-8.097	-0.428	-20.006	24.795	-39.225

35	-51.163	-17.097	-1.307	-18.231	23.823	-36.467
36	-47.196	-5.906	-1.042	-16.221	13.723	-32.990
37	-58.777	-12.772	-1.076	-22.006	22.124	-43.036
38	-64.916	-19.335	-0.619	-21.484	21.673	-41.340
39	-57.101	-5.351	-0.591	-21.499	16.419	-40.303
40	-59.137	-13.481	-1.027	-22.239	18.780	-38.063
41	-60.372	-15.229	-1.423	-20.693	18.209	-36.820
42	-50.824	-3.912	-0.547	-20.787	17.965	-38.409
43	-60.443	-8.276	-0.576	-21.699	17.525	-42.116
44	-65.923	-12.107	-0.908	-20.774	16.350	-40.615
45	-60.551	-11.724	-0.742	-21.850	15.998	-38.103
46	-59.091	-6.087	-0.410	-19.577	15.760	-39.740
47	-60.061	-15.718	-1.551	-21.676	21.188	-41.785
48	-63.252	-11.272	-0.753	-21.028	15.508	-39.336
49	-57.787	-17.000	-0.719	-19.929	20.304	-34.854
50	-53.317	-7.512	-0.625	-19.378	15.427	-38.290
51	-58.863	-10.587	-0.605	-19.586	16.550	-35.086
52	-62.323	-12.066	-1.066	-21.822	15.553	-40.372
53	-58.417	-8.853	-0.770	-18.624	16.683	-36.869
54	-70.958	-22.068	-1.608	-22.184	20.354	-41.535
55	-55.633	-4.760	-0.535	-19.732	15.223	-38.912
56	-67.264	-21.953	-1.096	-23.220	25.006	-42.241
57	-49.811	-3.265	-0.042	-19.545	18.139	-38.658
58	-57.115	-3.175	-0.125	-19.916	15.573	-39.570
59	-58.050	-1.081	-0.119	-23.896	19.325	-43.227
60	-55.269	-1.458	-0.003	-20.447	17.714	-41.935
61	-53.640	-2.911	-0.056	-19.437	14.261	-40.739
62	-55.581	-3.764	-0.028	-21.116	17.083	-37.662
63	-59.298	-11.563	-0.015	-21.582	17.891	-41.712
64	-59.715	-8.109	-0.680	-19.930	16.380	-38.120
65	-51.900	-8.410	-0.528	-17.593	18.347	-36.822
66	-52.645	-1.868	-0.060	-22.135	19.104	-39.237
67	-56.633	-3.944	-0.191	-23.030	19.029	-43.361
68	-55.095	-6.251	-0.560	-19.286	18.215	-38.142
69	-56.449	-12.107	-0.689	-22.820	16.684	-38.098
70	-54.834	-19.218	-1.087	-14.767	17.568	-29.026
71	-59.647	-17.548	-0.712	-19.745	23.338	-38.562
72	-53.062	-11.732	-0.561	-20.686	24.199	-39.985
73	-49.399	-6.055	-0.519	-16.518	15.253	-36.664

74	-52.491	-6.320	-0.019	-19.329	19.413	-39.048
75	-59.364	-23.150	-1.403	-19.521	22.231	-34.050
76	-54.893	-28.467	-1.327	-19.697	25.379	-31.623
77	-58.050	-6.318	-0.474	-22.709	14.842	-40.575
78	-52.865	-13.940	-0.716	-18.102	21.215	-32.640
79	-57.520	-9.179	-0.614	-20.618	17.378	-39.544
80	-54.989	-20.239	-1.084	-17.889	22.290	-32.620
81	-52.729	-21.613	-1.103	-15.346	21.251	-28.468
82	-52.461	-10.580	-0.020	-17.917	20.947	-40.167
83	-48.722	-2.176	-0.340	-18.275	18.231	-36.537
84	-52.805	-10.626	-0.526	-18.889	20.717	-37.791
85	-58.689	-13.399	-0.743	-19.935	18.497	-37.752
86	-55.109	-16.272	-0.315	-18.231	23.856	-37.962
87	-57.790	-6.216	-0.572	-22.095	15.715	-42.875
88	-61.826	-12.049	-1.230	-21.596	17.291	-37.412
89	-44.556	-14.023	-1.025	-14.762	19.741	-31.650
90	-59.956	-11.523	-0.561	-21.509	22.303	-41.620
91	-64.049	-19.143	-1.405	-20.933	22.327	-39.624
92	-59.067	-6.334	-0.553	-21.350	15.838	-41.913
93	-59.396	-11.386	-0.560	-21.578	17.877	-42.959
94	-62.700	-9.980	-0.630	-22.245	17.319	-39.972
95	-58.328	-11.131	-0.569	-21.391	20.010	-39.412
96	-52.029	-4.286	-0.609	-18.838	13.827	-34.751
97	-52.645	-4.869	-0.539	-19.296	12.393	-34.442
98	-60.816	-16.506	-0.598	-20.336	21.756	-40.150
99	-52.151	-10.805	-1.310	-20.403	20.782	-35.547
100	-73.102	-21.863	-1.384	-23.867	22.711	-45.364
Max.	-73.102	-31.449	-3.764	-23.896	8.327	-45.364
Min.	-18.914	-1.081	0.000	-2.789	31.078	-18.198
Avg.	-48.701	-10.686	-0.735	-16.730	18.475	-34.590
Std.	13.301	6.463	0.643	5.588	4.241	6.856

Table 6.6: Binding energy calculation of the virtual hit S1-2UUP complex and non-bonded interaction energies from MM-GBSA trajectories.

Energies (kcal/mol)	S1-2UUP complex
$\Delta G_{\text{Bind}}^{\text{a}}$	-48.701 ± 13.301
$\Delta G_{\text{Bind_Coul}}^{\text{b}}$	-10.686 ± 6.463
$\Delta G_{\text{Bind_Hbond}}^{\text{c}}$	-0.735 ± 0.643
$\Delta G_{\text{Bind_Lip}}^{\text{d}}$	-16.730 ± 5.588
$\Delta G_{\text{Bindsol_GB}}^{\text{e}}$	18.475 ± 4.241
$\Delta G_{\text{Bind_vdw}}^{\text{f}}$	-34.590 ± 6.856

a: Free energy of binding

b: Coulomb energy

c: Hydrogen-bonding energy

d: Lipophilic energy

e: solvation free energy

f: van der Waals energy

6.4. Prediction of ADMET properties of potential lead molecules: Prediction of compounds' pharmacokinetic properties by applying ADMET (Absorption, Distribution, Metabolism, Excretion, and Toxicity) modeling is frequently employed in drug discovery due to its high-throughput nature and cost-effectiveness. The results obtained after ADMET prediction and the Lipinski rule of five have been presented in Tables 6.7, 6.8 and 6.9. No violation was observed for molecular weight, hydrogen bond donor, or hydrogen bond acceptor values, as these were well in the accepted range (Table 6.9).

Structural, physicochemical, biochemical, pharmacokinetics and toxicity properties of top hits were calculated by using the Qikprop application of the Maestro suite of Schrodinger software (Fan et al., 2010) and underlined in Table 6.7 & 6.8. The ADMET (Absorption, Distribution, Metabolism, Excretion, and Toxicity) properties of various drugs provide preclinical data that play a significant role in the estimation of drug targeting after administration (Chandrasekaran et al., 2018). The n-octanol/water-octanol/water efficient (QPlogPo/w) is used

to measure the extent of distribution of a solute between water and the water-immiscible liquid phase. It is widely used to estimate a compound's lipophilic or hydrophobic properties and is widely used in the pharmaceutical sciences (Breindl et al., 1997). The QPlogPo/w value related to the hydrophobicity of the molecules from (S1–S20) was found in the range of -1.109 to 4.122 (Table 6.7), which was well within the recommended range of -2.0 to 6.5. As the MurD enzyme is an intracellular target (cytoplasmic enzyme) that may require the binding of agonists with a suitable lipophilic nature for effective action, based on QPlogPo/w values, the virtual hits from S1 to S20 displayed promising results. Human serum albumin (HSA), has a remarkable ability to bind to a variety of substances, including a broad range of medications. Therefore, a drug's interaction with HSA regulates its free and active concentration, acting as a reservoir for a prolonged duration of action and ultimately influencing the drug's ADMET (Absorption, Distribution, Metabolism, Excretion, and Toxicity) profile (Zsila et al., 2011). The estimation of QPlogKhsa (Prediction of binding to Human Serum Albumin) values displayed that the top twenty compounds have values from -0.422 to 0.794. The results shown in Table 6.7 demonstrated that all the top virtual hits displayed QPlogKhsa values within the recommended range of -1.5 to 1.5.

Caco-2 permeability is commonly used to predict the absorption of an oral medication into the human intestinal mucosa during *in vitro* analysis. As the intestine is the immediate site for the absorption of an orally administered drug, the QPPCaco values play a significant role in the prediction of the oral absorbability of a virtual hit (Husain et al., 2021). The final 20 virtual hits displayed QpCaco (cell permeability) values in the range of 2.51 to 1084.749. Most of the final virtual hits displayed average to good (compound S9 (50.42) and S15 (1084.749) cell permeability values except the virtual hit S14 which displayed a low Caco-2 permeability of 2.51 suggesting a structural modification to improve the permeability property. Percent Human Oral Absorption values of final virtual hits were found in the range of 21.488 to 100. Most of the compounds displayed average to good Percent Human Oral Absorption values (Table 6.7). The predicted blood brain barrier (QPlog BB) values of the highest virtual hits were found in the range of -2.236 to -0.238. Based on the Madin-Darby Canine Kidney (MDCK) cell line, the QPPMDCK ADMET (Absorption, Distribution, Metabolism, Excretion, and Toxicity) property

shows how small molecules are absorbed by the intestinal tract and is correlated with intestinal absorption in humans. This information is used to forecast small-molecule prioritization in drug-discovery projects (Patel et al.; 2018). The predicted QPPMDCK values of the highest virtual hits were found in the range of 0.847 (virtual hit S14) to 1334.432 (virtual hit S15) and most of the compounds displayed values better than the MurD controls already studied.

The most fascinating aspect of S1 is its admirable QPlogPo/w, related to the molecule's hydrophobicity of 2.94. It exhibits QPlogKhsa (Prediction of binding to Human Serum Albumin) and QPPCaco (cell permeability) values of 0.1 and 292.721 respectively (Table 6.7). Also, it exhibits a promising Percent Human Oral Absorption value of 88.348. The second-highest hit, S2, also displayed promising values of QPlog po/w, QPlogKhsa, and QPPCaco of 1.669, -0.296, and 164.06, respectively. It also exhibits an admirable Percent Human Oral absorption value of 76.36. Apart from these, virtual hit S3 also displays good values of QPlogpo/w, QPlogKhsa, and QPPCaco values of 4.122, 0.652, and 587.187, and an excellent Percent Human Oral absorption value of 100, respectively (Table 6.7).

While adding more progression criteria to discovery projects could help find high-quality compounds, it can also make the process more difficult, which could slow it down, increase costs, shorten patent durations, and make it less competitive. The early synthesis of compounds with desired properties and the deselection of compounds predicted to have unwanted features are the sources of speed. So, "predictive ADMET" has emerged from the application of traditional methods of structure-activity analysis and quantitative structure-activity relationship (QSAR) analysis to data on Absorption, Distribution, Metabolism, Excretion, and Toxicity (ADMET) (Davis et al., 2004).

The early stages of drug development have relied heavily on the estimation of pharmacokinetic parameters to guide hit-to-lead and lead-optimization efforts. Drug discovery players have actively sought molecular modeling techniques to find patterns in ADMET data and turn them into knowledge, given the exceptional complexity of the present R&D model. The field has developed in tandem with cheminformatics, which has progressed from conventional chemometrics to sophisticated machine learning techniques (Ferreira et al., 2019).

Table 6.7. Predicted ADMET parameters of top 20 virtual hits by Qikprop

Virtual Hits	Compound name/Molecule ID	QPlog Po/w ¹	QPlogKhsa ²	QPP Caco ³ (nm/sec)	%HOA ⁴	QPlogBB	QPPMDCK
MurD Inhibitors (Controls) https://pubchem.ncbi.nlm.nih.gov	CID84973005	1.722	-0.625	0.326	28.324	-3.091	0.505
	CID25181430	3.372	-0.225	0.467	40.763	-3.553	0.723
	CID84973004	1.907	-0.573	0.313	29.07	-3.345	0.498
	CID84972996	4.923	0.664	454.301	90.373	-1.342	560.064
S1	WZB117	2.947	0.1	292.721	88.348	-1.334	211.933
S2	EPZ015666	1.669	-0.296	164.065	76.36	-0.819	77.581
S3	SCH727965	4.122	0.652	587.187	100	-1.149	278.243
S4	Phloretin	2.113	0.025	73.638	72.737	-2.024	29.5
S5	S9428 Brazilin	1.294	-0.193	138.453	72.845	-1.346	58.372
S6	CRT0066101	2.393	0.133	110.758	77.545	-0.993	50.735
S7	EPI-001	3.817	0.212	429.092	96.414	-1.551	482.022
S8	TWS119	2.42	0.113	217.973	82.969	-1.305	95.333
S9	UM171	3.273	0.677	50.42	76.583	-1.221	21.672
S10	CP868569	4.115	0.789	342.873	96.415	-0.238	172.093
S11	TAK-659.cdx	1.481	0.058	73.8	69.054	-0.695	50.29
S12	AZD7762.cdx	1.568	0.001	15.199	57.279	-1.25	28.395
S13	S9395 N-Benzoyl-(2R,3S)-3-phenylisoserine.cdx	2.673	-0.271	84.503	77.084	-1.204	43.537
S14	S5159 Doxycycline.cdx	0.059	-0.111	2.51	21.488	-2.303	0.847
S15	WAY-631305	3.475	0.062	1084.749	100	-0.444	1334.432
S16	WAY-333718	2.096	0.064	380.094	85.396	-0.989	173.885
S17	S4722 (+)-Catechin.cdx	0.469	-0.422	52.764	60.519	-1.927	20.575
S18	CNX-774.cdx	3.883	0.361	170.488	89.623	-2.236	105.735
S19	KENACORT (triamcinolone).cdx	1.146	-0.22	67.263	66.367	-1.745	32.048
S20	Floxuridine.cdx	-1.109	-0.794	49.385	50.76	-1.513	33.620

1. QPlog Po/w: Predicted water partition coefficient (-2.0- 6.5)

2. QPlogKhsa : Predicted binding to Human serum albumin (-1.5-1.5)

3. QPPCaco: Predicted Apparent Caco-2 cell permeability in nm/sec (25 poor, >500 great)

4. %HOA : Percent Human Oral Absorption (> 80% high, < 25 poor)

5. QPlogBB: Predicted blood/brain coefficient (-3.0 to 1.2)

6. QPPMDCK: Predicted MDCK cell permeability in nm/sec (25 poor >500 great) . MDCK cells are considered to be a good mimic for the blood-brain barrier

Table 6.8. Evaluation of ADMET parameters of the lead molecules by Qikprop

Virtual Hits	Compound name/Molecule ID	SASA ^a	FOSA ^b	FISA ^c	PISA ^d
MurD Inhibitors (Controls) https://pubchem.ncbi.nlm.nih.gov	CID84973005	628.195	48.314	346.866	129.305
	CID25181430	798.012	114.294	330.492	251.705
	CID84973004	664.214	75.792	348.841	133.333
	CID84972996	805.64	17.837	141.153	569.202
S1	WZB117	637.836	0	161.283	438.483
S2	EPZ015666	695.684	314.888	124.2	256.597
S3	SCH727965	698.542	386.043	129.403	183.097
S4	Phloretin	529.015	49.88	224.485	254.649
S5	S9428 Brazilin	486.138	96.554	195.571	194.013
S6	CRT0066101	677.012	262.353	142.194	272.465
S7	EPI-001	732.234	303.398	143.768	214.626
S8	TWS119	562.625	0	174.786	387.839
S9	UM171	764.824	292.385	178.235	294.205
S10	CP868569	474.771	71.691	272.681	130.399
S11	TAK-659.cdx	612.845	335.995	160.787	81.973
S12	AZD7762.cdx	662.811	195.422	205.435	189.635
S13	S9395 N-Benzoyl-(2R,3S)-3-phenylisoserine.cdx	535.786	29.15	155.292	351.344
S14	S5159 Doxycycline.cdx	636.543	201.055	315.623	119.864
S15	WAY-631305	625.591	118.609	101.294	333.99
S16	WAY-333718	575.379	298.922	149.321	127.136
S17	S4722 (+)-Catechin.cdx	516.539	61.655	239.752	215.133
S18	CNX-774.cdx	884.145	170.143	186.039	498.698
S19	KENACORT (triamcinolone).cdx	589.983	267.282	228.633	79.741
S20	Floxuridine.cdx	428.537	126.166	242.782	14.98

a: SASA(Solvent Accessible Surface Area): Total solvent surface area in square angstroms using a probe with 1.4 Å radius

b: FOSA: Hydrophobic component of SASA (saturated carbon and attached hydrogen)

c: FISA: Hydrophobic component of SASA (SASA on N , O and H on heteroatoms)

d: PISA: Phi (carbon and attached hydrogen) component of SASA.Volume; Estimated number of hydrogen bonds that would be accepted by the solute from the water molecules in aqueous solution.Values are averages taken over a number of configurations,so they can be non-integer.

The surface area components were used to estimate the volume (total solvent-accessible volume), PISA (β component of SASA), FOSA (hydrophobic component of SASA), FISA (hydrophilic component of SASA), and SASA (total solvent accessible surface area) properties.

The SASA (total solvent accessible surface area) value of lead molecules were found in the range of 474.77 (Virtual hit S10) to 884.14 (Virtual hit S18) (Table 6.8) that were found to be well within the acceptable range of 300.0 – 1000.0 while FOSEA (Hydrophobic component of SASA (saturated carbon and attached hydrogen)) were in the range of 0 (Virtual hit S1) to 386.04 (Virtual hit S3) (Table 6.8), and were well in the accepted range of 0.0 – 750.0 as predicted in (https://gohom.win/ManualHom/Schrodinger/Schrodinger_20152_docs/qikprop/qikprop_user_manual). Likewise FOSEA, Hydrophobic component of SASA (SASA on N, O and H on heteroatoms) were in the range of 101.294 (Virtual hit S15) to 315.62 (Virtual hit S14) and were again in the acceptable range of 7.0 – 330.0 while PISA π (carbon and attached hydrogen) component of the SASA values were found in the range of 14.98 (Virtual hit S20) to 498.69 (Virtual hit S18). Most of the compounds displayed values within the acceptable range of 0.0 – 450.0 except few which suggested structural modification. Most of the above described properties of the lead molecules were within the acceptable range (https://gohom.win/ManualHom/Schrodinger/Schrodinger_20152_docs/qikprop/qikprop_user_manual.pdf). Likewise these properties of lead molecules were found to be comparable or better than the molecules already studied against MurD enzyme (Table 6.8).

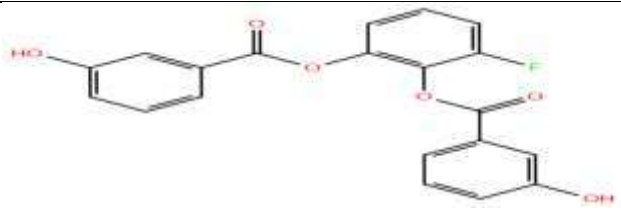
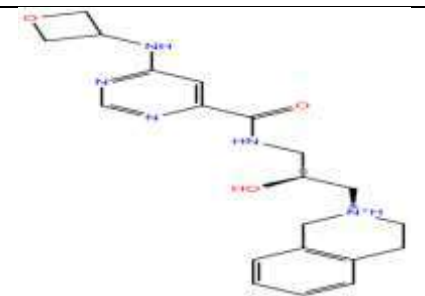
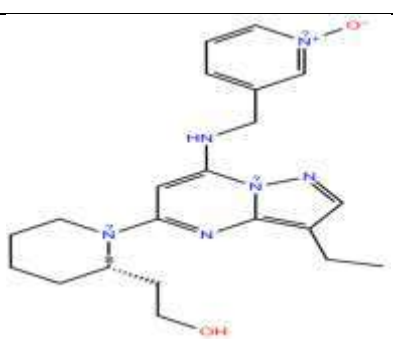
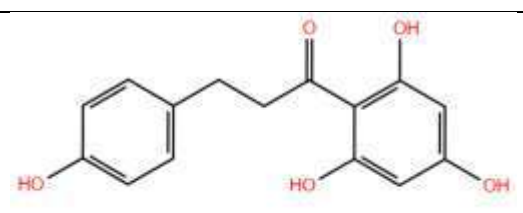
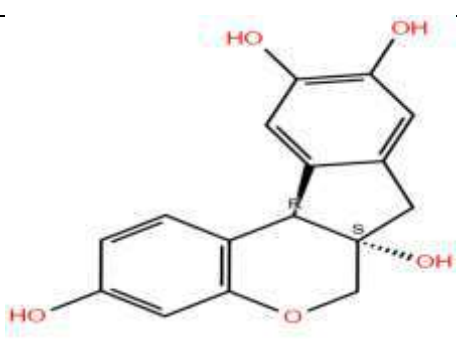
All of the top 20 virtual hits finalized against the Mur D enzyme (Mur D) PDB ID 2UUP) were found to obey the Lipinski rule of Five (0 to 1) (Table 6.9).

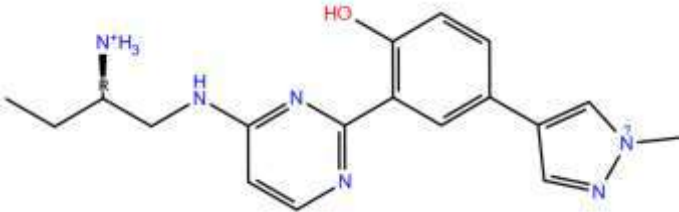
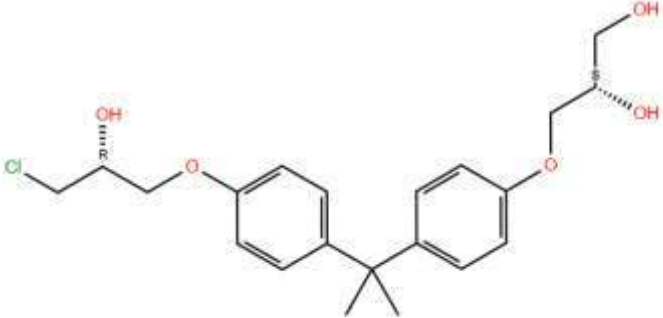
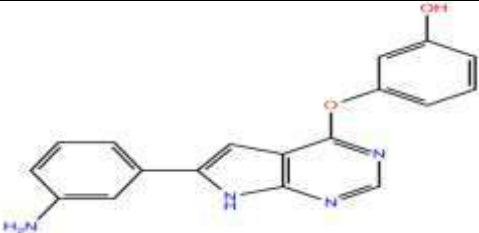
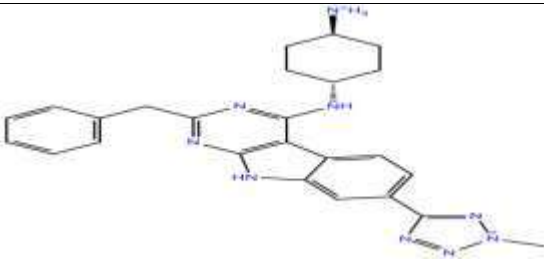
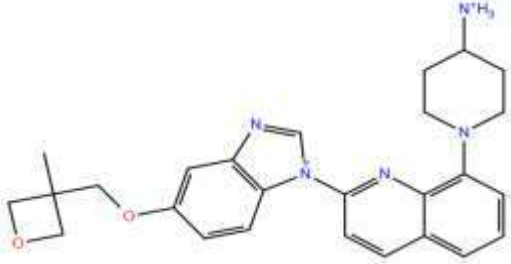
Table 6.9. Predicted Lipinski parameters of top 20 lead molecules

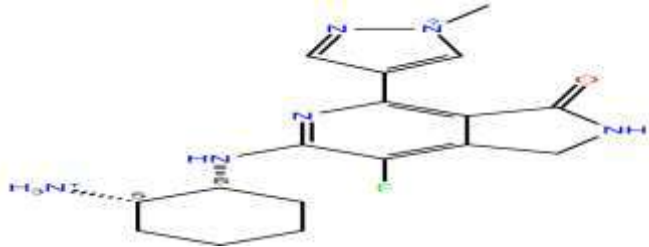
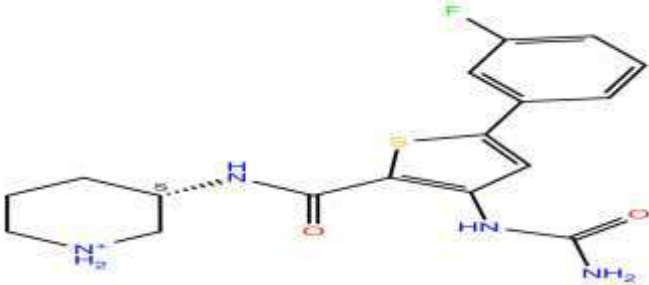
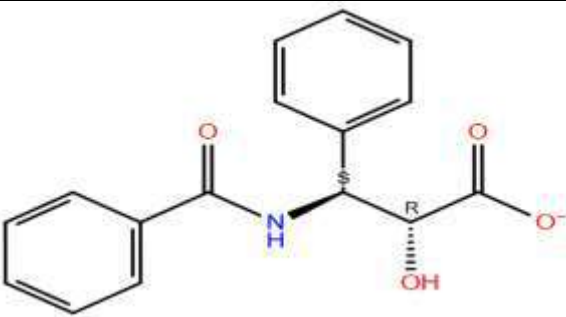
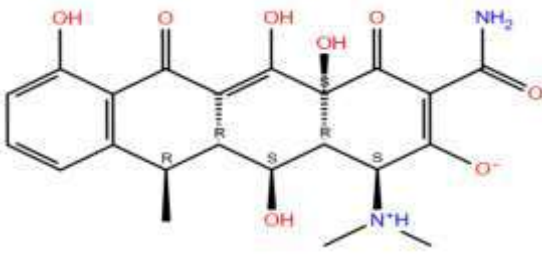
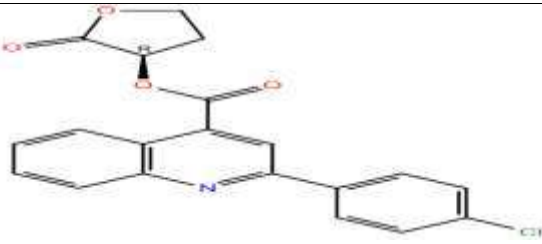
Virtual Hits	Compound name/Molecule ID	M.Wt ¹	Volume ²	donorHB ³	acceptHB ⁴	Rule of Five ⁵
MurD Inhibitors (Controls) https://pubchem.ncbi.nlm.nih.gov	CID84973005	394.416	1102.262	3.25	8.25	0
	CID25181430	499.555	1436.206	4.25	9.25	0
	CID84973004	394.416	1139.181	3.25	8.25	0
	CID84972996	508.388	1395.845	2	7	1
S1	WZB117	304.256	876.116	4	6.45	0
S2	EPZ015666	280.205	856.614	0	9	0
S3	SCH727965	219.584	613.226	2	3.5	0
S4	Phloretin	175.1	554.328	1	5.5	0
S5	S9428 Brazilin	288.256	903.495	3	4.75	0
S6	CRT0066101	197.19	641.262	2	3.5	0
S7	EPI-001	311.337	1042.446	5	6.25	0
S8	TWS119	272.257	882.221	2	4	0
S9	UM171	444.486	1381.051	4	9.9	1
S10	CP868569	237.012	564.096	1	5	0
S11	TAK-659.cdx	344.391	1076.666	4	6.5	0
S12	AZD7762.cdx	362.421	1121.225	4	5	0
S13	S9395 N-Benzoyl-(2R,3S)-3-phenylisoserine.cdx	285.299	927.189	2	5.2	0
S14	S5159 Doxycycline.cdx	444.44	1205.013	3	9.2	1
S15	WAY-631305	367.788	1094.149	0	6	0
S16	WAY-333718	305.33	987.919	1	6	0
S17	S4722 (+)-Catechin.cdx	290.272	871.955	5	5.45	0
S18	CNX-774.cdx	499.503	1540.845	4	9.5	1
S19	KENACORT (triamcinolone).cdx	394.439	1106.377	3	8.85	0
S20	Floxuridine.cdx	246.192	710.426	3	8.6	0

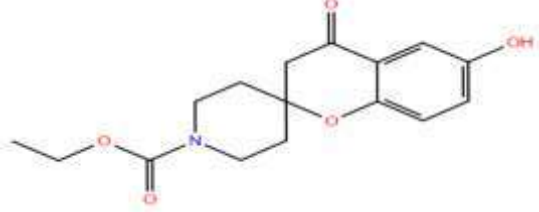
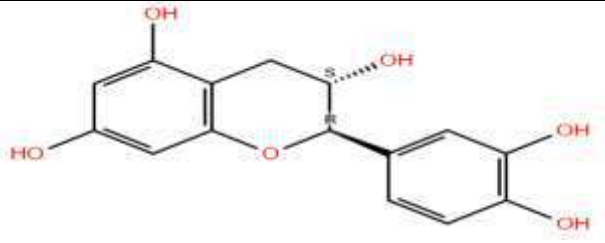
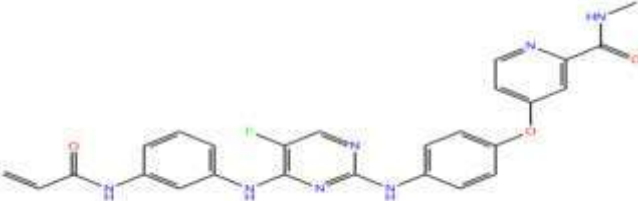
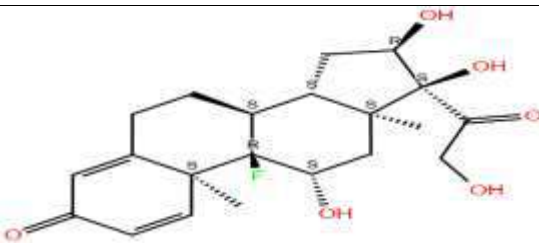
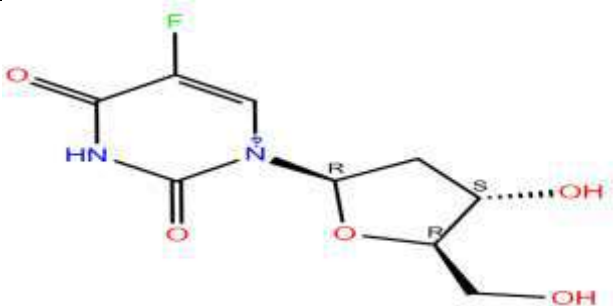
1. M.Wt: Molecular weight of the molecule
2. Volume: Total solvent-accessible volume in cubic angstroms using a probe with a 1.4Å^o
3. donor HB: Estimated number of hydrogen bonds that would be donated by solute to water molecule in aqueous solution (<5)
4. accept HB : Estimated number of hydrogen bonds that would be accepted (<10)
5. Rule of Five: Number of violations of Lipinski's rule

Table 6.10: Chemical structures of various lead molecules against MurD

Virtual Hit	Molecule ID	Chemical Structure
S1	WZB117	
S2	EPZ015666	
S3	SCH727965	
S4	Phloretin	
S5	S9428 Brazilin	

S6	CRT0066101	
S7	EPI-001	
S8	TWS119	
S9	UM171	
S10	CP868569	

S11	TAK-659	
S12	AZD7762	
S13	S9395	
S14	S5159 Doxycycline	
S15	WAY-631305	

S16	WAY-333718	
S17	S4722 (+)-Catechin.cdx	
S18	CNX-774.cdx	
S19	KENACORT (triamcinolone)	
S20	Floxuridine.cdx	

6.5 Determination of Antibacterial Activity: The final two top lead molecules were procured commercially (Cayman chemicals, USA).



Fig 6.24 : Top two virtual lead compounds

Standard strains of *Escherichia coli* (ATCC 8739), *Staphylococcus aureus* (ATCC 6538), *Pseudomonas aeruginosa* (ATCC 9027), and *Bacillus subtilis* (ATCC 6633) were procured commercially. The antibacterial activities of the lead molecules S1 and S2 were determined by the agar well diffusion method. Sterile agar plates were seeded with selected bacterial strains (10^8 CFU) and were allowed to remain at 37 °C for 3 hours. Ciprofloxacin at the concentration of 5µg/ ml was used as a control drug (Azam et al., 2020) . The zone surrounding the well that inhibits bacterial growth was measured and the average in millimeters (three independent evaluations) was computed.

Table 6.11 & Fig 6.25a demonstrated that the zone of inhibition of the compound S1 against *Escherichia coli* (ATCC 8739) falls in the range of from 14 ± 0.08 mm at the concentration of 100 µg/ml, While the compound S2 did not exhibit any inhibitory activity against *Escherichia coli* (ATCC 8739) (Table 6.11 & Fig 6.25b) at the highest tested concentration of 100 µg/ml. Compound S1 exhibited encouraging antibacterial activity against the Gram-negative bacteria *Pseudomonas aeruginosa* (ATCC 9027) at a concentration of 100 µg/ml (zone of inhibition 13 ± 0.04 mm) (Table 6.12 & Fig 6.26 a) while compound S2 was found to be ineffective against the same strain even at the most heightened tested concentration of 100 µg/ml (Table 6.12 & Fig 6.26 b). (Table 6.13 & Fig 6.27 a) demonstrated that the zone of inhibition of the compound S1 against *Staphylococcus aureus* (ATCC 6538) falls in the range of from 20 ± 0.05 mm at the

concentration of 100 $\mu\text{g/ml}$, while the compound S2 displayed a zone of 18 ± 0.03 mm at the concentration of 100 $\mu\text{g/ml}$ (Table 6.13 & Fig 6.27b). Compound S1 also displayed antibacterial activity against the Gram-positive bacteria *Bacillus subtilis* (ATCC 6633) at a concentration of 100 $\mu\text{g/ml}$ (zone of inhibition 21 ± 0.05 mm), (Table 6.14 & Fig 6.28a) while compound S2 demonstrated zone of inhibition against *Bacillus subtilis* (ATCC 6633) in the range of from 19 ± 0.06 mm at the concentration of 100 $\mu\text{g/ml}$ (Table 6.14 & Fig 6.28b). Studies on antibacterial activity of Pyridin-2-yl-Carbamodithioates against various bacterial species also displayed significant antibacterial activity against *E. coli* NCIM 2065 and *Pseudomonas aeruginosa* NCIM 2200 (Azam et al., 2020)

Table 6.11: Antibacterial studies of compounds S1 & S2 on *Escherichia coli* (ATCC 8739)

S.No.	Treatment	Concentration ($\mu\text{g/ml}$)	Diameter of Zone of Inhibition (mm)
1	DMSO	-	-
2	Ciprofloxacin	5	23 ± 0.00
3	S1	100	14 ± 0.08
4	S2	100	-

The data represents the mean of three independent experiments

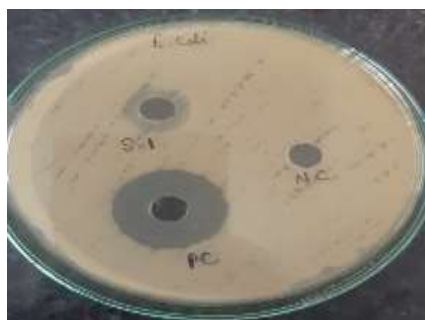


Fig. 6.25a

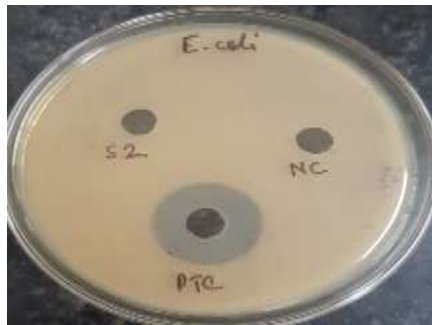


Fig. 6.25b

Fig. 6.25: Fig. 6.25a Antibacterial studies of compound S1 against *Escherichia coli* (ATCC 8739) & Fig. 6.25b Antibacterial studies of compound S2 against *Escherichia coli* (ATCC 8739)

Table 6.12. Antibacterial studies of compounds S1 & S2 on *Pseudomonas aeruginosa* (ATCC 9027)

S.No.	Treatment	Concentration (µg/ml)	Diameter of Zone of inhibition (mm)
1	DMSO	-	-
2	Ciprofloxacin	5	22± 0.00
3	S1	100	13± 0.04
4	S2	100	-

The data represents the mean of three independent experiments



Fig. 6.26 a



Fig 6.26 b

Fig. 6.26: Fig. 6.26a Antibacterial studies of virtual hit S1 against *Pseudomonas aeruginosa* (ATCC 9027) & Fig. 6.26b virtual hit S2 against *Pseudomonas aeruginosa* (ATCC 9027)

Table 6.13: Antibacterial studies of compounds S1 & S2 on *Staphylococcus aureus* (ATCC 6538)

S.No.	Treatment	Concentration ($\mu\text{g/ml}$)	Diameter of zone of Inhibition (mm)
1	DMSO	-	-
2	Ciprofloxacin	5	24 ± 0.00
3	S1	100	20 ± 0.05
4	S2	100	18 ± 0.03

The data represents the mean of three independent experiments

Fig. 6.27: Fig. 6.27a Antibacterial studies of virtual hit S1 against *Staphylococcus aureus* (ATCC 6538) & Fig. 6.27b Antibacterial studies of virtual hit S2 against *Staphylococcus aureus* (ATCC 6538)



Fig. 6.27 a



Fig 6.27 b

Table.6.14: Antibacterial studies of compounds S1 & S2 against *Bacillus subtilis* (ATCC 6633)

S.No.	Treatment	Concentration ($\mu\text{g/ml}$)	Diameter of zone of Inhibition (mm)
1	DMSO	-	-
2	Ciprofloxacin	5	25 \pm 0.00
3	S1	100	21 \pm 0.05
4	S2	100	19 \pm 0.06

The data represents the mean of three independent experiments

Fig. 6.28: Fig. 6.28a Antibacterial studies of virtual hit S1 against *Bacillus subtilis* (ATCC 6633) & Fig. 6.28b Antibacterial studies of virtual hit S2 against *Bacillus subtilis* (ATCC 6633)



Fig 6.28a

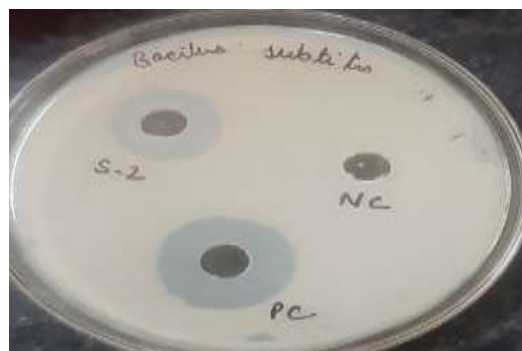


Fig 6.28 b

6.6 Determination of Minimum Inhibitory Concentration (MIC) :

The minimal inhibitory concentration (MIC) test was performed using Muller Hinton Broth (MHB) by using standard protocol. The lowest dilution that exhibits an inhibition percentage of greater than 95% is known as the minimum inhibitory concentration, or MIC (CLSI, 2020; Berhanu et al, 2013). The MIC of compound S1 was found to be at 40 µg /ml against *Escherichia coli* (ATCC 8739) at which 95.17 % of the growth was inhibited (Table 6.15 , Fig 6.29). The compound S1 exhibited an MIC of 50 µg/ml against *Pseudomonas aeruginosa* (ATCC 9027) at which 95.23 % growth was inhibited (Table 6.16 , Fig 6.30) The compound S1 exhibited an MIC of 30 µg /ml against *Staphylococcus aureus* (ATCC 6538) at which 95.11 % growth was inhibited Table 6.17 , Fig 6.31) while it displayed an MIC of 20 µg /ml with an inhibition percentage of 95.28 against *Bacillus subtilis* (ATCC 6633) (Table 6.18 , Fig 6.32) . The compound S2 was found to be ineffective against *Escherichia coli* (ATCC 8739) (Table 6.19) and *Pseudomonas aeruginosa* (ATCC 9027) (Table 6.20) at the highest tested concentration of 100 µg /ml while it displayed an MIC of 50 µg/ml against *Staphylococcus aureus* (ATCC 6538) (Table 6.21, Fig 6.33) and an MIC of 40 µg/ml against *Bacillus subtilis* (ATCC 6633) (Table 6.22, Fig 6.34). According to the findings, Gram-positive bacteria had lower MIC values for the tested compound than did Gram-negative bacteria. The Minimal Inhibitory Concentration (MIC) of novel lipopeptides (FT97) produced employing the Ugi-4CR process against *Staphylococcus aureus* was found to be 62.5 µg/mL displaying the moderate inhibitory effect of these lipopeptides (Valdes et al., 2023). Variations in the chemical makeup of bacterial cell walls and the tested compound's capacity to penetrate bacterial membranes may account for the diversity in antibacterial efficacy (Rashdan et al., 2021). A group of d-glutamic acid-containing dual inhibitor of MurD and MurE ligases from *Escherichia coli* and *Staphylococcus aureus* were designed, synthesized, and evaluated. It has minimal inhibitory concentration (MIC) values of 8 µg /mL, and it has antibacterial activity against Gram-positive *Staphylococcus aureus* and its methicillin-resistant strain (MRSA) (Tomašić et al., 2012). 5-benzylidenetherhodanine- and 5-benzylidenethiazolidine2,4dione-based compounds displayed MIC of > 128 µg/mL when tested against *Escherichia coli* ATCC 25922, *Pseudomonas aeruginosa* 27853, *Staphylococcus aureus* ATCC 29213, and *Enterococcus faecalis* ATCC 2921 (Zidar et

al.,2010). Compound T1827917 from Enamine library displayed MIC of 128,128,256 µg/mL against *Staphylococcus aureus* NCIM 5021, *Staphylococcus aureus* NCIM 5022 and methicillin resistant *Staphylococcus aureus* (MRSA strain 43300) while the compound was found to be ineffective against tested Gram negative bacterial strains (Azam et al., 2019). The increase in absorbance with increasing concentration of tested compounds is attributed to absorption of light by the compounds and cell lysis fragments but at the same time overall bacterial growth is decreasing as demonstrated by increase in percentage inhibition. A study that investigated the use of ethanol extracts from *Vinca rosea* leaves as a green corrosion inhibitor produced similar findings. Higher extract concentrations resulted in greater absorbance at particular wavelengths in the inhibitor solution's UV-Vis absorption spectra (Selvi et al.,2020). Certain plant extracts were also found to absorb light in the visible range displaying increased OD with extract concentration even when bacterial growth was inhibited or absent (Eloff, J. N., 1998).

Table 6.15. MIC determination of compound S1 against *Escherichia coli* (ATCC 8739)

conc.of compound S1 (µg/ml)	Absorbance (O.D at 600 nm)		% Inhibition
	Initial	Final	
100	0.641	0.54	99.05
50	0.52	0.421	97.11
40	0.47	0.373	95.17
30	0.368	0.294	72.84
20	0.237	0.184	52.45
10	0.132	0.083	48.57
5	0.099	0.067	32.06
4	0.08	0.052	28.18
3	0.07	0.05	20.41
Negative Growth Control	0.049	0.152	

The data represent the mean value of three independent experiments: $p < 0.05$

Fig 6.29: Concentration (of compound S1) vs inhibition % chart against *Escherichia coli* (ATCC 8739) vs control

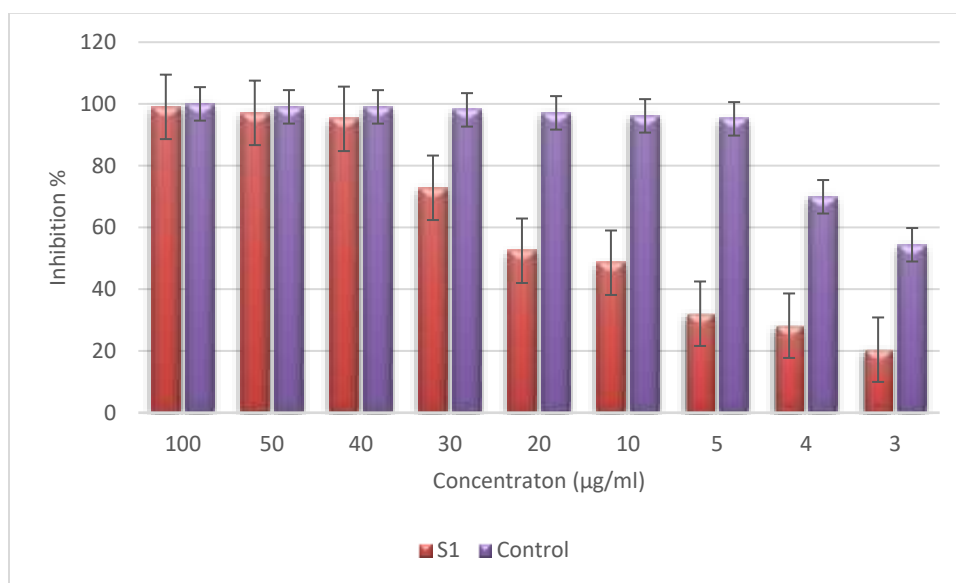


Table 6.16. MIC determination of compound S1 against *Pseudomonas aeruginosa* (ATCC 9027)

conc. of compound S1 (µg/ml)	Absorbance (O.D at 600 nm)		% Inhibition
	Initial	Final	
100	0.642	0.541	98.11
50	0.524	0.426	95.23
40	0.472	0.383	86.57
30	0.369	0.292	75.03
20	0.237	0.167	68.3
10	0.135	0.088	46.19
5	0.105	0.068	36.57
4	0.084	0.059	25.03
3	0.072	0.057	15.42
Negative Growth control	0.051	0.155	

The data represent the mean value of three independent experiments; $p < 0.05$

Fig 6.30. Concentration (of compound S1) vs inhibition % chart against *Pseudomonas aeruginosa* (ATCC 9027) vs control

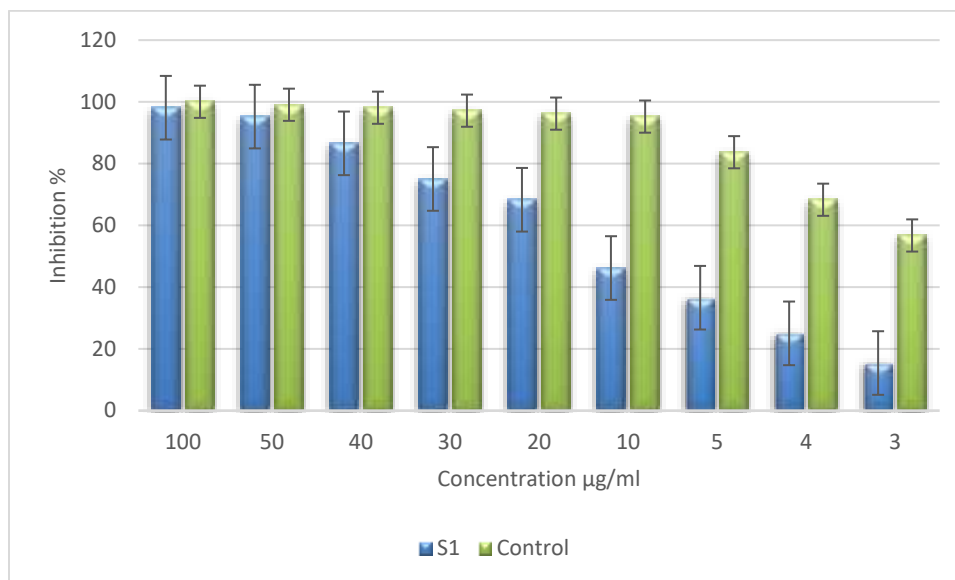


Table 6.17. MIC determination of compound S1 against *Staphylococcus aureus* (ATCC 6538)

conc. of compound S1 (µg/ml)	Absorbance (OD at 600 nm)		% Inhibition
	Initial	Final	
100	0.647	0.547	99.03
50	0.525	0.427	97.07
40	0.462	0.365	96.09
30	0.362	0.266	95.11
20	0.238	0.145	92.17
10	0.137	0.062	74.52
5	0.096	0.035	60.8
4	0.078	0.032	46.09
3	0.07	0.039	31.39
Negative Growth control	0.053	0.155	

The data represents the mean of three independent experiments; $p < 0.05$

Fig. 6.31. Concentration (of compound S1) vs inhibition % chart against *Staphylococcus aureus* (ATCC 6538) vs control

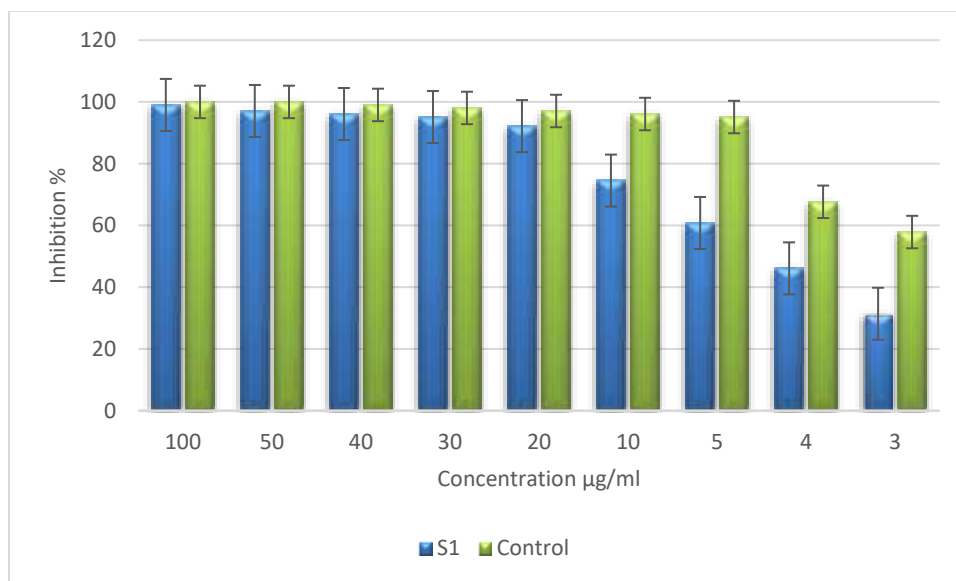


Table 6.18 MIC determination of compound S1 against *Bacillus subtilis* (ATCC 6633)

conc. of compound S1 (µg/ml)	Absorbance (O.D at 600 nm)		% Inhibition
	Initial	Final	
100	0.644	0.54	99.09
50	0.523	0.421	98.14
40	0.474	0.373	97.19
30	0.366	0.266	96.23
20	0.234	0.135	95.28
10	0.125	0.049	73.38
5	0.098	0.032	63.85
4	0.079	0.022	55.28
3	0.073	0.027	44.8
Negative Growth control	0.054	0.159	

The data represent the mean value of three independent experiments; *p<0.01 vs control

Fig 6.32 Concentration (of compound S1) vs inhibition % chart against *Bacillus subtilis* (ATCC 6633) vs control

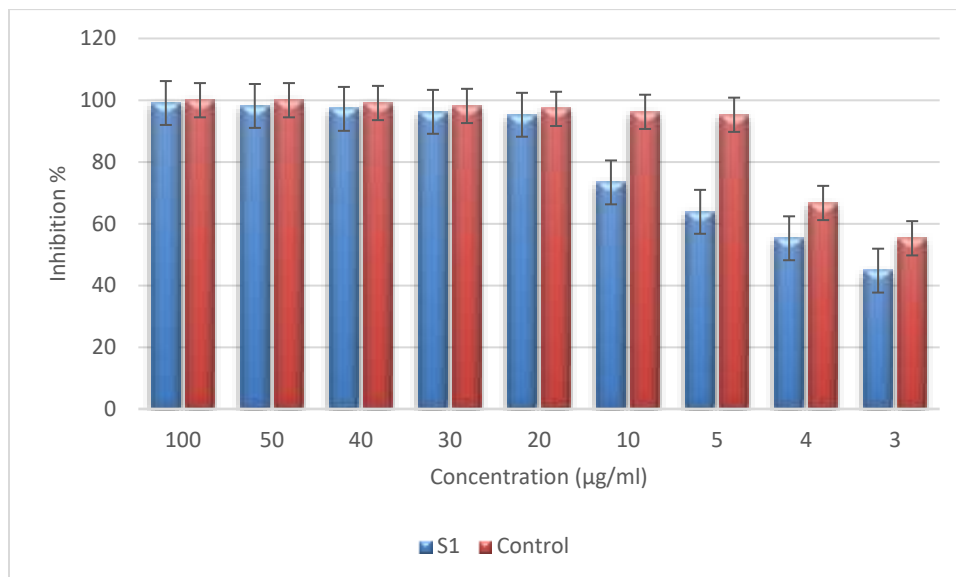


Table 6.19: MIC determination of Compound S2 against *Escherichia coli* (ATCC 8739)

conc.of compound S2 (µg/ml)	Absorbance (O.D at 600 nm)		% Inhibition
	Initial	Final	
100	0.685	0.686	-
50	0.559	0.56	-
40	0.496	0.497	-
30	0.427	0.429	-
20	0.363	0.366	-
10	0.256	0.257	-
5	0.137	0.14	-
4	0.103	0.109	-
3	0.075	0.086	-
Negative Growth Control	0.049	0.152	

Table 6.20: : MIC determination of compound S2 against *Pseudomonas aeruginosa* (ATCC 9027)

conc.of compound S2 (µg/ml)	Absorbance (O.D at 600 nm)		% Inhibition
	Initial	Final	
100	0.683	0.684	-
50	0.557	0.558	-
40	0.494	0.495	-
30	0.425	0.427	-
20	0.361	0.365	-
10	0.258	0.262	-
5	0.139	0.143	-
4	0.104	0.109	-
3	0.079	0.087	-
Negative Growth control	0.051	0.155	

Table 6.21. MIC determination of compound S2 against *Staphylococcus aureus* (ATCC 6538)

conc.of compound S2(µg/ml)	Absorbance (O.D at 600 nm)		
	Initial	Final	% Inhibition
100)	0.682	0.583	98.05
50	0.558	0.462	95.11
40	0.495	0.41	84.33
30	0.424	0.354	69.62
20	0.362	0.305	56.88
10	0.254	0.206	48.05
5	0.135	0.01	35.31
4	0.106	0.078	28.45
3	0.08	0.06	20.6
Negative Growth control	0.053	0.155	-

The data represent the mean value of three independent experiments: $p < 0.05$ vs control

Fig 6.33. Concentration (of compound S2) vs inhibition % chart against *Staphylococcus aureus* (ATCC 6538) vs control

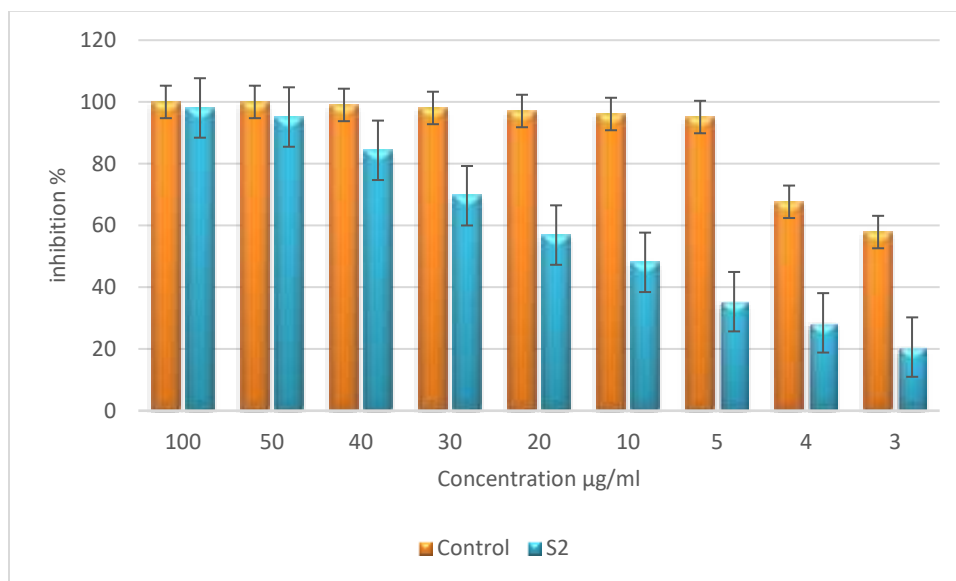


Table 6.22. MIC determination of Compound S2 against *Bacillus subtilis* (ATCC 6633)

conc.of compound S2(µg/ml)	Absorbance (O.D at 600 nm)		% Inhibition
	Initial	Final	
100	0.684	0.581	99.09
50	0.561	0.46	97.19
40	0.498	0.399	95.28
30	0.426	0.353	70.52
20	0.364	0.298	63.85
10	0.257	0.198	57.19
5	0.138	0.091	45.76
4	0.107	0.073	33.38
3	0.085	0.058	26.71
Negative Growth control	0.054	0.159	

The data represent the mean value of three independent experiments: $p < 0.05$ versus control

Fig 6.34. Concentration (compound S2) vs inhibition % chart against *Bacillus subtilis* (ATCC 6633) vs control

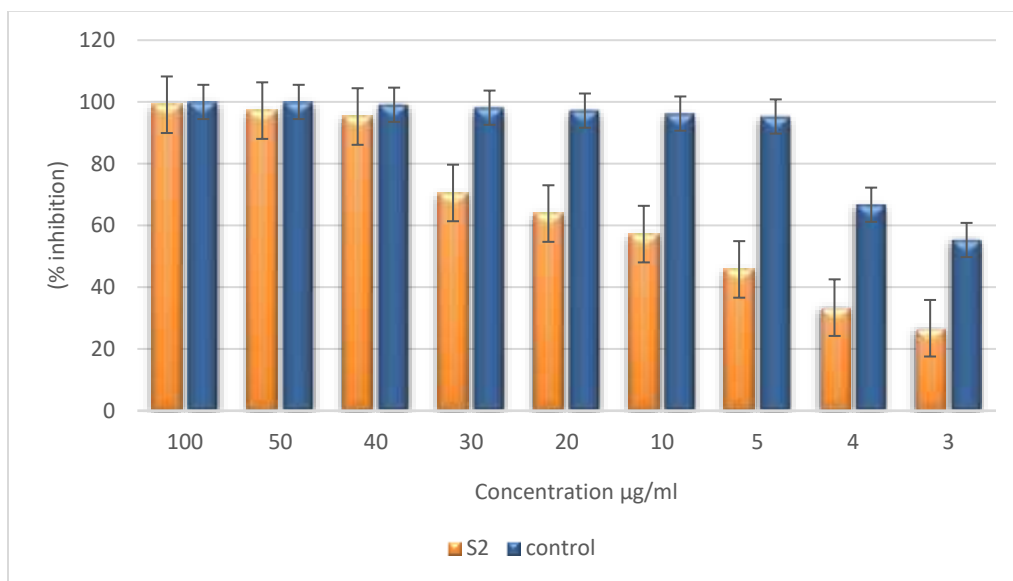


Table 6.23: MIC values against tested bacterial strains

Compound	Minimum Inhibitory Concentration (µg/ml)			
	<i>E. coli</i>	<i>Pseudomonas aeruginosa</i>	<i>Staphylococcus aureus</i>	<i>Bacillus subtilis</i>
S1	40	50	30	20
S2	-	-	50	40
Ciprofloxacin	5	5	5	5

Escherichia coli (ATCC 8739), *Pseudomonas aeruginosa* (ATCC 9027), *Staphylococcus aureus* (ATCC 6538) , *Bacillus subtilis* (ATCC 6633)

6.7: Determination of Minimum Bactericidal Concentration (MBC):

Table 6.24: MBC values obtained against tested bacterial species

Bacterial strain		Compound S1	Compound S2
<i>Escherichia coli</i>	MIC	40	-
	MBC	50	-
<i>Pseudomonas aeruginosa</i>	MIC	50	-
	MBC	100	-
<i>Staphylococcus aureus</i>	MIC	30	50
	MBC	30	50
<i>Bacillus subtilis</i>	MIC	20	40
	MBC	20	40

Escherichia coli (ATCC 8739), *Pseudomonas aeruginosa* (ATCC 9027), *Staphylococcus aureus* (ATCC 6538), *Bacillus subtilis* (ATCC 6633)

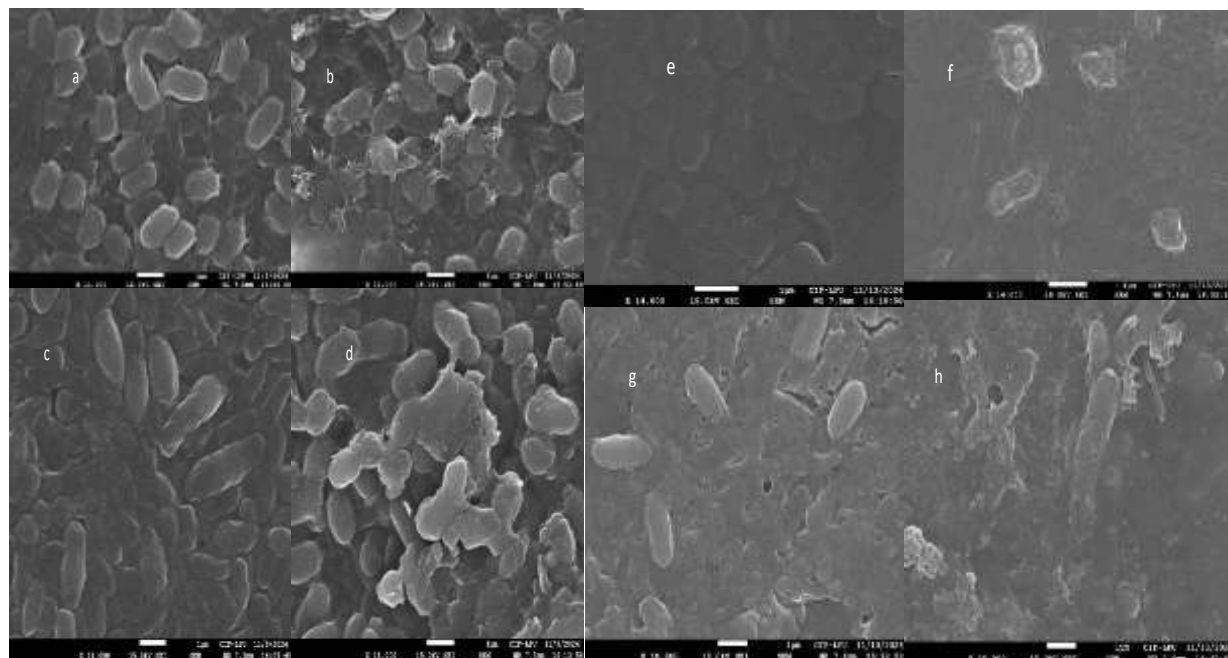
The MBC results are enlisted in Table 6.24 revealed that the compound S1 displayed MBC of 50 µg/ml against *Escherichia coli* (ATCC 8739), 30µg/ml against *Staphylococcus aureus* (ATCC 6538), 100 µg/ml against *Pseudomonas aeruginosa* (ATCC 9027), and 20µg/ml against *Bacillus subtilis* (ATCC 6633). The compound S2 was ineffective against *Escherichia coli* (ATCC 8739) and *Pseudomonas aeruginosa* (ATCC 9027) while displayed MBC of 50µg/ml against *Staphylococcus aureus* (ATCC 6538), and 40µg/ml against *Bacillus subtilis* (ATCC 6633). During the determination of MIC and MBC of uglans regia fraction along with *Terminalia arjuna* and *Acacia nelotica* against various bacterial species, many fractions displayed MBC at a higher concentration than the respective MIC. In the present study, the MBC values were either higher or the same as those of calculated MIC values as was also demonstrated in earlier studies (Croshaw B ,1983; Abubakar et al., 2009).

6.8: Effect of Lead Compounds on Bacterial Cell Morphology

Scanning Electron Microscopy (SEM) is a powerful imaging technique that uses focused beams of electrons to produce high-resolution images of a sample's surface. SEM is widely used in materials science, biology, and nanotechnology for its ability to provide detailed topographic and compositional information (Goldstein et al., 2017). SEM operates by producing a beam of high-energy electrons, typically accelerated by a voltage in the range of 1-30 kV. This electron beam is generated by an electron gun and focused through a series of lenses and apertures. The electron beam is scanned in a raster pattern over the sample surface. When electrons strike the sample, they interact with the atoms in the material, resulting in the emission of various signals (Egerton, 2005).

JEOL Scanning electron microscopy (SEM) was used to examine the damaging effects of lead compounds (highest virtual hits S1 & S2) on the cellular structures of tested microorganisms (Figure 6.35). Bacterial cells cultivated in the absence of lead molecules had a smooth surface, but when cells were grown in the presence of lead compounds at their MIC concentrations, their surface were shattered and disordered. The surface of the *Escherichia coli* (ATCC 8739) cells that had been treated with S1 (40 µg/ml) appeared corrugated, with some depressions and changes in length (Figure 6.35 a & b). *Pseudomonas aeruginosa* (ATCC 9027) cells were likewise demonstrated to be broken and destructed when treated with S1 at its MIC concentration of 50 µg/ml (Figure 6.35 c & d). The treated cells became much more compressed, which prevented them from proliferating and dividing. Damages to cell wall were observed in addition to the atypical cellular architecture. Damage to cellular faces were also observed in treated *Staphylococcus aureus* (ATCC 6538) cells with S1 (30 µg/ml) (Figure 6.35 e & f) and S2 (50 µg/ml) (Figure 6.35 i & j) at their MIC concentrations. In *Bacillus subtilis* (ATCC 6633) cells, at the MIC concentration of lead compound S1 (20 µg/ml) (Figure 6.35 g & h) and S2 (40 µg/ml), the effects resulted in shattering and distortion of cell envelopes (Figure 6.35 k & 6.35 l) and damage to cell structures. Furthermore, all four bacterial cell envelopes developed cell damage as a result of the lead compounds exposure.

The increased roughness, which correlates with the cell debris from cellular breakdown seen under SEM, revealed that the cell was disorganized which was due to damage to the outer covering of the bacterial cell resulting in loss of osmotic pressure and ultimate destruction of the cellular structure. According to some authors, the loss of structural integrity is triggered by damage to the cell wall (Zengin et al., 2014). All these findings pointed to physical, mechanical, and morphological harm to the bacterial cell wall that were also found in the studies on effect on cell wall when tested against different agents (Denney, 2019; Ahmed et al., 2020). The bacterial cell wall damage that results in cell death is shown by these morphological alterations. The images from the scanning electron microscope showed that the nanohybrids significantly altered the bacterial cells' morphology, as shown in similar studies about the deleterious effects of inhibitors. The bacterial cells in the control group had a uniform surface and seemed smooth and undamaged. The bacterial cells treated with the CNH nanohybrids, on the other hand, displayed a surface that was uneven and rough, with cracks and deformations (Agrawal et al., 2024). The impact of the antimicrobial peptide BCp12 on *Staphylococcus aureus* was investigated using SEM and proteomics studies. The findings also showed that *Staphylococcus aureus*'s cell wall integrity was severely compromised by BCp12, which led to the subsequent development of pores (Shi et al., 2023).



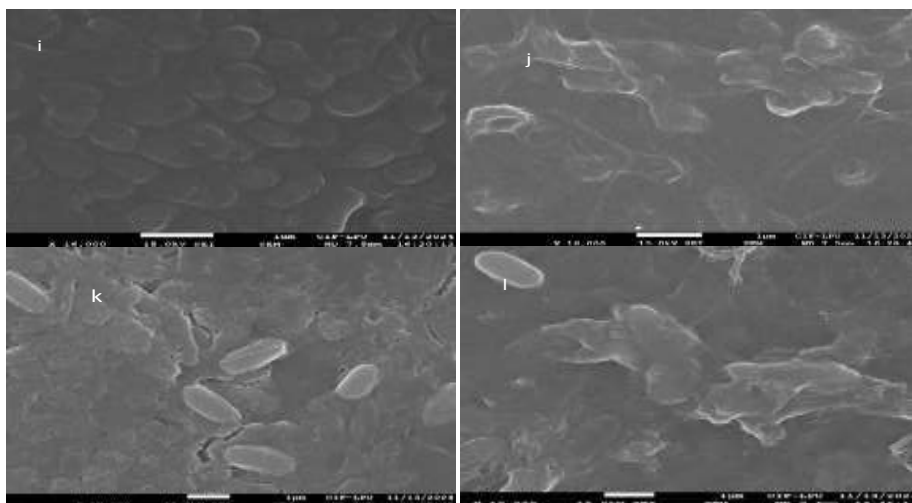


Figure 6.35: Scanning electron micrographs of (a) *Escherichia coli* (ATCC 8739) before treatment (b) *Escherichia coli* (ATCC 8739) after treatment with compound S1 (c) *Pseudomonas aeruginosa* (ATCC 9027) before treatment (d) *Pseudomonas aeruginosa* (ATCC 9027) after treatment with compound S1 (e) *Staphylococcus aureus* (ATCC 6538) before treatment (f) *Staphylococcus aureus* (ATCC 6538) after treatment with compound S1 (g) *Bacillus subtilis* (ATCC 6633) before treatment (h) *Bacillus subtilis* (ATCC 6633) after treatment with compound S1 (i) *Staphylococcus aureus* (ATCC 6538) before treatment (j) *Staphylococcus aureus* (ATCC 6538) after treatment with compound S2 (k) *Bacillus subtilis* (ATCC 6633) before treatment (l) *Bacillus subtilis* (ATCC 6633) after treatment with compound S2

Chapter 7

Conclusion & Future Remarks

7. Conclusion:

The formation of a peptide bond between D-glutamic acid and the cytoplasmic intermediate molecule UDP-MurNAc-L-Ala mostly depends on Mur D. MurD is a great target for accelerating the development of innovative antibacterial medications because it is absent in mammals.

In the current study, high-throughput virtual screening (HTVS) was done by using *in silico* tools to detect prospective inhibitors of *E. coli* Mur D (PDB ID 2UUP) enzyme. In this study, several small compound libraries containing about 0.3 million small ligands were used to target the enzyme molecule. Twenty virtual hits S1–S20 were finalized corresponding to the extra-precision (XP) Glide score. Among top 20 selected virtual hits, most of the compounds showed favorable ADMET (Absorption, Distribution, Metabolism, Excretion, and Toxicity) profiles. Docking-free energy score and binding mechanism studies demonstrated virtual hit S1 (WZB117) to be noteworthy. Compound S1's stability with the MurD complex has been verified using a 100-ns MD simulation studies. The analysis of interactions over the course of the 100 ns trajectory revealed that the protein and residue GLY73 were interacting through hydrogen bonds. The residues GLU164 and TYR187 interacted through a water bridge interaction with the protein molecule. Hydrophobic, H-bond, and water bridge interactions performed a critical function in the inhibitor's stability inside the catalytic pocket. Calculating binding free energy using the MM-GBSA strategy of S1-2UUP complex established that Van der Waals, hydrogen bonding, lipophilic, as well as Coulomb energy were the main factors that favor ligand binding.

Also, the top two tested lead molecules displayed significant antibacterial activity and minimum inhibitory concentration (MIC) and minimum bactericidal concentration (MBC) against various groups of bacterial species except the compound S2 (EPZ015666) that did not exhibit measurable inhibitory activity against the tested Gram-negative organisms in MIC assays. However, these findings should be considered inconclusive, as factors such as outer membrane permeability or efflux mechanisms may have influenced the outcome. Further studies are required to clarify its potential efficacy against Gram-negative bacteria. SEM observations demonstrated that all studied Gram-positive and Gram-negative bacteria had significant

morphological changes and that the structural integrity of the cells had been damaged following treatment with the lead compound molecules. Of all the established targets for drug research, the Mur enzymes involved in the cytoplasmic phases of cell wall production have received the greatest attention. Since most common antibiotics currently in use (e.g., tetracyclines, aminoglycosides, macrolides, quinolones, β -lactams, etc.) target the enzymes taking part in the later stages of cell wall synthesis, incidences of resistance are being reported against these antibiotics. Only fosfomycin, a known drug, is active against the Mur A enzyme, and many susceptible bacterial species are developing resistance against fosfomycin by modification of the target site, overexpression, or recycling pathway. In this context, there is an urgent need to develop newer inhibitors against novel drug targets like the Mur D enzyme. In this context, the virtual hits shortlisted by this study, particularly the highest virtual hit S1, have displayed promising molecular docking and simulation results. Additionally, the introduction of cationic groups as well as amphiphilic groups together with inhibitors targeting MurD may be considered to enhance permeability within bacterial cell. Additionally, siderophores were suggested to affix with inhibitors that use iron absorption mechanism to increase permeability of microbial cells.

Collectively, this detailed study provides a comprehensive understanding of the molecular interactions governing the stability of the inhibitor -2UUP (Mur D) complex, which is essential for rational drug design and optimization efforts.

7.1. Future Aspects:

1. Compounds explored and discovered through the present study might be helpful in clinical trials to develop potential antimicrobial drugs of pharmaceutical importance .
2. Currently newly developed antimicrobial drugs (against enzymes of PG synthesis pathway) lagging behind due to their limited permeable efficacy through the bacterial cell wall or membrane. The compounds discovered in this study might be helpful to enhance the penetration power of existing marketed drugs via selective and synergistic way.
3. The present study might open a new field of research about *in vivo* regulation of Mur D enzyme while they are interacting with the selected inhibitors discovered through this study .
4. The chemical structure of the identified anti-microbial compounds might be helpful to redesign and engineer the existing synthetic drugs for specificity enhancement and alteration of mode of action for Mur D enzyme inhibitor.

Bibliography

Bibliography:

- Abubakar, E. M. M. (2009). Efficacy of crude extracts of garlic (*Allium sativum* Linn.) against nosocomial *Escherichia coli*, *Staphylococcus aureus*, *Streptococcus pneumoniae* and *Pseudomonas aeruginosa*. *Journal of Medicinal Plants Research*, 3(4), 179-185.
- Agrawal, O., Sharma, H. K., Chaurasia, R., Bakshi, G. K., Agarwal, A., Sen, M., ... & Mukherjee, M. (2024). Propene-bridged cyanurate tetramers decorated on carbon nanosheets with antibacterial activity: insights from molecular modeling and in vitro studies. *RSC Applied Interfaces*.
- Ahmed, B., Ameen, F., Rizvi, A., Ali, K., Sonbol, H., Zaidi, A., ... & Musarrat, J. (2020). Destruction of cell topography, morphology, membrane, inhibition of respiration, biofilm formation, and bioactive molecule production by nanoparticles of Ag, ZnO, CuO, TiO₂, and Al₂O₃ toward beneficial soil bacteria. *ACS omega*, 5(14), 7861-7876.
- Akinduti, P. A., Motayo, B., Idowu, O. M., Isibor, P. O., Olasehinde, G. I., Obafemi, Y. D., ... & Adeyemi, G. A. (2019, August). Suitability of spectrophotometric assay for determination of honey microbial inhibition. In *Journal of Physics: Conference Series* (Vol. 1299, No. 1, p. 012131). IOP Publishing.
- Amineni, U., Pradhan, D., & Marisetty, H. (2010). In silico identification of common putative drug targets in *Leptospira interrogans*. *Journal of chemical biology*, 3(4), 165-173.
- Antane, S., Caufield, C. E., Hu, W., Keeney, D., Labthavikul, P., Naughton, S. M., . . . Yang, Y. (2006). Pulvinones as bacterial cell wall biosynthesis inhibitors. *Bioorganic & medicinal chemistry letters*, 16(1), 176-180.
- Andualem, B. (2013). Synergistic antimicrobial effect of Tenegn honey (*Trigona iridipennis*) and garlic against standard and clinical pathogenic bacterial isolates. *International Journal of Microbiological Research*.
- Auger, G., van Heijenoort, J., Blanot, D., & Deprun, C. (1995). Synthesis of N-acetylmuramic acid derivatives as potential inhibitors of the D-glutamic acid-adding enzyme. *Journal für Praktische Chemie/Chemiker-Zeitung*, 337(1), 351-357.
- Azam, M., Jupudi, S., Saha, N., & Paul, R. (2019). Combining molecular docking and molecular dynamics studies for modelling *Staphylococcus aureus* MurD inhibitory activity. *SAR and QSAR in Environmental Research*, 30(1), 1-20.
- Azam, M. A., & Jupudi, S. (2017). Extra precision docking, free energy calculation and molecular dynamics studies on glutamic acid derivatives as MurD inhibitors. *Computational biology and chemistry*, 69, 55-63.
- Azam, M. A., & Jupudi, S. (2019). Structure-based virtual screening to identify inhibitors against *Staphylococcus aureus* MurD enzyme. *Structural Chemistry*, 30(6), 2123-2133.
- Azam, M. A., & Jupudi, S. (2020). MurD inhibitors as antibacterial agents: a review. *Chemical Papers*, 74(6), 1697-1708.
- Azam, M. A., & Jupudi, S. (2020). Synthesis, Molecular Docking and Antibacterial Activity of Some Novel Pyridin-2-yl-Carbamodithioates. *FABAD Journal of Pharmaceutical Sciences*, 45(1), 9-18.
- Bachelier, A., Mayer, R., & Klein, C. D. (2006). Sesquiterpene lactones are potent and irreversible inhibitors of the antibacterial target enzyme MurA. *Bioorganic & medicinal chemistry letters*, 16(21), 5605-5609.

- Barreteau, H., Sosič, I., Turk, S., Humljan, J., Tomašić, T., Zidar, N., . . . Kikelj, D. (2012). MurD enzymes from different bacteria: evaluation of inhibitors. *Biochemical pharmacology*, 84(5), 625-632.
- Baum, E. Z., Montenegro, D. A., Licata, L., Turchi, I., Webb, G. C., Foleno, B. D., & Bush, K. (2001). Identification and characterization of new inhibitors of the Escherichia coli MurA enzyme. *Antimicrobial agents and chemotherapy*, 45(11), 3182-3188.
- Bauer, A. W. M. M., Kirby, W. M. M., & Sherris, J. C. T. (1966). turck, Turck M. Antibiotic susceptibility testing by a standardized single disk method. *American journal of clinical pathology*, 45(4), 493.
- Belete, T. M. (2019). Novel targets to develop new antibacterial agents and novel alternatives to antibacterial agents. *Human Microbiome Journal*, 11, 100052.
- Bensen, D., Rodriguez, S., Nix, J., Cunningham, M., & Tari, L. (2012). Structure of MurA (UDP-N-acetylglucosamine enolpyruvyl transferase) from Vibrio fischeri in complex with substrate UDP-N-acetylglucosamine and the drug fosfomycin. *Acta Crystallographica Section F: Structural Biology and Crystallization Communications*, 68(4), 382-385.
- Benson, T. E., Marquardt, J. L., Marquardt, A. C., Etzkorn, F. A., & Walsh, C. T. (1993). Overexpression, purification, and mechanistic study of UDP-N-acetylenolpyruvylglucosamine reductase. *Biochemistry*, 32(8), 2024-2030.
- Bertrand, J. A., Auger, G., Fanchon, E., Martin, L., Blanot, D., Van Heijenoort, J., & Dideberg, O. (1997). Crystal structure of UDP-N-acetylmuramoyl-L-alanine: D-glutamate ligase from Escherichia coli. *The EMBO journal*, 16(12), 3416-3425.
- Bertrand, J. A., Auger, G., Martin, L., Fanchon, E., Blanot, D., Le Beller, D., . . . Dideberg, O. (1999). Determination of the MurD mechanism through crystallographic analysis of enzyme complexes. *Journal of molecular biology*, 289(3), 579-590.
- Bertrand, J. A., Fanchon, E., Martin, L., Chantalat, L., Auger, G., Blanot, D., . . . Dideberg, O. (2000). "Open" structures of MurD: domain movements and structural similarities with folylpolyglutamate synthetase. *Journal of molecular biology*, 301(5), 1257-1266.
- Bratkovič, T., Lunder, M., Urleb, U., & Štrukelj, B. (2008). Peptide inhibitors of MurD and MurE, essential enzymes of bacterial cell wall biosynthesis. *Journal of basic microbiology*, 48(3), 202-206.
- Breindl, A., Beck, B., Clark, T., & Glen, R. C. (1997). Prediction of the n-octanol/water partition coefficient, logP, using a combination of semiempirical MO-calculations and a neural network. *Molecular modeling annual*, 3, 142-155.
- Chakkyarath, V., & Natarajan, J. (2019). Identification of Ideal multi-targeting bioactive compounds against mur ligases of Enterobacter aerogenes and its binding mechanism in comparison with chemical inhibitors. *Interdisciplinary Sciences: Computational Life Sciences*, 11(1), 135-144.
- Chandrasekaran, B., Abed, S. N., Al-Attraqchi, O., Kuche, K., & Tekade, R. K. (2018). Computer-aided prediction of pharmacokinetic (ADMET) properties *Dosage form design parameters* (pp. 731-755): Elsevier.
- Chen, M. W., Lohkamp, B., Schnell, R., Lescar, J., & Schneider, G. (2013). Substrate channel flexibility in Pseudomonas aeruginosa MurB accommodates two distinct substrates. *PloS one*, 8(6), e66936.

- Chopra, I. (2013). The 2012 Garrod lecture: discovery of antibacterial drugs in the 21st century. *Journal of Antimicrobial Chemotherapy*, 68(3), 496-505.
- CLSI . M100 Performance Standards for Antimicrobial Susceptibility Testing. 30th ed. *Clinical and Laboratory Standards Institute*; Wayne, PA, USA: 2020.
- Croshaw B ,1983). Evaluation of non-antibiotic antimicrobial agents. In : *Pharmaceutical Microbiology*,3 rd edn.,(Hugo WB and Russell AD eds. Blackwell, Oxford, pp. 237-257).
- Cutinho, P. F., Shankar, R. C., Anand, A., Roy, J., Mehta, C. H., Nayak, U. Y., & Murahari, M. (2020). Hit identification and drug repositioning of potential non-nucleoside reverse transcriptase inhibitors by structure-based approach using computational tools (part II). *Journal of Biomolecular Structure and Dynamics*, 38(13), 3772-3789.
- Daniel, R. A., & Errington, J. (1993). DNA sequence of themurE-murD region of *Bacillus subtilis* 168. *Microbiology*, 139(2), 361-370.
- Davis, A. M., & Riley, R. J. (2004). Predictive ADMET studies, the challenges and the opportunities. *Current opinion in chemical biology*, 8(4), 378-386.
- Denney, B. M. (2019). Production of Rhamnolipidic biosurfactant by *Pseudomonas libanensis* strain IHB 17501 and its antibacterial and cytolytic effect on *Streptococcus pneumoniae* ATCC 49619. *Int. Res. J. Pharm*, 10(1), 32-36.
- De Smet, K. A., Kempseell, K. E., Gallagher, A., Duncan, K., & Young, D. B. (1999). Alteration of a single amino acid residue reverses fosfomycin resistance of recombinant MurA from *Mycobacterium tuberculosis*The EMBL accession number for the sequence in this paper is X96711. *Microbiology*, 145(11), 3177-3184.
- Egerton, R. F. (2005). *Physical principles of electron microscopy* (Vol. 56). New York: Springer.
- El-Sherbeini, M., Geissler, W. M., Pittman, J., Yuan, X., Wong, K. K., & Pompliano, D. L. (1998). Cloning and expression of *Staphylococcus aureus* and *Streptococcus pyogenes* murD genes encoding uridine diphosphate N-acetylmuramoyl-L-alanine: D-glutamate ligases. *Gene*, 210(1), 117-125.
- El Zoeiby, A., Sanschagrin, F., & Levesque, R. C. (2003). Structure and function of the Mur enzymes: development of novel inhibitors. *Molecular microbiology*, 47(1), 1-12.
- Eloff, J. N. (1998). A sensitive and quick microplate method to determine the minimal inhibitory concentration of plant extracts for bacteria. *Planta medica*, 64(08), 711-713.
- Elokely, K. M., & Doerksen, R. J. (2013). Docking challenge: protein sampling and molecular docking performance. *Journal of chemical information and modeling*, 53(8), 1934-1945.
- Eschenburg, S., Priestman, M., & Schönbrunn, E. (2005). Evidence that the fosfomycin target Cys115 in UDP-N-acetylglucosamine enolpyruvyl transferase (MurA) is essential for product release. *Journal of Biological Chemistry*, 280(5), 3757-3763.
- Fan, Y., Unwalla, R., Denny, R. A., Di, L., Kerns, E. H., Diller, D. J., & Humblet, C. (2010). Insights for predicting blood-brain barrier penetration of CNS targeted molecules using QSPR approaches. *Journal of chemical information and modeling*, 50(6), 1123-1133.
- Favini-Stabile, S., Contreras-Martel, C., Thielens, N., & Dessen, A. (2013). M re B and M ur G as scaffolds for the cytoplasmic steps of peptidoglycan biosynthesis. *Environmental microbiology*, 15(12), 3218-3228.
- Ferreira, L. L., & Andricopulo, A. D. (2019). ADMET modeling approaches in drug discovery. *Drug discovery today*, 24(5), 1157-1165.

- Friesner, R. A., Banks, J. L., Murphy, R. B., Halgren, T. A., Klicic, J. J., Mainz, D. T., Repasky, M. P., Knoll, E. H., Shelley, M. and Perry, J. K. (2004). Glide: a new approach for rapid, accurate docking and scoring 1 method and assessment of docking accuracy. *Journal of Medicinal Chemistry* 47(7): 1739-1749.
- Friesner, R. A., Murphy, R. B., Repasky, M. P., Frye, L. L., Greenwood, J. R., Halgren, T. A., . . . Mainz, D. T. (2006). Extra precision glide: Docking and scoring incorporating a model of hydrophobic enclosure for protein– ligand complexes. *Journal of medicinal chemistry*, 49(21), 6177-6196.
- García-Ortegón, M., Simm, G. N., Tripp, A. J., Hernández-Lobato, J. M., Bender, A., & Bacallado, S. (2022). DOCKSTRING: easy molecular docking yields better benchmarks for ligand design. *Journal of chemical information and modeling*, 62(15), 3486-3502.
- Gaur, V., & Bera, S. (2022). Recent developments on UDP-N-acetylmuramoyl-L-alanine-D-gutamate ligase (Mur D) enzyme for antimicrobial drug development: An emphasis on in-silico approaches. *Current Research in Pharmacology and Drug Discovery*, 3, 100137.
- Gaur, V., Kumar, N., Vyas, A., Chowdhury, D., Singh, J., & Bera, S. (2023). Identification of potential inhibitors against Escherichia coli Mur D enzyme to combat rising drug resistance: an in-silico approach. *Journal of Biomolecular Structure and Dynamics*, 1-11.
- Gegnag, L. D., Waddell, S. T., Chabin, R. M., Reddy, S., & Wong, K. K. (1998). Inhibitors of the bacterial cell wall biosynthesis enzyme Mur D. *Bioorganic & medicinal chemistry letters*, 8(13), 1643-1648.
- Gilson, M. K., & Zhou, H. X. (2007). Calculation of protein-ligand binding affinities. *Annual Review of Biophysics*, 36(1), 21-42.
- Gobec, S., Urleb, U., Auger, G., & Blanot, D. (2001). Synthesis and biochemical evaluation of some novel N-acyl phosphono- and phosphinoalanine derivatives as potential inhibitors of the D-glutamic acid-adding enzyme. *Die Pharmazie*, 56(4), 295-297.
- Goldstein, J. I., Newbury, D. E., Michael, J. R., Ritchie, N. W., Scott, J. H. J., & Joy, D. C. (2017). *Scanning electron microscopy and X-ray microanalysis*. springer.
- Halgren, T. A., Murphy, R. B., Friesner, R. A., Beard, H. S., Frye, L. L., Pollard, W. T. and Banks, J. L. (2004). Glide: a new approach for rapid, accurate docking and scoring 2. enrichment factors in database screening. *Journal of Medicinal Chemistry* 47(7): 1750-1759.
- Hara, H., Yasuda, S., Horiuchi, K., & Park, J. T. (1997). A promoter for the first nine genes of the Escherichia coli mra cluster of cell division and cell envelope biosynthesis genes, including ftsI and ftsW. *Journal of bacteriology*, 179(18), 5802-5811.
- Hendlin, D., Stapley, E., Jackson, M., Wallick, H., Miller, A., Wolf, F., . . . Foltz, E. (1969). Phosphonomycin, a new antibiotic produced by strains of Streptomyces. *Science*, 166(3901), 122-123.
- Horton, J. R., Bostock, J. M., Chopra, I., Hesse, L., Phillips, S. E., Adams, D. J., . . . Fishwick, C. W. (2003). Macrocyclic inhibitors of the bacterial cell wall biosynthesis enzyme Mur D. *Bioorganic & medicinal chemistry letters*, 13(9), 1557-1560.
- Hrast, M., Knez, D., Zdovc, I., Barreateau, H., & Gobec, S. (2021). Mur ligases inhibitors with azastilbene scaffold: Expanding the structure–activity relationship. *Bioorganic & medicinal chemistry letters*, 40, 127966.

- Hrast, M., Rožman, K., Ogris, I., Škedelj, V., Patin, D., Sova, M., . . . Zega, A. (2019). Evaluation of the published kinase inhibitor set to identify multiple inhibitors of bacterial ATP-dependent mur ligases. *Journal of enzyme inhibition and medicinal chemistry*, 34(1), 1010-1017.
- Humljan, J., Kotnik, M., Boniface, A., Šolmajer, T., Urleb, U., Blanot, D., & Gobec, S. (2006). A new approach towards peptidosulfonamides: synthesis of potential inhibitors of bacterial peptidoglycan biosynthesis enzymes MurD and MurE. *Tetrahedron*, 62(47), 10980-10988.
- Humljan, J., Kotnik, M., Contreras-Martel, C., Blanot, D., Urleb, U., Dessen, A., . . . Gobec, S. (2008). Novel naphthalene-N-sulfonyl-D-glutamic acid derivatives as inhibitors of MurD, a key peptidoglycan biosynthesis enzyme. *Journal of medicinal chemistry*, 51(23), 7486-7494.
- Husain, A., Bhutani, M., Parveen, S., Khan, S. A., Ahmad, A., & Iqbal, M. A. (2021). Synthesis, in vitro cytotoxicity, ADME, and molecular docking studies of benzimidazole-bearing furanone derivatives. *Journal of the Chinese Chemical Society*, 68(2), 362-373.
- Ikeda, M., Wachi, M., Ishino, F., & Matsushashi, M. (1990). Nucleotide sequence involving murD and an open reading frame ORF-Y spacing murF and ftsW in Escherichia coli. *Nucleic acids research*, 18(4), 1058.
- Ikeda, M., Wachi, M., Jung, H. K., Ishino, F., & Matsushashi, M. (1990). Homology among MurC, MurD, MurE and MurF proteins in Escherichia coli and that between E. coli MurG and a possible MurG protein in Bacillus subtilis. *The Journal of General and Applied Microbiology*, 36(3), 179-187.
- Isa, M. A. (2019). Homology modeling and molecular dynamic simulation of UDP-N-acetylmuramoyl-l-alanine-d-glutamate ligase (MurD) from Mycobacterium tuberculosis H37Rv using in silico approach. *Computational biology and chemistry*, 78, 116-126.
- Jha, R. K., Khan, R. J., Amera, G. M., Singh, E., Pathak, A., Jain, M., . . . Singh, A. K. (2020). Identification of promising molecules against MurD ligase from Acinetobacter baumannii: insights from comparative protein modelling, virtual screening, molecular dynamics simulations and MM/PBSA analysis. *Journal of Molecular Modeling*, 26(11), 1-17.
- Jorgensen, W. L., & Duffy, E. M. (2002). Prediction of drug solubility from structure. *Advanced drug delivery reviews*, 54(3), 355-366.
- Jorgensen, W. L., Maxwell, D. S., & Tirado-Rives, J. (1996). Development and testing of the OPLS all-atom force field on conformational energetics and properties of organic liquids. *Journal of the American Chemical Society*, 118(45), 11225-11236.
- Jukič, M., Gobec, S., & Sova, M. (2019). Reaching toward underexplored targets in antibacterial drug design. *Drug development research*, 80(1), 6-10.
- Jupudi, S., Azam, M. A., & Wadhvani, A. (2021). Design, synthesis and molecular modelling of phenoxyacetohydrazide derivatives as Staphylococcus aureus MurD inhibitors. *Chemical Papers*, 75(3), 1221-1235.
- Kahler, C. M., Sarkar-Tyson, M., Kibble, E. A., Stubbs, K. A., & Vrielink, A. (2018). Enzyme targets for drug design of new anti-virulence therapeutics. *Current opinion in structural biology*, 53, 140-150.

- Kapetanovic, I. (2008). Computer-aided drug discovery and development (CADD): in silico-chemico-biological approach. *Chemico-biological interactions*, 171(2), 165-176.
- Kotnik, M., Humljan, J., Contreras-Martel, C., Oblak, M., Kristan, K., Hervé, M., . . . Dessen, A. (2007). Structural and functional characterization of enantiomeric glutamic acid derivatives as potential transition state analogue inhibitors of MurD ligase. *Journal of molecular biology*, 370(1), 107-115.
- Kouidmi, I., Levesque, R. C., & Paradis-Bleau, C. (2014). The biology of Mur ligases as an antibacterial target. *Molecular microbiology*, 94(2), 242-253.
- Kumari, M., & Subbarao, N. (2021). Identification of novel multitarget antitubercular inhibitors against mycobacterial peptidoglycan biosynthetic Mur enzymes by structure-based virtual screening. *Journal of Biomolecular Structure and Dynamics*, 1-12.
- Meng, X. Y., Zhang, H. X., Mezei, M., & Cui, M. (2011). Molecular docking: a powerful approach for structure-based drug discovery. *Current computer-aided drug design*, 7(2), 146-157.
- Mengin-Lecreulx, D., Parquet, C., Desviat, L. R., Plá, J., Flouret, B., Ayala, J. A., & van Heijenoort, J. (1989). Organization of the murE-murG region of Escherichia coli: identification of the murD gene encoding the D-glutamic-acid-adding enzyme. *Journal of bacteriology*, 171(11), 6126-6134.
- Miyachiro, M. M., Granato, D., Trindade, D. M., Ebel, C., Paes Leme, A. F., & Dessen, A. (2019). Complex formation between Mur enzymes from Streptococcus pneumoniae. *Biochemistry*, 58(30), 3314-3324.
- Mobley, D. L., & Dill, K. A. (2009). Binding of small-molecule ligands to proteins: “what you see” is not always “what you get”. *Structure*, 17(4), 489-498.
- N Sangshetti, J., S Joshi, S., H Patil, R., G Moloney, M., & B Shinde, D. (2017). Mur ligase inhibitors as anti-bacterials: a comprehensive review. *Current pharmaceutical design*, 23(21), 3164-3196.
- Naclerio, G. A., & Sintim, H. O. (2020). Multiple ways to kill bacteria via inhibiting novel cell wall or membrane targets. *Future Medicinal Chemistry*, 12(13), 1253-1279.
- Nakagawa, H., Saio, T., Nagao, M., Inoue, R., Sugiyama, M., Ajito, S., . . . Kawakita, Y. (2021). Conformational dynamics of a multidomain protein by neutron scattering and computational analysis. *Biophysical Journal*, 120(16), 3341-3354.
- Nikolaidis, I., Favini-Stabile, S., & Dessen, A. (2014). Resistance to antibiotics targeted to the bacterial cell wall. *Protein science*, 23(3), 243-259.
- Patel, R. D., Prasanth Kumar, S., Pandya, H. A., & Solanki, H. A. (2018). MDCKpred: a web-tool to calculate MDCK permeability coefficient of small molecule using membrane-interaction chemical features. *Toxicology Mechanisms and Methods*, 28(9), 685-698.
- Patin, D., Boniface, A., Kovač, A., Hervé, M., Dementin, S., Barreateau, H., . . . Blanot, D. (2010). Purification and biochemical characterization of Mur ligases from Staphylococcus aureus. *Biochimie*, 92(12), 1793-1800.
- Perdih, A., Kovač, A., Wolber, G., Blanot, D., Gobec, S., & Solmajer, T. (2009). Discovery of novel benzene 1, 3-dicarboxylic acid inhibitors of bacterial MurD and MurE ligases by structure-based virtual screening approach. *Bioorganic & medicinal chemistry letters*, 19(10), 2668-2673.

- Perdih, A., Hrast, M., Barreteau, H. I. n., Gobec, S., Wolber, G., & Solmajer, T. (2014). Inhibitor design strategy based on an enzyme structural flexibility: a case of bacterial MurD ligase. *Journal of chemical information and modeling*, 54(5), 1451-1466.
- Perdih, A., Wolber, G., & Solmajer, T. (2013). Molecular dynamics simulation and linear interaction energy study of d-Glu-based inhibitors of the MurD ligase. *Journal of computer-aided molecular design*, 27, 723-738.
- Rashdan, H. R., Shehadi, I. A., Abdelrahman, M. T., & Hemdan, B. A. (2021). Antibacterial activities and molecular docking of novel sulfone biscompound containing bioactive 1, 2, 3-triazole moiety. *Molecules*, 26(16), 4817.
- Repasky, M. P., Murphy, R. B., Banks, J. L., Greenwood, J. R., Tubert-Brohman, I., Bhat, S., & Friesner, R. A. (2012). Docking performance of the glide program as evaluated on the Astex and DUD datasets: a complete set of glide SP results and selected results for a new scoring function integrating WaterMap and glide. *Journal of computer-aided molecular design*, 26, 787-799.
- Saio, T., Ogura, K., Kumeta, H., Kobashigawa, Y., Shimizu, K., Yokochi, M., . . . Inagaki, F. (2015). Ligand-driven conformational changes of MurD visualized by paramagnetic NMR. *Scientific reports*, 5(1), 1-11.
- Samal, H. B., Das, J. K., Mahapatra, R. K., & Suar, M. (2015). Molecular modeling, simulation and virtual screening of MurD ligase protein from *Salmonella typhimurium* LT2. *Journal of Pharmacological and Toxicological Methods*, 73, 34-41.
- Schleifer, K. H., & Kandler, O. (1972). Peptidoglycan types of bacterial cell walls and their taxonomic implications. *Bacteriological reviews*, 36(4), 407-477.
- Selvi, J. A., Arthanareeswari, M., Pushpamalini, T., Rajendran, S., & Vignesh, T. (2020). Effectiveness of *Vinca rosea* leaf extract as corrosion inhibitor for mild steel in 1 N HCl medium investigated by adsorption and electrochemical studies. *Int. J. Corros. Scale Inhib*, 9(4), 1429-1443.
- Sheng, J., Huang, L., Zhu, X., Cai, J., & Xu, Z. (2014). Reconstitution of the peptidoglycan cytoplasmic precursor biosynthetic pathway in cell-free system and rapid screening of antisense oligonucleotides for Mur enzymes. *Applied microbiology and biotechnology*, 98, 1785-1794.
- Shi, Y., Li, Y., Yang, K., Wei, G., & Huang, A. (2023). A novel milk-derived peptide effectively inhibits *Staphylococcus aureus*: Interferes with cell wall synthesis, peptidoglycan biosynthesis disruption reaction mechanism, and its application in real milk system. *Food Control*, 144, 109374.
- Shivakumar, D., Williams, J., Wu, Y., Damm, W., Shelley, J., & Sherman, W. (2010). Prediction of absolute solvation free energies using molecular dynamics free energy perturbation and the OPLS force field. *Journal of chemical theory and computation*, 6(5), 1509-1519.
- Silver, L. L. (2017). Fosfomycin: mechanism and resistance. *Cold Spring Harbor perspectives in medicine*, 7(2), a025262.
- Simčič, M., Pureber, K., Kristan, K., Urleb, U., Kocjan, D., & Grdadolnik, S. G. (2014). A novel 2-oxoindolinyldene inhibitor of bacterial MurD ligase: enzyme kinetics, protein-inhibitor binding by NMR and a molecular dynamics study. *European journal of medicinal chemistry*, 83, 92-101.

- Simčič, M., Sosič, I., Hodošek, M., Barreateau, H., Blanot, D., Gobec, S., & Grdadolnik, S. G. (2012). The binding mode of second-generation sulfonamide inhibitors of MurD: clues for rational design of potent MurD inhibitors. *PloS one*, 7(12), e52817.
- Šink, R., Barreateau, H., Patin, D., Mengin-Lecreulx, D., Gobec, S., & Blanot, D. (2013). MurD enzymes: some recent developments. *Biomolecular concepts*, 4(6), 539-556.
- Šink, R., Kotnik, M., Zega, A., Barreateau, H., Gobec, S., Blanot, D., . . . Contreras-Martel, C. (2016). Crystallographic study of peptidoglycan biosynthesis enzyme MurD: domain movement revisited. *PloS one*, 11(3), e0152075.
- Šink, R., Kovač, A., Tomašić, T., Rupnik, V., Boniface, A., Bostock, J., . . . Gobec, S. (2008). Synthesis and biological evaluation of N-acylhydrazones as inhibitors of MurC and MurD ligases. *ChemMedChem: Chemistry Enabling Drug Discovery*, 3(9), 1362-1370.
- Skarzynski, T., Mistry, A., Wonacott, A., Hutchinson, S. E., Kelly, V. A., & Duncan, K. (1996). Structure of UDP-N-acetylglucosamine enolpyruvyl transferase, an enzyme essential for the synthesis of bacterial peptidoglycan, complexed with substrate UDP-N-acetylglucosamine and the drug fosfomycin. *Structure*, 4(12), 1465-1474.
- Smith, C. A. (2006). Structure, function and dynamics in the mur family of bacterial cell wall ligases. *Journal of molecular biology*, 362(4), 640-655.
- Sosič, I., Barreateau, H., Simčič, M., Šink, R., Cesar, J., Zega, A., . . . Amoroso, A. (2011). Second-generation sulfonamide inhibitors of D-glutamic acid-adding enzyme: activity optimisation with conformationally rigid analogues of D-glutamic acid. *European journal of medicinal chemistry*, 46(7), 2880-2894.
- Sova, M., Kovač, A., Turk, S., Hrast, M., Blanot, D., & Gobec, S. (2009). Phosphorylated hydroxyethylamines as novel inhibitors of the bacterial cell wall biosynthesis enzymes MurC to MurF. *Bioorganic Chemistry*, 37(6), 217-222.
- Steinbach, A., Scheidig, A. J., & Klein, C. D. (2008). The unusual binding mode of cnicin to the antibacterial target enzyme MurA revealed by X-ray crystallography. *Journal of medicinal chemistry*, 51(16), 5143-5147.
- Štrancar, K., Blanot, D., & Gobec, S. (2006). Design, synthesis and structure–activity relationships of new phosphinate inhibitors of MurD. *Bioorganic & medicinal chemistry letters*, 16(2), 343-348.
- Thakur, M., & Chakraborti, P. K. (2008). Ability of PknA, a mycobacterial eukaryotic-type serine/threonine kinase, to transphosphorylate MurD, a ligase involved in the process of peptidoglycan biosynthesis. *Biochemical Journal*, 415(1), 27-33.
- Tiwari, P., Sharma, P., Kumar, M., Kapil, A., Abdul Samath, E., & Kaur, P. (2022). Identification of novel natural MurD ligase inhibitors as potential antimicrobial agents targeting *Acinetobacter baumannii*: In silico screening and biological evaluation. *Journal of Biomolecular Structure and Dynamics*, 40(24), 14051-14066.
- Tomašić, T., Šink, R., Zidar, N., Fic, A., Contreras-Martel, C., Dessen, A., . . . Gobec, S. (2012). Dual inhibitor of MurD and MurE ligases from *Escherichia coli* and *Staphylococcus aureus*. *ACS medicinal chemistry letters*, 3(8), 626-630.
- Tomašić, T., Zidar, N., Kovač, A., Turk, S., Simčič, M., Blanot, D., . . . Zega, A. (2010). 5-Benzylidenethiazolidin-4-ones as multitarget inhibitors of bacterial Mur ligases. *ChemMedChem: Chemistry Enabling Drug Discovery*, 5(2), 286-295.

- Tomašić, T., Zidar, N., Sink, R., Kovač, A., Blanot, D., Contreras-Martel, C., . . . Gobec, S. (2011). Structure-based design of a new series of D-glutamic acid based inhibitors of bacterial UDP-N-acetylmuramoyl-L-alanine: D-glutamate ligase (MurD). *Journal of medicinal chemistry*, 54(13), 4600-4610.
- Tripathi, N. M., & Bandyopadhyay, A. (2022). High throughput virtual screening (HTVS) of peptide library: Technological advancement in ligand discovery. *European Journal of Medicinal Chemistry*, 243, 114766.
- Turk, S., Kovač, A., Boniface, A., Bostock, J. M., Chopra, I., Blanot, D., & Gobec, S. (2009). Discovery of new inhibitors of the bacterial peptidoglycan biosynthesis enzymes MurD and MurF by structure-based virtual screening. *Bioorganic & medicinal chemistry*, 17(5), 1884-1889.
- Umetsu, S., Tsunoda, T., Kiyanagi, H., Inahashi, Y., Nonaka, K., Dairi, T., & Ogasawara, Y. (2024). Identification of a new oligomycin derivative as a specific inhibitor of the alternative peptidoglycan biosynthetic pathway. *The Journal of Antibiotics*, 77(3), 182-184.
- Valdes, O., Ali, A., Carrasco-Sánchez, V., Cabrera-Barjas, G., Duran-Lara, E., Ibrahim, M., ... & Abril, D. (2023). Ugi efficient synthesis of novel N-alkylated lipopeptides, antimicrobial properties and computational studies in *Staphylococcus aureus* via MurD antibacterial target. *Computational Biology and Chemistry*, 106, 107932.
- Van Der Spoel, D., Lindahl, E., Hess, B., Groenhof, G., Mark, A. E., & Berendsen, H. J. (2005). GROMACS: fast, flexible, and free. *Journal of computational chemistry*, 26(16), 1701-1718.
- Victor, F., Tebbe, M., Birch, G., Smith, M., Letourneau, D., & Wu, C. (1999). *D-Glutamic acid analogs as Streptococcus pneumoniae UDP-N-acetyl muramoyl-alanine: D-glutamate ligase (MurD) inhibitors [abstract 1276]*. Paper presented at the Program and Abstracts of the 39th Interscience Conference on Antimicrobial Agents and Chemotherapy, San Francisco. Washington, DC: American Society for Microbiology.
- Vollmer, W., Blanot, D., & De Pedro, M. A. (2008). Peptidoglycan structure and architecture. *FEMS microbiology reviews*, 32(2), 149-167.
- Walsh, A. W., Falk, P. J., Thanassi, J., Discotto, L., Pucci, M. J., & Ho, H.-T. (1999). Comparison of the D-glutamate-adding enzymes from selected gram-positive and gram-negative bacteria. *Journal of bacteriology*, 181(17), 5395-5401.
- Wang, H., Jin, K., Wang, C., Guo, X., Chen, Z., & Tao, J. (2019). Effect of fiber surface functionalization on shear behavior at carbon fiber/epoxy interface through molecular dynamics analysis. *Composites Part A: Applied Science and Manufacturing*, 126, 105611.
- Watanabe, H., Mori, H., Itoh, T., & Gojobori, T. (1997). Genome plasticity as a paradigm of eubacteria evolution. *Journal of molecular evolution*, 44(1), S57-S64.
- Wiegand, I., Hilpert, K., & Hancock, R. E. (2008). Agar and broth dilution methods to determine the minimal inhibitory concentration (MIC) of antimicrobial substances. *Nature protocols*, 3(2), 163-175.
- Zdouc, M., Schink, J., Lešnik, S., Rožman, K., Konc, J., Janežič, D., & Gobec, S. (2018). Docking study with biological validation on bacterial enzyme MurD. *Chemical Data Collections*, 13, 139-155.

- Zengin, H., & Baysal, A. H. (2014). Antibacterial and antioxidant activity of essential oil terpenes against pathogenic and spoilage-forming bacteria and cell structure-activity relationships evaluated by SEM microscopy. *Molecules*, 19(11), 17773-17798.
- Zheng, X., Zheng, T., Liao, Y., & Luo, L. (2021). Identification of Potential Inhibitors of MurD Enzyme of *Staphylococcus aureus* from a Marine Natural Product Library. *Molecules*, 26(21), 6426.
- Zidar, N., Tomašić, T., Šink, R., Kovač, A., Patin, D., Blanot, D., . . . Zega, A. (2011). New 5-benzylidenethiazolidin-4-one inhibitors of bacterial MurD ligase: design, synthesis, crystal structures, and biological evaluation. *European journal of medicinal chemistry*, 46(11), 5512-5523.

Web References:

<https://www.rcsb.org>
<https://www.asinex.com>
<https://lifechemicals.com>
<https://www.chemdiv.com>
<https://enamine.net>
<https://www.selleckchem.com>
<https://www.ibscreen.com>
<https://pubchem.ncbi.nlm.nih.gov>
https://gohom.win/ManualHom/Schrodinger/Schrodinger_20152_docs/qikprop/qikprop_user_manual
 Schrödinger, LLC. (2021). Glide User Manual. Schrödinger Release

Publications



Contents lists available at ScienceDirect

Current Research in Pharmacology and Drug Discovery

journal homepage: www.journals.elsevier.com/current-research-in-pharmacology-and-drug-discovery



Recent developments on UDP-N-acetylmuramoyl-L-alanine-D-glutamate ligase (Mur D) enzyme for antimicrobial drug development: An emphasis on in-silico approaches



Vinita Gaur, Surojit Bera*

Department of Microbiology, School of Bioengineering and Biosciences, Lovely Professional University, Punjab, 144411, India

ARTICLE INFO

Keywords:

Antibiotic resistance

Peptidoglycan

MurD

In-silico

ABSTRACT

Introduction: The rapid emergence of antibiotic resistance among various bacterial pathogens has been one of the major concerns of health organizations across the world. In this context, for the development of novel inhibitors against antibiotic-resistant bacterial pathogens, UDP-N-Acetylmuramoyl-L-Alanine-D-Glutamate Ligase (MurD) enzyme represents one of the most apposite targets.

Body: The present review focuses on updated advancements on MurD-targeted inhibitors in recent years along with genetic regulation, structural and functional characteristics of the MurD enzyme from various bacterial pathogens. A concise account of various crystal structures of MurD enzyme, submitted into Protein Data Bank is also discussed.

Discussion: MurD, an ATP dependent cytoplasmic enzyme is an important target for drug discovery. The genetic organization of MurD enzyme is well elucidated and many crystal structures of MurD enzyme are submitted into Protein Data bank. Various inhibitors against MurD enzyme have been developed so far with an increase in the use of in-silico methods in the recent past. But cell permeability barriers and conformational changes of MurD enzyme during catalytic reaction need to be addressed for effective drug development. So, a combination of in-silico methods along with experimental work is proposed to counter the catalytic machinery of MurD enzyme.



Identification of potential inhibitors against *Escherichia coli* Mur D enzyme to combat rising drug resistance: an *in-silico* approach

Vinita Gaur^a, Neeraj Kumar^b , Ashish Vyas^a, Debabrata Chowdhury^c, Joginder Singh^{a*} and Surojit Bera^a 

^aDepartment of Microbiology, School of Bioengineering and Biosciences, Lovely Professional University, Punjab, India; ^bDepartment of Pharmaceutical Chemistry, Bhupal Nobles' University, Udaipur, Rajasthan, India; ^cSchool of Medicine – Infectious Diseases, Stanford University, Stanford, CA, USA

Communicated by Ramaswamy H. Sarma

ABSTRACT

Indiscriminate use of anti-microbial agents has resulted in the inception, frequency, and spread of antibiotic resistance among targeted bacterial pathogens and the commensal flora. Mur enzymes, playing a crucial role in cell-wall synthesis, are one of the most appropriate targets for developing novel inhibitors against antibiotic-resistant bacterial pathogens. In the present study, *in-silico* high-throughput virtual (HTVS) and Standard-Precision (SP) screening was carried out with 0.3 million compounds from several small-molecule libraries against the *E. coli* Mur D enzyme (PDB ID 2UUP). The docked complexes were further subjected to extra-precision (XP) docking calculations, and highest Glide-score compound was further subjected to molecular simulation studies. The top six virtual hits (S1–S6) displayed a glide score (G-score) within the range of -9.013 to -7.126 kcal/mol and compound S1 was found to have the highest stable interactions with the Mur D enzyme (2UUP) of *E. coli*. The stability of compound S1 with the Mur D (2UUP) complex was validated by a 100-ns molecular dynamics simulation. Binding free energy calculation by the MM-GBSA strategy of the S1-2UUP (Mur D) complex established van der Waals, hydrogen bonding, lipophilic, and Coulomb energy terms as significant favorable contributors for ligand binding. The final lead molecules were subjected to ADMET predictions to study their pharmacokinetic properties and displayed promising results, except for certain modifications required to improve QPlogHERG values. So, the compounds screened against the Mur D enzyme can be further studied as preparatory points for *in-vivo* studies to develop potential drugs.

HIGHLIGHTS

- *E. coli* is a common cause of urinary tract infections.
- *E. coli* MurD enzyme is a suitable target for drug development.
- Novel inhibitors against *E. coli* MurD enzyme were identified.

ARTICLE HISTORY

Received 2 May 2023
Accepted 13 December 2023

KEYWORDS

E. coli; hTVS; XP; MD simulation; MM-gbsa; ADMET predictions; Mur enzymes



LOVELY
PROFESSIONAL
UNIVERSITY

Transforming Education Transforming India

Certificate No.257721



Bioclues
Organization

Certificate of Participation

This is to certify that **Prof./Dr./Mr./Ms. Vinita Gaur** of has participated in **Poster Presentation** on the topic entitled **Identification of potential inhibitors against E.coli Mur enzymes through virtual screening and in - vitro assay** in the International Conference on **Bioengineering and Biosciences (ICBB-2022)** held on **18-19 November 2022** organized by the Department of Biotechnology, School of Bio-engineering and Biosciences in association with the Society of Bioinformatics for Experimenting Scientists (Bioclues) organized at Lovely Professional University, Punjab.

Date of Issue : 07-12-2022

Place: Phagwara (Punjab), India



ICMBSDG
Microbial Bioprospecting Towards Sustainable
Development Goals



**LOVELY
PROFESSIONAL
UNIVERSITY**

Transforming Education Transforming India

**NAAC
GRADE A++**

Certificate No. 298803

Certificate of Participation

This is to certify that **Prof./Dr./Mr./Ms. Vinita Gaur** of **Lovely Professional University** has Participated/Presented a Oral Presentation entitled **Identification of prospective inhibitors against E. coli Mur D enzyme through virtual screening & in-vitro assay** in International Conference on “**Microbial Bioprospecting Towards Sustainable Development Goals**” held on **24th- 25th November 2023** organized by Association of Microbiologist of India-LPU Unit and Society of Chemical and Synthetic Biology at Lovely Professional University, Punjab.

Date of Issue : 12-12-2023

Place : Phagwara (Punjab), India

Prepared by
(Administrative Officer-Records)

Dr. Arun Karnwal
President
AMI-LPU Unit

Dr. Karthik Loganathan
President
SCSB

Dr. Ashish Vyas
Organizing Secretary
AMI-LPU Unit

Dr. Neeta Raj Sharma
Senior Dean
SBEB, LPU



Appendix:

Mueller Hinton Broth (M-H Broth)

A liquid medium for antibiotic susceptibility studies (MIC-determination).

Ingredients	Grams/Liter
Beef infusion solids	2.0
Starch	1.5
Casein hydrolysate	17.5

Final pH 7.4 +/- 0.2 at 25°C.

Directions: Dissolve 21 g in 1 liter of distilled water. Sterilize by autoclaving at 121°C for 15 minutes.

Muller Hinton Agar

Ingredients	Grams/Liter
HM infusion solids B # (from 300g)	2.000
Acicase ##	17.500
Starch	1.500
Agar	17.000
Final pH (at 25°C)	7.3±0.1

- Equivalent to Beef heart infusion ## - Equivalent to Casein acid hydrolysate
Directions
Suspend 38.0 grams in 1000 ml purified/ distilled water. Heat to boiling to dissolve the medium completely. Sterilize by autoclaving at 15 lbs pressure (121°C) for 15 minutes. Cool to 45-50°C. Mix well and pour into sterile Petri plates.

Nutrient Broth Medium

Nutrient Broth Medium is used as a sterility-testing medium

Composition

Ingredients	Gms / Litre
Peptone	10.000
Beef extract	10.000
Sodium chloride	5.000

pH after sterilization 7.3 ± 0.1

Directions Suspend 25 grams in 1000 ml purified/distilled water. Heat if necessary to dissolve the medium completely. Sterilise by autoclaving at 10 lbs pressure (115°C) for 30 minutes or alternatively at 15lbs pressure(121°C) for 15 minutes or as per validated cycle

Tryptic Soy Broth (TSB)

TSB is a general-purpose medium that is routinely used to grow bacteria which tend to have high nutritional requirements

Composition

Ingredients	Grams / L
Pancreatic digest of casein	17
Peptic digest of soybean	3
Sodium chloride	5
Dipotassium phosphate (K_2HPO_4)	2.5
Dextrose	2.5

Phosphate Buffered Saline (PBS) pH 7.4

Intended use: Phosphate-Buffered Saline (PBS), pH 7.4 is used for the preparation of dilution, blanks for the examination of samples from food, water, and other clinical and non-clinical specimens.

Composition

Ingredients	Gms / Litre
Sodium chloride	7.650
Disodium phosphate, Anhydrous	0.724
Dipotassium hydrogen phosphate	0.210
Final pH (at 25°C)	7.40

Directions Suspend 8.58 grams in 1000 ml purified /distilled water. Dispense in test tubes or flasks as desired. Sterilize by autoclaving at 15 lbs pressure (121°C) for 15 minutes.